SEMMELWEIS EGYETEM

DOKTORI ISKOLA

Ph.D. értekezések

2958.

MISKOLCZI CHRISTINA

Neuroendokrinológia
című program

Programvezető: Dr. Fekete Csaba, tudományos tanácsadó

Témavezető: Dr. Mikics Éva, csoportvezető

BEHAVIORAL AND PLASTICITY-RELATED EFFECTS OF POST-WEANING SOCIAL ISOLATION IN RATS AND MICE

PhD thesis

Christina Miskolczi

János Szentágothai Doctoral School of Neuroscience

Semmelweis University

Supervisor: Éva Mikics, Ph.D

Official reviewers: Nóra Bunford, Ph.D

Gergely Zachar, Ph.D

Head of the Complex Examination Committee: Dániel Bereczki, MD, D.Sc

Members of the Complex Examination Committee: Xénia Gonda, Ph.D

István Tarnawa, Ph.D

Budapest

2023

Table of Contents

List of Abbreviations

ACC	anterior cingulate cortex
AD	Alzheimer's disease
ADHD	attention deficit hyperactivity disorder
ANX	anxiety or phobic disorders
ASD	autism spectrum disorder
BD	bipolar disorder
BDNF	brain-derived neurotrophic factor
BLA	basolateral amygdala
CA1	cornu Ammonis 1
CP	critical period
ELM	early-life maltreatment
EPM	elevated plus-maze test
FLX	fluoxetine
GABA	gamma-aminobutyric acid
GAD65	65 kDa isoform of glutamic acid decarboxylase
GMV	grey matter volume
HPC	hippocampus
IL	infralimbic cortex
IL	infralimbic cortex
IN	interneuron
Iso	isolation
Kv2.1	Potassium voltage-gated channel, Shab-related subfamily, member1
LGN	lateral geniculate nucleus
MDD	major depressive disorder
mPFC	medial prefrontal cortex
MRI	magnetic resonance imaging
mRNA	messenger ribonucleic acid
NDS	normal donkey serum
OF	open field test
OFC	orbitofrontal cortex
PBS	phosphate buffered saline

PFC	prefrontal cortex
PN	postnatal day
PNN	perineuronal net
PrL	prelimbic cortex
PV	parvalbumin
PWSI	post-weaning social isolation
Reg	regrouping
Res	resocialization
RI	resident-intruder test
ROI	region of interest
RT-PCR	real-time polymerase chain reaction
SCZ	schizophrenia
SI	social interaction test
SPT	sucrose preference test
TrkB	tyrosine receptor kinase B
V1	primary visual cortex
VEH	vehicle
vGAT	vesicular GABA transporter
vGluT1	vesicular glutamate transporter 1
vGluT2	vesicular glutamate transporter 2
vHPC	ventral hippocampus
WFA	*Wisteria floribunda* agglutinin
WMV	white matter volume
yr	year

1. Introduction

1.1. The devastating consequences of early-life maltreatment.

Maltreatment experienced in early life (early-life maltreatment; ELM), i.e. during childhood and adolescence, represents a major risk factor in the development of psychopathologies in later life [1–7]. ELM includes any acts or series of acts of commission or omission by a parent or other caregiver that causes harm, potential for harm, or threat of harm to a child (generally interpreted as under 18 years of age), even if harm was not intended [8]. It is usually divided into five types: physical, sexual and emotional abuse and physical and emotional neglect [9]. Out of these subtypes, neglect has often received the least attention, even though it is one of the most common forms of maltreatment and can be even more detrimental than physical or sexual abuse [8,10,11]. Overall, ELM is a widespread issue affecting millions of children worldwide each year, with global prevalence rates ranging from 12-36% per each subtype according to self-reports [9].

A history of ELM shows an especially high incidence in individuals with psychiatric disorders. A study by Struck et al. revealed that while a history of moderate to severe ELM was present in 15.0% of healthy controls, patients diagnosed with schizophrenia/schizoaffective disorder, bipolar disorder, major depressive disorder, or persistent depressive disorder had an ELM prevalence of 56.1%, 56.3%, 57.1% and 75.4%, respectively [12]. Another study by Li et al. reported that 58.59% of depression and anxiety cases can be potentially attributed to ELM globally, and estimate that reducing ELM by 10-25% could prevent 31.4 – 80.3 million depression and anxiety cases worldwide [7].

It has been proposed that ELM induces a cascade of molecular and neurobiological changes, leading to ecophenotypic variants that form a clinically distinct population compared to non-maltreated psychiatric patients [13]. Indeed, ELM has been linked to younger age of onset [12,14–17], greater severity of symptoms [12,16,18], a more unfavorable course of disease [14,16,17,19], elevated risk of suicide [16,18,20] and higher chance of comorbidities [14–16,18]. Patients with a history of ELM also show poor treatment response compared to non-maltreated controls [17–19].

ELM-induced psychopathologies commonly affect the social domain, and may include disruptive, aggressive, or withdrawn behavior that begins at an early age [21].

These and additional internalizing and externalizing problems extend into adulthood [22,23], carrying a potential increase of self-harm [24–27] and criminal behavior [2,28,29], including violence [30,31]. Social interactions form an essential part of our society. Navigating through social networks with aberrant social behavior can generate constant difficulties for people with a history of ELM, causing additional distress and increasing allostatic load, which may result in a cycle of worsening symptoms and lead to altered stress-reactivity [21].

Apart from individual effects, the consequences of ELM also place a heavy burden on society, as reflected by exorbitant, ever-increasing economic costs [32,33].

The above highlights that ELM-induced psychopathologies are linked to grave consequences involving both the self and others and warrant intervention. The added difficulty of ELM-related mental health disorders displaying increased treatment-resistance urges the development of novel treatment methods. However, in order to devise effective intervention strategies, elucidating the neurobiological mechanisms underlying ELM-induced psychopathological effects is imperative.

1.2. Early life as a vulnerable developmental period for social adversity.

Childhood and adolescence represent time windows when dynamic changes take place in the central nervous system. Grey matter volume increases at a fast pace in the first few years after birth as synapses are formed and overproduced in waves during synaptogenesis [34–36]. This is followed by synaptic pruning, when unused synapses are weakened or eliminated, whereas active synapses are maintained and strengthened in a neuronal activity-dependent way [37]. Experience-driven activation of neural systems thus ensures that each individual's brain networks are selectively molded to environmental demands.

Total grey matter volume peaks before 5-7 years of age in humans [38,39], after which it begins to decrease as pruning takes place [34–36,39]. Parallel to this, white matter volume gradually increases with the myelinization of existing axons, solidifying neural pathways and restricting plasticity [38,40–42]. The developmental curves of grey matter volume are sequential and hierarchical; lower-order sensory cortices develop first, while regions that subserve more complex functions and thus integrate more information, e.g. higher-order association cortices, mature later [43]. Concordantly, commissural and projection fibers involved in more basic processes mature earlier, whereas association

fibers partaking in more complex tasks, especially frontal-temporal ones (such as the cingulum, uncinate fasciculus and superior longitudinal fasciculus), show prolonged maturation and decline at a slower rate [38,40,41].

Given that, as highlighted by studies with humans, most grey and white matter restructuring takes place during childhood and adolescence (**Fig. 1.**), and pruning is selectively influenced by environmental stimuli [44], social adversities experienced during this time could leave a devastating impact on the developing brain and lead to subsequent psychopathologies [45]. Indeed, a history of ELM has been associated with disturbances in grey matter volume [46], white matter volume [47], or even altered functional connectivity between regions of the social behavioral network [48–50].

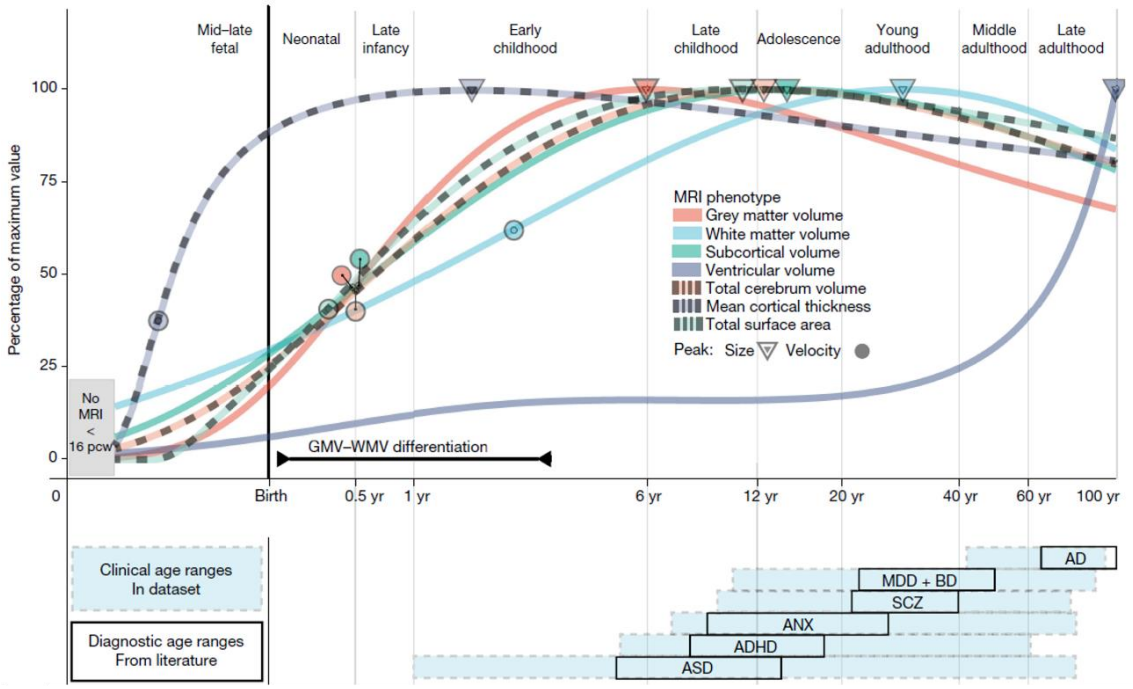

Figure 1. Developmental trajectories based on MRI scans and age ranges of incidence for major psychiatric disorders. *Top, normative developmental trajectories of the median for each global MRI phenotype and key maturational milestones, as a function of age (log-scaled). Circles show the peak rate of growth trajectories for each category. Triangles show the peak volume of each category. Bottom, age range of incidence for each of the major psychiatric disorders represented in the MRI dataset; black boxes indicate the age when these conditions are generally diagnosed. MRI, magnetic resonance imaging; AD, Alzheimer's disease; ADHD, attention deficit hyperactivity disorder; ASD, autism spectrum disorder (with the inclusion of high-risk individuals that*

have a confirmed diagnosis at a later age); ANX, anxiety or phobic disorders; BD, bipolar disorder; GMV, grey matter volume; MDD, major depressive disorder; SCZ, schizophrenia. WMV, white matter volume; yr, year; Figure adapted from Bethlehem et al. [51] licensed under CC BY 4.0.

To summarize this section, childhood and the adolescent period are characterized by dynamic, large-scale changes in brain structure and function, and these changes are influenced by environmental experiences. As such, early life marks a vulnerable period when social adversities could leave a lasting impact on developing brain networks.

Still, human neuroimaging studies allow for large-scale observations and conclusions only, whereas the precise understanding of cellular and molecular processes underlying ELM-induced behavioral and structural changes is crucial in order to develop novel treatment methods, highlighting the importance of preclinical research.

1.3. Critical period plasticity.

Critical periods (CP) denote time windows of heightened plasticity during brain development when networks possess the ability to make fast, dynamic changes as an adaptive response to environmental experience [52,53].

CPs have first been described in the visual system of cats in the groundbreaking work of Wiesel and Hubel [54–56]. In these studies, one eye was deprived of vision in kittens either from birth or later in life for various periods of time, after which the responsiveness to light stimulation of neurons in the visual thalamus (lateral geniculate nucleus – LGN) and primary visual cortex (V1) were measured. Closure of one eye for a brief postnatal period (2-3 months in kittens but varies from weeks to years proportionally to the lifespan of the species) caused amblyopia or permanent loss of vision through the deprived eye despite no damage in the retina, LGN or V1. Under normal conditions, the LGN sends thalamocortical axons that serve each eye to layer IV of V1. In V1, inputs from each eye converge and compete for space, producing alternating ocular dominance columns [57,58]. Monocular deprivation during development expands the columns serving the normal/open eye at the expense of columns responding to the deprived eye, which become reduced in size and complexity [59,60].

Much of what we know about critical period regulation comes from preclinical studies investigating the visual cortex and other, mainly sensory systems. Based on these

findings, key principles and processes have been described pertaining to critical period plasticity.

First of all, critical periods denote temporary time windows during development, and high plasticity associated with critical periods substantially decreases after closure [61]. For example, monocular deprivation in adulthood produces no detectable effects as opposed to early-life deprivation [56]. Though some level of plasticity can remain in adulthood, the magnitude and speed of changes differentiate CP plasticity from adult plasticity, the latter of which is slower and involves more modest alterations in brain networks [44,62].

Second, though the basic wiring and connections of networks are genetically determined [63–66], refinement of brain circuits involves neuronal activity. At first, internally generated spontaneous activity shapes connections [67], which eventually gives way to experience-dependent neuronal activity to fine-tune networks according to environmental demands [68]. As such, it has been shown that experience can influence the onset and course of CPs. Lack of experience, e.g. rearing animals in the dark since birth causes delayed onset and decelerated course of the critical period in the visual system [69]. However, environmental enrichment is enough to induce critical period closure in dark-reared rats similarly to normally-reared ones [70].

Third, the maturation of inhibitory neurotransmission constitutes a key part of CP processes [52,71]. It has been proposed that inhibition gradually represses the response to spontaneous intrinsic activity and promotes experience-driven input, switching learning from internal cues to external signals [72].

CP plasticity is tied to the maturation of a particular interneuron subtype, parvalbumin-expressing (PV+) interneurons (INs). PV+ INs are the most abundant interneuron subtype in the neocortex [73]. Owing to their specialized cellular and molecular properties, PV+ INs exert reliable, fast, strong and temporally precise inhibition onto neighboring pyramidal neurons, making them crucial players in the generation of network oscillations [74]. Maturation of PV+ INs follow a functional hierarchy, appearing first in sensory regions and progressively extending to more complex association cortices (**Fig. 2.**) [75,76], coinciding with the developmental timing of grey matter volume changes and suggesting that critical periods progress sequentially also. PV+ IN maturation and gamma-aminobutyric acid (GABA) neurotransmission are

sensitive to sensory experience [77,78] and have strongly been implicated in the regulation of critical period onset [52,79–84], establishing their role as pivotal plasticity switches [82].

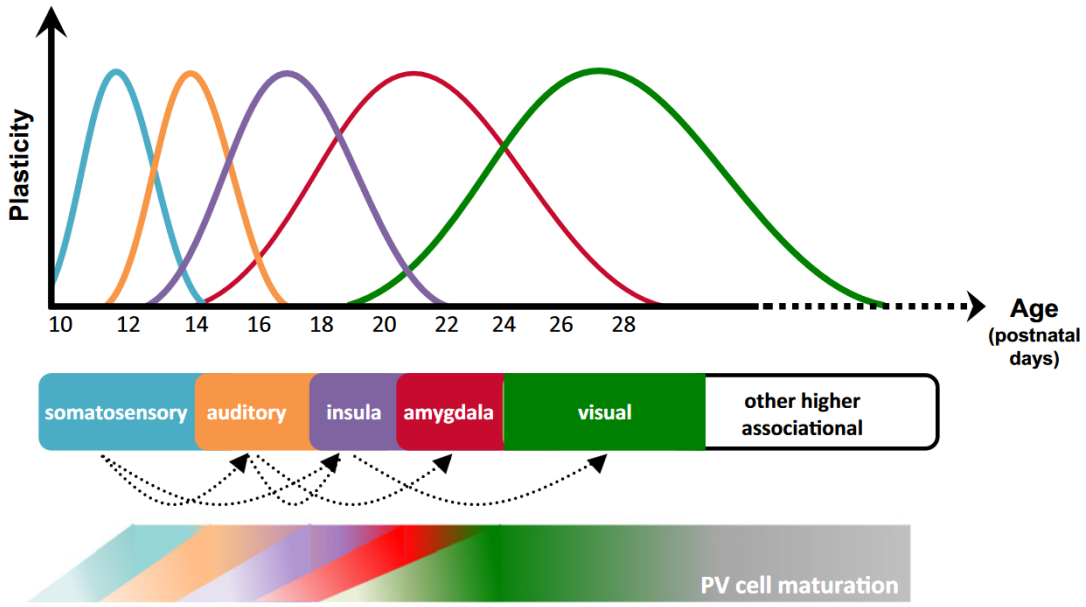

Figure 2. Sequential CP plasticity periods described in the mouse brain. *The trajectories denote the time windows for peak plasticity in the barrel cortex, auditory cortex, insular cortex, amygdala, visual cortex, and higher associational cortices. Local maturation of parvalbumin-containing interneuron circuits in each brain region is associated with decreased plasticity and critical period closure. PV, parvalbumin. Figure used from Reh et al. [71].*

Fourth, brain-derived neurotrophic factor (BDNF), arguably the most studied member of the neurotrophin family of growth factors, partakes in several plasticity-related processes, including neuronal differentiation and maturation [85], synapse formation [86,87], modulation of synaptic strength [88,89], and critical period onset [90,91]. Unlike other growth factors that are mainly secreted in a constitutive way, BDNF possesses neuronal activity-dependent promoters [92–94], which allow environmental stimuli to induce BDNF expression via experience-dependent activation of relevant neuronal circuits. In line with this, it has been shown that activity-dependent promoter IV of BDNF is necessary for the maturation of cortical inhibition [95]. Visual system experiments have displayed that light regulates the expression of BDNF messenger ribonucleic acid (mRNA) in the visual cortex, but even in absence of light, i.e. in dark

rearing conditions, CP can be induced by overexpression of BDNF [96,97]. Under normal rearing conditions, BDNF overexpression induces precocious CP [90] which involves the accelerated maturation of inhibition [91].

Fifth, CP closure involves both functional and physical molecular brakes that consolidate the changes made during maturation [82]. One of these well-described physical brakes are perineuronal nets (PNN). PNNs are specialized extracellular matrix structures that preferentially surround PV+ INs, dividing PV+ INs into two main subpopulations: those that are enwrapped by PNNs (PV+PNN+) and those that lack PNN (PV+PNN-) [98–102]. PNNs restrict developmental plasticity [79,103,104], likely by (**I**) acting as a physical barrier between neurons and advancing axons [105–107], (**II**) acting as a scaffold for chemorepulsive axon guidance signals [108], (**III**) limiting lateral diffusion of receptors at synapses [109], and (**IV**) enabling fast-spiking properties of PV+ INs by acting as an ionic buffer [110,111]. Organization of PNNs is experience-dependent [112] and begins by the end of the critical period [103]. Lack of experience delays PNN appearance, and degradation of PNNs induces CP-like plasticity [103].

In summary, CPs are finite time windows of high plasticity during development that are dynamically regulated by experience. Experience-driven neuronal activity induces the expression of critical period onset regulators, such as BDNF, which promote the maturation of inhibition. Cortical information processing becomes more efficient as mature PV+ INs increase the signal-to-noise ratio. Finally, experience-dependent changes made during the CP are consolidated with the appearance of PNNs and other factors that promote CP closure.

1.4. Prefrontal cortex maturation: a critical period for social behavior?

Social behavior, defined as „all behavior that influences, or is influenced by, other members of the same species" [114], involves the rapid **(I)** perception and broadscale integration of various factors related to the opponent or group (e.g. rank, emotional state) and inner state of the self (e.g. motivational or emotional state); **(II)** prediction of the potential consequences of actions; and **(III)** response-selection: selecting an action that maximizes reward and/or minimizes harm [115]. Social interactions are thus highly complex and are regulated by various overlapping and densely interconnected circuits, where each brain region can participate in the regulation of multiple behaviors, while each type of behavior is regulated by multiple regions [116,117]. As such, key hubs of the

social behavioral network, including (but not limited to) the hippocampus, amygdala and prefrontal cortex (PFC), show protracted development, with a peak in adolescence [39,43,118–120].

Neural processing of social information is of heightened importance in adolescence, as this is a period when family likely becomes a less prominent factor in the life of children and peers become more so [121,122]. Therefore, in order to maintain a social support network, adolescents must go through social re-orientation as they integrate themselves into a new network, which places added stress on brain regions regulating social behavior [122].

Among these brain regions, the PFC is especially notable: aside from regulating emotional behavior and controlling basic drives, the PFC has been regarded as the region mainly responsible for the temporal organization of behavior in goal-directed actions [123]. As such, the PFC is heavily involved in all three stages of social interaction mentioned above [115], denoting it as a cardinal conductor of social behavioral networks. Owing to its widespread intricate connections, the PFC is one of the last brain regions to reach full maturation - it has been shown that the overproduction of dendritic spines reaches a peak in late childhood and subsequent pruning begins in early adolescence, but can last even until the third decade of life [124,125].

The protracted development of the PFC marks it vulnerable for an extended period of time. Given its important role in emotion regulation and the organization of social behavior, altered PFC maturation due to ELM could lead to abnormal social interactions. Indeed, reports do show that ELM has been coupled with smaller PFC volume or reduced cortical thickness [46,126–128], blunted PFC function [129], and ELM-induced changes in the PFC have been associated with subsequent lifetime perpetration of aggression in adulthood [130]. However, the neurobiological processes that could link ELM-induced deficits in prefrontal networks to ELM-associated abnormal aggression and other disturbances in social behavior remain largely unknown.

Current knowledge on CPs mainly came from the observation of sensory and motor systems, but it remains to be seen if CP processes are universal across all cortical areas. If so, do the same mechanisms govern CP plasticity in higher-order association areas, i.e. the PFC?

Recently, studies have begun to consider adolescence as a critical period for social learning and PFC maturation [113,131–133]. As with sensory CPs, adolescence involves the functional maturation of prefrontal PV+ INs: PV expression and GABAergic activity increases during adolescence in rodents [134–137], and so does the build-up of PNNs [136]. Humans and non-human primates also display PV+ IN maturation during adolescence in the PFC as shown by PV mRNA expression, suggesting that PFC development is conserved across mammalian species [138,139].

Signalling involving BDNF and its receptor, tyrosine receptor kinase B (TrkB), are necessary for the development of PV+ IN-mediated perisomatic inhibition across cortical areas [140]. In line with this, a study has shown that transgenic mice with reduced TrkB/BDNF signalling displayed reduced PV+ IN-mediated inhibition, which was associated with deficient prefrontal network dynamics and increased aggression [141]. Other studies have also strengthened the link between prefrontal PV+ INs and social behavior: the number of PV+ INs has been shown to be associated with aggressive behavior [142]; chemogenetic inhibition of PV+ INs impairs social interaction [143]; and absence of social experience (i.e. social isolation) during adolescence has been shown to disrupt PFC PV+ INs [144].

As mentioned before, prefrontal PNNs also appear over the adolescent period [136,145,146]. Preclinical studies have revealed that PNNs are sensitive to perturbations in early life including maternal deprivation, which decreases PNN expression around PV+ INs in subregions of the PFC [147]; and social threat, which increases PNN expression and reduces inhibition in a subregion of the PFC, the anterior cingulate cortex (ACC) [148].

The studies highlighted above suggest that PFC maturation shows a peak during adolescence and involves similar mechanisms to those seen in sensory and motor cortical CPs. Considering this, early-life adversities could have important implications in the context of CP mechanisms. First of all, different types of ELMs could offset CP in opposing ways: if we consider social adversities analogous to visual system experiments, social isolation (i.e. lack of experience, analogous to dark rearing) could delay CP onset whereas abuse (i.e. adverse ‘environmental enrichment’) could cause early onset of maturation [149,150]. Second, the potential of manipulating CP plasticity in PFC

development and social learning could bear promising therapeutic implications [151,152].

Still, knowledge regarding the development of social behavior and PFC maturation in association with CP mechanisms is scarce. Additionally, while increasing evidence outlines the close relationship between PV+ IN maturation and PNN deposition in CP plasticity and social experience-dependent learning, there is an astonishing lack of information on the specific role and properties of the PNN-enwrapped PV+ IN population itself. To add further difficulties, the reliable differentiation between prefrontal PV+PNN+ and PV+PNN- interneurons is not possible yet with current *in vivo* methods. Thus, whether each subpopulation plays different roles in the regulation of social behavior, whether ELM influences the two subpopulations in a distinct way, and whether these potential changes contribute to ELM-induced abnormal social behavior remain to be elucidated [153].

1.5. Fluoxetine induces critical period-like plasticity.

Fluoxetine is an antidepressant belonging to the selective serotonin reuptake inhibitor (SSRI) class. Developed in the 1970s and approved for the treatment of depression by the US FDA in 1987 [154], research on its mechanisms of action focused on 5-hydroxytryptamine (5-HT)-neurotransmission, leaving its other properties unexplored for years.

Some earlier studies have already suggested that fluoxetine is capable of amplifying neuroplasticity [155], but it wasn't until the groundbreaking paper of Maya Vetencourt et al. [156] that induced CP-like plasticity by fluoxetine gained widespread attention.

In the study, Maya Vetencourt et al. have shown that in rats that underwent monocular deprivation, ocular dominance plasticity can be reinstated and visual functions can be recovered in adulthood by chronic administration of fluoxetine. This was accompanied by reduced inhibition and increased expression of BDNF in the visual cortex. Indeed, it has been shown that BDNF/TrkB signalling is crucial for antidepressant-induced behavioral effects [157], and that chronic, but not acute treatment increases BDNF mRNA expression [158] via its activity-dependent promoters IV and VI [159]. Apart from increasing BDNF, fluoxetine also exerts its effects by upregulating

genes related to CP and synaptic plasticity [159,160], decreasing PV+ IN-mediated inhibition, and decreasing PNNs that surround PV+ INs [160].

Fluoxetine also shows promising results in emotion-related paradigms: in a study investigating fear extinction, only the combined treatment of extinction training and chronic fluoxetine administration was successful in long-term fear erasure, whereas neither treatment alone was capable of inducing an enduring loss of the fear memory in adult animals [161]. Fluoxetine likely induced CP-like plasticity in the fear circuitry, as shown by increased expression of BDNF in the basolateral amygdala (BLA) and the hippocampus (HPC), reduction in the percentage of PV+PNN+ cells in the BLA and cornu Ammonis 1 (CA1) region of the HPC, and increased excitation in the BLA, allowing experience-dependent remodeling of fear networks guided by extinction training [161]. Other paradigms involving chronic social defeat stress have shown that fluoxetine treatment is able to reverse social defeat stress-induced anxiety- and depression-like behavior [162,163], and even some parameters of social behavior, i.e. sniffing and rearing [162].

These findings could have crucial implications in the context of early-life adversities and social learning, but the detailed investigation of chronic fluoxetine treatment on social behavior in general and on ELM-induced abnormal social behavior has not been performed yet. Such investigations require a robust preclinical model of early-life adversity in which fluoxetine-induced mechanisms and behavior can be reliably observed [164,165].

1.6. Modelling early-life neglect: post-weaning social isolation in rats.

Post-weaning social isolation (PWSI) is a laboratory model of early-life neglect. In this model, following weaning on postnatal day 21 (PN21) rats are either housed socially (in groups of 4) or are isolated (housed alone) for 8 weeks, until adulthood.

As mentioned before, ELM carries an increased risk for social behavior-related disturbances [166], including the perpetration of violent crimes [167]. Comparably to human studies, prior results from our research group show that PWSI in male rats induces disturbances in social behavior. Notably, isolated rats display abnormal aggression in adulthood that disregards species-specific rules, including an increased number of total attacks, attacks aimed at the vulnerable body parts of the opponent, unsignaled attacks (i.e. attack without warning or threat) and dismissal of the opponent's behavioral cues,

e.g. continued attack even when the opponent shows submission [168–170]. Isolated rats also show increased defensive behavior and display behavioral fragmentation (i.e. fast abnormal switching between elements of social behavior) [168–170]. Resocialization, a laboratory model for behavioral therapy [171], fails to ameliorate PWSI-induced violent aggression [172]. These results highlight that PWSI leads to enduring, treatment-resistant social behavioral abnormalities, providing a suitable basis for finding novel approaches in the intervention of ELM-induced psychopathologies.

While behavioral repertoires are largely specific to each species, aggression is a general behavioral capacity that is seen across mammalians. Such class-common behaviors have been shown to share elemental neural processes, and despite the functional and anatomical differences of human and rodent PFC, it could be argued that rodent models provide valuable insight into the prefrontal regulation of social functions, including aggression [173].

Human studies show that the PFC is activated by aggressive actions [174], more so in subjects with aggression-related psychopathologies [175,176]. Additionally, violent offenders display chronic structural alterations in the PFC [177]. Preclinical models also underline the PFC as a key regulator of aggressive behavior [178,179], and in the context of modelling ELM, PWSI in rats induces hyperactivation in both main regions of the PFC, i.e. the orbitofrontal cortex (OFC) and medial prefrontal cortex (mPFC) following aggressive interaction [170,180]. In addition to functional changes, PWSI induces structural changes also, which include the reduced thickness of the mPFC, reduced vascularization, and decreased dendritic and glial density [180].

Based on our earlier research, PWSI induces a robust and enduring behavioral phenotype, which is accompanied by structural and functional changes in the PFC, making it an ideal model system to study the neurobiological underpinnings of early-life adversities and explore novel treatment opportunities [165]. PWSI has largely been investigated in rats, carrying certain advantages over mice: rats show a wider range of social behavioral repertoire [181,182], show more affiliative social behavior [182], and are the standard approach to test drug toxicology, efficacy and dosage in the pharmaceutical industry versus mice [181]. Additionally, the studies investigating CP-like induced plasticity by fluoxetine have been performed in rats [156,161].

Still, studies in mice are rapidly gaining importance due to the increased use of transgenic techniques. Mice also display more aggressive behavior than rats [182], which could be beneficial in the investigation of the neural background behind PWSI-induced abnormal aggression. However, before further experiments can take advantage of the widespread technical opportunities offered by transgenic strains in the investigation of PWSI and fluoxetine treatment, a detailed characterization of PWSI-induced behavioral changes is imperative, which has not been performed in mice so far.

1.7. Summary of introduction.

Early-life social adversities leave a devastating impact on both the individual and its environment. ELM-associated psychopathologies are clinically distinct, characterized by increased severity and resistance to treatment, which warrants the development of novel treatment methods.

Human neuroimaging studies show that early life is a dynamic period of large-scale changes. Notably, brain regions of the social circuitry go through active remodeling in adolescence as reintegration into new social groups takes place. The PFC is a central hub in the regulation of social behavior and is characterized by protracted development that peaks in adolescence, making it vulnerable to social adversities experienced in early life.

Research suggests that adolescence is a CP for PFC maturation and is probably governed by similar processes as those described in sensory CPs. Still, little is known about social learning and PFC maturation in the context of CP mechanisms and how maltreatment in early life may derail these. Additionally, PV+ INs and the PNNs that enwrap them are critical orchestrators of CP timing, and PV+ INs have been established to play a role in social information processing. But whether the two major PV+ IN subpopulations are affected differently by early-life social adversities remains to be investigated.

PWSI is a robust laboratory model of childhood neglect and its effects on social behavior have been well-established in rats, making it an ideal candidate to study social learning in the context of CP plasticity. Fluoxetine has been shown to affect plasticity in sensory and even emotion-related paradigms in rats, and research suggests that social, PFC-related tasks would be similarly affected.

Still, despite the advantages of rats in social behavioral paradigms, the eventual need for transgenic strains that facilitate the manipulation of selective circuits and neuronal populations necessitate the use of mouse models. Unfortunately, a detailed behavioral characterization of PWSI has not been performed yet in mice. Additionally, while PWSI has been shown to induce disturbances in the structure and function of the prefrontal cortex (PFC), little is known about how PWSI might impact PV+ INs and the PNNs that enwrap these, CP regulators specifically associated with the closure of cortical network development.

Here, I hypothesize that PWSI in rodents leads to social behavioral abnormalities in adulthood, accompanied by changes affecting CP plasticity regulators, which potentially contribute to the emergence of abnormal social behavior. Plasticity of social behavior, i.e. the capacity for social learning presumably decreases by adulthood, rendering social abnormalities resistant to change. Inducing CP plasticity in adulthood with chronic fluoxetine treatment could allow for social learning beyond adolescence, carrying exciting therapeutic implications in the treatment of childhood maltreatment-induced psychopathologies.

2. Objectives

In two sets of experiments, we aimed to investigate PWSI-induced social disturbances, their association with social learning in adulthood, and PWSI-induced changes in critical period regulators, i.e. PV+ interneurons and PNNs, in the PFC.

Experiment 1 - Fluoxetine and social learning in adulthood in PWSI rats:

In the first set of experiments described in the thesis, we aimed to investigate whether fluoxetine, by inducing CP-like plasticity in adulthood, can provide capacity for social learning.

- Since PWSI takes place during the presumed critical period of social learning, we wished to verify that PWSI, i.e. social deprivation from weaning to adulthood, disrupts the development of social behavior, leading to the emergence of abnormal social behavior during social interactions.
- We wished to investigate whether PWSI-induced social abnormalities are resistant to resocialization in adulthood, possibly reflecting critical period closure of social behavioral development and prefrontal network maturation.
- We aimed to study whether reinstating critical period-like plasticity in adulthood with chronic fluoxetine treatment could enable the possibility of social learning and thus ameliorate PWSI-induced abnormalities in social behavior.

Experiment 2 – Behavioral characterization of PWSI in mice and the effects of PWSI on prefrontal PV+ neurons and PNNs:

The second set of experiments investigates the behavioral output of PWSI in mice including a detailed social behavioral characterization, and studies how PWSI affects PV+ interneurons and perineuronal nets, established regulators of CP plasticity, in the PFC. We differentiated between the two main regions of the PFC, the ventromedially located OFC and the dorsomedially located mPFC, as they subserve different tasks and could be impacted by PWSI in distinct ways.

- We aimed to investigate PWSI-induced behavioral changes via an extensive behavioral test battery. We assume that PWSI-induced behavioral disturbances in mice parallel those seen in rats. Notably, since PWSI takes place during the presumed critical period of social behavioral development, we propose that disturbances induced by PWSI will be specific to the social domain.

- The maturation of PV+ interneurons and the deposition of PNNs around PV+ INs are tied to critical period closure, and it has been shown that prefrontal PV+ interneurons are involved in the regulation of social behavior. Therefore, PWSI-induced disturbances in social behavior must be reflected in changes affecting PV+ interneuronal networks. Here, we aimed to characterize changes in PV+ INs and PNNs by measuring fluorescent intensity, studying input and output properties of PV+ neurons and investigating whether PWSI-induced changes in PV+ neurons are dependent on the presence of PNNs, i.e. whether PWSI affects PV+PNN- and PV+PNN+ interneurons differently.

3. Methods

3.1. Fluoxetine and social learning in adulthood in PWSI rats

3.1.1. Animals

Male Wistar rats (Charles-River) acquired from the breeding facility of the Institute of Experimental Medicine (Budapest, Hungary) were used in the first experiment. Subjects were maintained at a temperature of 22 ± 1°C and a relative humidity of 60 ± 10% in a 12:12h light cycle with lights off at 08:00AM. Food and water were available ad libitum. Following weaning on PN21, rats were randomly assigned to social housing (maintained in groups of 4) or isolation (maintained individually) in cages sized 42 x 26 x 19 cm (**Fig. 3.**). As soon as socially-reared rats weighed 200 g, they were transferred to cages measuring 60 x 38 x 19 cm. Behavioral testing started in adulthood at PN77, when animals weighed 400-450 g.

Intruders used in the resident-intruder (RI) test were also male Wistar rats obtained from the same source as the experimental subjects, and were kept under similar conditions in groups of 6. Intruders weighed ~300 g at the time of testing.

All experiments were carried out in accordance with the European Communities Council Directive of November 24, 1986 (86/609/EEC) and were reviewed and approved by the Animal Welfare Committee of the Institute of Experimental Medicine (PEI/001/30-4/2013).

3.1.2. Experimental design

3.1.2.1. Post-weaning social isolation and the first resident-intruder test

Following weaning, rats were either housed in groups of 4 (social rearing, n = 40), or were housed alone (PWSI, n = 80) for 8 weeks, until reaching adulthood. In order to avoid litter effects, rats from all litters were randomly placed into social or isolation rearing. As such, socially-reared groups consisted of members from different litters.

To investigate the social behavioral effects of PWSI, rats underwent an RI test right after the isolational period (RI Test 1), during the 11th postnatal week (**Fig. 3.** and **Fig. 5A**).

3.1.2.2. Resocialization and chronic fluoxetine treatment

After RI Test 1, PWSI rats either remained in individual housing (isolation; n = 40), or were placed into social groups consisting of four PWSI rats (resocialization; n = 40). Half of both groups, i.e. isolation-reared and resocialized, received chronic fluoxetine (FLX) treatment over the three-week treatment period, while the other half of animals were used as controls and received normal drinking water. FLX (fluoxetine hydrochloride; Sigma-Aldrich, Budapest, Hungary) was administered via drinking water, at a concentration of 0.2 mg/ml. Regularly recorded fluid intake and body weights indicated that the average FLX intake was 5.9 ± 0.1 mg/day for each rat (~14 mg/kg). Under similar conditions, FLX has been shown to significantly increase neural plasticity in rats [156,183]. FLX was added to the drinking water following the 1-hour observation period, meaning that it did not influence behavior right after resocialization. PWSI rats were allocated into the following four treatment groups: (**I**) '**Isolation**', wherein subjects were maintained in isolation following the first RI test, without receiving FLX treatment (**IsoVEH**); (**II**) '**Resocialization**'; wherein subjects were resocialized into groups of 4 after the first RI test, without receiving FLX treatment (**ResVEH**); (**III**) '**Isolation+fluoxetine**'; denoting subjects that were maintained in isolation after the first RI and received FLX treatment (**IsoFLX**) and (**IV**) '**resocialization+fluoxetine**'; denoting subjects that were resocialized after RI Test 1 and received FLX treatment (**ResFLX**) (**Fig. 3. and Fig. 5B**). Resocialization and FLX administration lasted for 3 weeks. The social behavior of the newly created groups (resocialization and resocialization+fluoxetine) was monitored throughout as described below.

After the first RI test, socially-reared rats were regrouped into groups of 4 where at least 2 rats in the new groups remained unfamiliar to each other. This was done in order to mimic resocialization in PWSI animals. Half of socially-reared rats received chronic FLX treatment, resulting in two groups: (**I**) '**Regrouping**'; regrouped after the RI Test 1 and did not receive FLX treatment and (**II**) '**Regrouping+fluoxetine**'; regrouped and received FLX treatment (**Fig. 3 and 6**). The two groups were euthanized at the end of the treatment period, along with PWSI rats. Brain samples were split into 2 main groups: 1) immunohistochemical analysis of PV+ INs and PNNs; and retrograde viral tracing, 2) gene expression-analysis using quantitative real-time polymerase chain reaction (RT-

PCR). Due to the current regulations involving doctoral thesis requirements, the results of brain sample analysis do not form part of the thesis, please refer to these in [184].

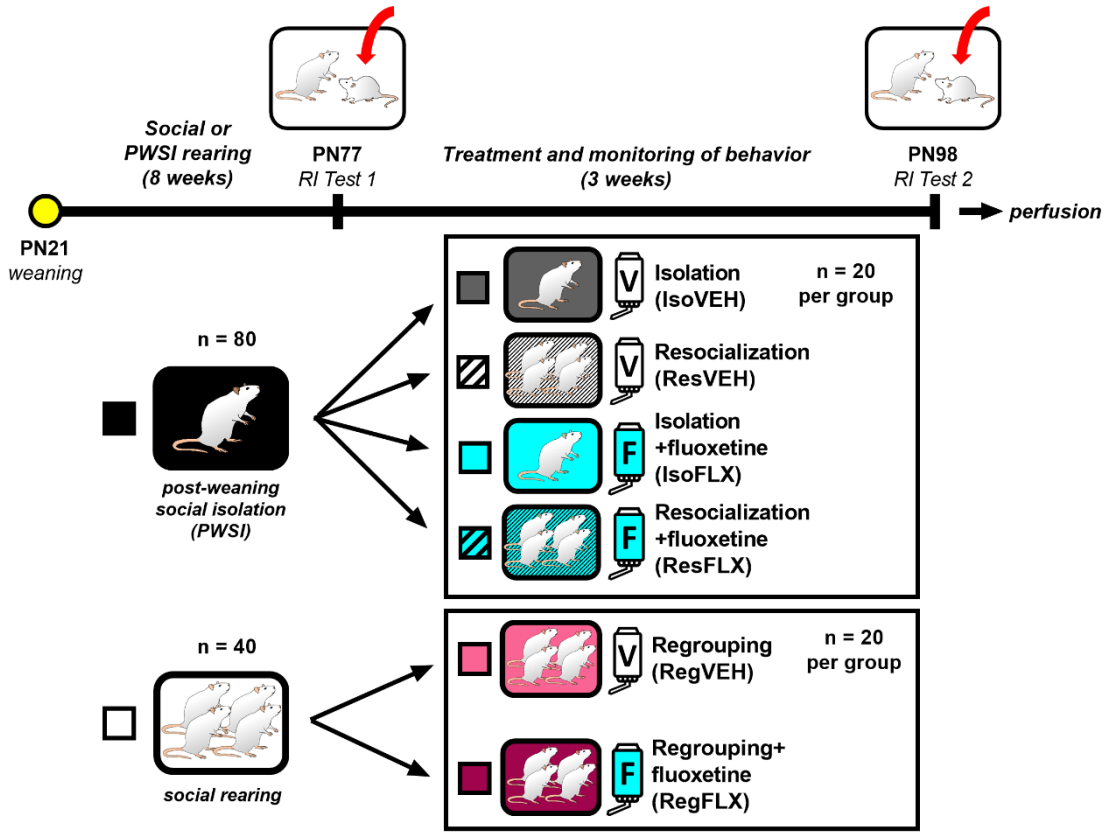

Figure 3. Experimental timeline. *After weaning on PN21, rats were subjected to social rearing or PWSI for 8 weeks. Following the 8-week period, rats were subjected to a resident-intruder test (RI Test 1) on PN77 in adulthood. After RI Test 1, PWSI rats were divided into four groups for 3 weeks: half of the animals remained in isolation and either received normal drinking water (IsoVEH) or chronic fluoxetine treatment administered through their drinking water (IsoFLX), whereas the other half was resocialized into groups of 4 PWSI animals and either received normal drinking water (ResVEH) or chronic fluoxetine treatment (ResFLX). After RI Test 1, social rats were regrouped into groups of 4 to mimic resocialization in PWSI rats, and either received normal drinking water (RegVEH) or chronic fluoxetine treatment (RegFLX) for 3 weeks. The behavior of rats was monitored throughout the 3 weeks. Following the 3-week treatment period, rats were subjected to an RI test (RI Test 2), and were perfused under resting conditions. F, fluoxetine; IsoFLX, isolation+fluoxetine; IsoVEH, isolation+vehicle; PN, postnatal day; PWSI, post-weaning social isolation; RegFLX, regrouping+fluoxetine; RegVEH,*

regrouping+vehicle; ResFLX, resocialization+fluoxetine; ResVEH, resocialization+vehicle; RI, resident-intruder test; V, vehicle.

3.1.3. Experimental procedures

3.1.3.1. The resident-intruder (RI) test

3 days prior to the test rats were placed into individual cages measuring 22 x 38 x 28 cm to establish territorial behavior. The test took place at the beginning of the dark period under dim red illumination. During the test, a smaller-sized male intruder was placed into the subject's homecage for 20 mins. Behavior was recorded and analyzed by an experimenter blinded to the conditions at low speed, with frame-by-frame analysis when needed. We investigated the total number of biting attacks, their type (i.e. soft bite, hard bite or skin pulling), and whether they were aimed at vulnerable or non-vulnerable targets [169] (**Fig. 4.**). Hard bites were defined as attacks involving a forceful body movement of the subject, usually jumping or stomping with the two hind legs, eliciting a strong startle response and subsequent fleeing or other defensive/submissive behaviors from the opponent. In contrast, soft bites involved minimal movement and elicited little to no reaction from the opponent. Skin pulls denoted pulling the opponent's skin with the mouth. 'Vulnerable target bites' defined attacks aimed at vulnerable body parts of the opponent, including the head, throat or belly.

Attack counts denoted quantitative aspects of aggression, while qualitative aspects, i.e. the share of hard bites in the total attack count or aiming attacks at vulnerable body parts of the opponent (i.e. the head, throat or belly) were used to differentiate abnormal aggression from species-specific normal attacks [171].

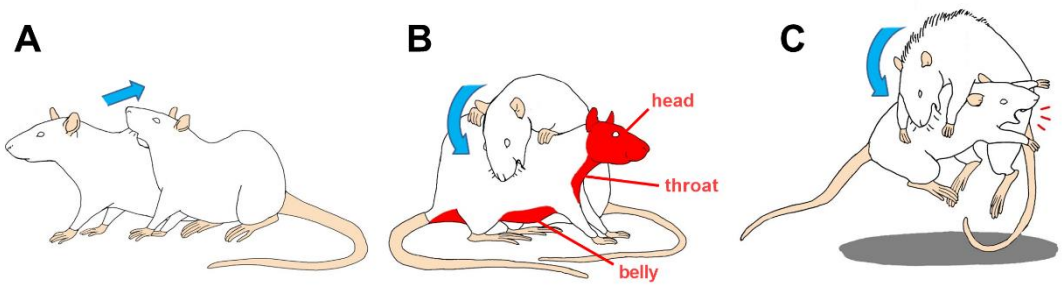

Figure 4. Schematic drawings depicting types of attacks measured during RI. A, *Skin pull: a weak attack involving pulling the opponent's skin with the mouth.* ***B,*** *Soft bite: a*

weak attack involving minimal movement from the attacker and little to no reaction from the opponent. Vulnerable areas on the opponent, i.e. the head, throat and belly, are marked with red. ***C,*** *Hard bite: a strong attack involving the forceful body movement of the attacker (attack jump or stomping with the two hind legs) that elicit a strong startle response in the opponent and subsequent fleeing or other defensive/submissive behaviors. RI, resident-intruder test. Figures were drawn by the author of the thesis.*

3.1.3.2. Group monitoring during the 3-week treatment period

To investigate behavior during cohabitation, we studied aggressive behaviors during the dark/active phase of the day (not included in the current thesis) and huddling during sleep in the light/inactive phase, which is thought to indicate social cohesion [172]. Rats were distinguished using individual marks made with permanent hair dye. Webcameras were placed above the cages and automatically took pictures 1, 2, 4, 6, and 10 hours after the beginning of the light/inactive period of each day. Huddling during sleep denoted direct physical contact with cagemates while sleeping. Absence of contact was scored as "0", whereas at least one contact was scored as "1" irrespective to the number of contacted cagemates. Scores coming from the 5 timepoints were averaged for each individual daily to give their huddling score. Huddling was investigated every day of the 3-week treatment/resocialization period.

3.1.4. Statistical analysis

Values shown in the text and figures indicate mean ± SEM. For main effects we used two-way or repeated-measures ANOVA, as described in the text. When necessary, square-root-transformation was used on behavioral data to fulfill ANOVA requirements. Post hoc analysis was performed by the Duncan test unless otherwise specified. The StatSoft 12.0 software was used for regression analysis. Comparison between the treatment groups and socially-reared groups was done by Student's t-test. P-values lower than 0.05 were considered statistically significant.

3.2. Behavioral characterization of PWSI in mice and the effects of PWSI on prefrontal PV+ neurons and PNNs

3.2.1. Animals

Male Crl:CD1 mice (Charles-River Laboratories) acquired from the breeding facility of the Institute of Experimental Medicine (Budapest, Hungary) were used in the second series of experiments. Animals were maintained in a 12:12 hour light-dark cycle with lights off at 07:00AM, at a temperature of 22 ± 1ºC and a relative humidity of 60 ± 10%. Food and water were available ad libitum, with the exception of the delay discounting training and test period. Over the course of the experiment, body weights of mice were regularly measured and did not show significant differences between groups at any given time point. On PN21, mice were weaned and randomly subjected to social (four animals per cage) or isolation (housed alone) rearing. Mice were housed in Plexiglas cages measuring 36.5 x 20.7 x 14 cm. Intruders used in the resident-intruder test were also male Crl:CD1 mice obtained from the same source, housed socially (in groups of 4-5 mice per cage), and kept under similar conditions as the test subjects. All experiments were carried out according to the Directive of the European Parliament and the Council from 22 September 2010 (2010/63/EU) and were reviewed and approved by the Animals Welfare Committee of the Institute of Experimental Medicine (PEI/001/2056-4/2015).

3.2.2. Experimental design

Following weaning on PN21, mice were housed in groups of four (social rearing) or underwent PWSI (single housing) for 6 weeks. Mice from all litters were randomly assigned to social or PWSI rearing to eliminate litter effects. Mice were subjected to a behavioral test battery after reaching adulthood (PN63), which lasted from PN64 until PN109 (refer to **Fig. 5.** for detailed timeline). Behavioral experiments were performed at 09:00AM, during the first half of the dark/active cycle. Following the open field test on PN64, we subjected all test animals to single housing and kept animals as such until the end of the test battery. Mice underwent a resident-intruder test on PN67 (**RI1**) in order to verify the appearance of PWSI-induced social disturbances and abnormal aggression described in our previous studies in rats [168,170], and another RI test (**RI2**) was conducted after the behavioral battery (PN109), to verify whether the PWSI-induced

abnormal aggressive phenotype remained stable over time and to investigate fighting-induced changes in the PFC.

Mice were perfused on PN109 under resting conditions or 90 minutes after the second RI test. Sample sizes were n = 22 for PWSI mice, and n = 20 for social mice. All test subjects underwent the behavioral test battery, except for the RI2 test. Here, mice were divided into 4 groups: '**social, baseline**' (i.e. perfused under resting conditions, did not undergo RI2; n = 6), '**PWSI, baseline**' (perfused under resting conditions, no RI2; n = 6), '**social, aggressive interaction**' (underwent the RI2 test; n = 14) and '**PWSI, aggressive interaction**' (underwent the RI2 test; n = 16). As such, every mouse endured the same conditions up until they were split into four groups, whereas the split itself was made in order to have baseline control groups for our histological analyses (i.e. resting conditions versus aggressive interaction-induced prefrontal activation). Sample size varied slightly between tests because of minor technical issues (e.g. damaged video footage). Two social animals were excluded from the final analysis due to statistically extremely outlying behavioral parameters in the RI tests (i.e. total bite and vulnerable target bite values surpassed the mean by over 3 standard deviations; further description of biting attacks can be found in *3.2.3.2.*).

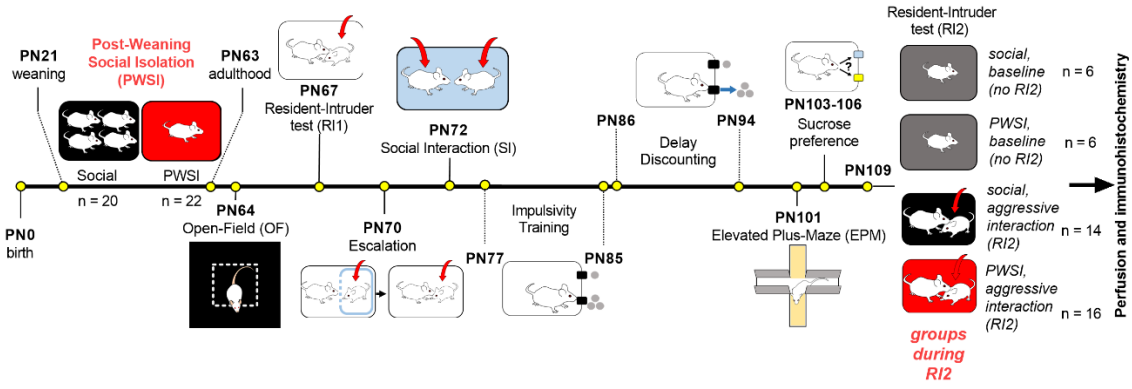

Figure 5. Experimental timeline. *Following weaning on PN21, mice were housed socially (in groups of 4 animals per cage) or were subjected to PWSI (one animal per cage) for 6 weeks, until adulthood (PN63). Afterwards, mice underwent a behavioral battery that lasted until PN109. On PN109 subjects were split into 4 groups, and were euthanized under baseline conditions or 90 minutes after aggressive interaction [153]. EPM, elevated plus-maze; OF, open field test; PN, postnatal day; PWSI, post-weaning social isolation; RI, resident-intruder test; SI, social interaction test.*

3.2.3. Behavioral test battery

3.2.3.1. Open field test (OF)

A square black Plexiglas box measuring 40 x 36 x 15 cm was used to conduct the OF test. Animals were placed into the middle of the box and were allowed to explore the apparatus for 10 minutes under low light illumination (70 lux). After each test, the apparatus was cleaned with water and dried thoroughly. Behavior was video-recorded and the videos were subsequently analyzed by a blind experimenter using the H77+ event-recording software (József Haller, Institute of Experimental Medicine, Budapest, Hungary). Locomotion was measured via the number of line-crossings using a grid placed over the recording. Other investigated parameters included the latency to enter the center and percentage of time spent in the center. The center was defined as the central 20 x 18 cm area of the box.

3.2.3.2. Resident-intruder tests (RI1, RI2) and escalation

All test subjects were transferred into individual cages with fresh corn cob bedding 3 days prior to the first RI test on PN67 (**RI1**). This was done to ensure the emergence of territorial behavior.

Resident-intruder tests: in the early hours of the dark cycle (09:00AM) under dim red illumination, a smaller-sized novel male intruder was placed into the homecage of the resident for 10 minutes. Behavior was video-recorded and analyzed as described below.

Escalation: in the early hours of the dark cycle (09:00AM) under dim red illumination, a smaller-sized male opponent was placed into the resident's homecage for 5 minutes in a wire box the size of 18 x 12 x 10 cm. The test subject was able to see and smell the opponent but was unable to make direct contact with it [185]. After the escalation period was over, the wire box and the opponent contained in the wire box were removed, and a novel smaller-sized male intruder was placed into the homecage of the test subject for 10 minutes (the resident could interact freely with the intruder). Behavior was recorded and analyzed as described below.

On PN109, mice were either perfused under baseline (resting) conditions or 90 minutes after aggressive interaction, i.e. the second RI test (**RI2**). Behavior was video-recorded and videos were analyzed by an experimenter blinded to the conditions, at low

speed, with frame-by-frame analysis when needed. Test subjects were differentiated by marks placed with permanent hair-dye. Parameters investigated were the latency to the first biting attack, the total number of bites, the intensity of biting attacks (categorized as soft or hard), and whether attacks were aimed at the vulnerable body parts of the opponent, such as the head, throat, or belly (see **Fig. 8B**) [168,169]. Hard bites denoted attacks delivered with a forceful body movement of the resident that induced a strong startle response in the intruder (a large jump, fleeing, or other defensive behaviors). Contrarily, soft bites did not involve excessive movement of the resident and induced little to no response from the intruder at most [168]. We also analyzed the duration and frequency of each behavioral type using the Solomon Coder event-recording software (RRID:SCR_016041). The following behavioral types were differentiated: exploration (rearing and any exploratory activity that is not directed towards the conspecific), sniffing (non-aggressive sniffing of any body part of the opponent), grooming (self-grooming movements), offensive behavior (attack bouts, chasing, tail-rattling, aggressive grooming, mounting, punching and kicking), defensive behavior (defensive upright posture, fleeing from the opponent), submission (being unmoving while being sniffed or aggressively groomed by the conspecific, usually crouched low with eyes shut) and vigilance (continuous tense or agitated observation of the intruder from a distance, with the body constantly being directed towards the intruder) [153,186,187].

3.2.3.3. Social interaction test (SI)

Two unfamiliar experimental mice belonging to the same housing group (i.e. social versus social, isolated versus isolated) were placed into a novel Plexiglas test cage the size of 35 x 20 x 25 cm under low light illumination (70 lux). On the day before testing, each animal was separately habituated to the novel cage for 15 minutes. Mice were differentiated by marks painted with permanent hair-dye. On PN72, the pairs were placed into the cage for 10 minutes and their behavior was video-recorded and analyzed by an experimenter blinded to the conditions. We investigated the duration and frequency of exploration (rearing and any exploratory activity that is not directed towards the conspecific), sniffing (non-aggressive sniffing of any body part of the opponent), defensive behaviors (defensive upright posture, fleeing from the opponent), offensive behaviors (attack bouts, chasing, tail-rattling, aggressive grooming, mounting, punching

and kicking), grooming (any self-grooming behavior) and digging activity (digging through the corn cob bedding).

3.2.3.4. Delay discounting test

Our protocol outlined here follows the work of Adriani et al [188] and Aliczki et al. [189]. Automated operant chambers were used for the test, equipped with two nose-poke holes with LED lights and infrared sensors, a feeding device with a magazine where sugar pellets could be held, and a chamber light (Med Associates, St. Albans, VT, USA). The chambers were placed into soundproof wooden cubicles and were controlled by the Med-PC IV software (Med Associates, St. Albans, VT, USA). The chamber lights signalled the start of each trial. Between trials, the chambers were cleaned with 20% ethanol and then dried. Mice were subjected to a restricted feeding protocol four days before the start of the experiment (maintaining 85-95% of their original body weight) to increase their motivation for food rewards.

Training phase: subjects were placed into the chambers for 30 minutes each day during 8 consecutive days. Nose-poke responses given into one of the holes got rewarded with a 45 mg sugar pellet (small reward), while responses given into the other hole were rewarded with three 45 mg pellets (large reward). Both small or large rewards were presented immediately after the response was given, and were followed by a 25 second timeout period during which responses were registered but not rewarded. The side of the nose-poke hole (left or right) associated with the large reward was balanced over subjects. Throughout training, all mice developed a strong preference for the side that was associated with the large reward.

Test phase: following the training, mice were subjected to a protocol that was similar to the training phase, except the delivery of the larger reward was preceded by a delay. The delay of the large reward was progressively increased each day (5, 10, 20, 30, 45, 60, 75, 90 s from day 1 to day 8, respectively). Small rewards were still delivered immediately following the response. Responses made during the delays and timeout periods were recorded but not rewarded. With the increasing delay in delivery, mice gradually shifted their preference from the large reward to the small, but immediate reward.

The number of total responses during training and testing can be used to characterize the motivational state of mice, while inadequate responses (nose pokes made

for the large reward during the delay and timeout periods) are considered to indicate impulsive responses [190].

3.2.3.5. Elevated plus-maze (EPM)

The EPM consisted of two open arms (30 x 7 cm), two closed arms (30 x 7 cm with 30 cm high walls) and a central platform (7 x 7 cm) 50 cm above the ground. The EPM was made of gray Plexiglas. Mice were placed into the central part facing an open arm and were allowed to explore the apparatus for 5 minutes under low light illumination (70 lux). After each test, the EPM was cleaned with water and dried thoroughly. Behavior was video-recorded and subsequently analyzed with the event-recording software Solomon Coder. We measured locomotion via the number of closed arm entries. We also investigated the percentage of time spent in the open arms and the ratio of open arm entries and total arm entries.

3.2.3.6. Sucrose preference test (SPT)

A bottle was filled with 2% sucrose solution and was placed next to the bottle containing drinking water in the homecage of the mice. The two bottles were left there overnight (in the sense of human time and not the reversed dark/light cycle that mice were kept under) and then measured on the following day for four consecutive days. The starting side (left or right) of the sucrose solution bottle was balanced over subjects. The position of the sucrose solution bottle and water bottle was switched daily. Sucrose preference was measured as the percentage of sucrose consumption (g) divided by total consumption (g).

3.2.4. Immunohistochemistry and confocal imaging

3.2.4.1. Fixation and tissue processing

Mice were placed under anesthesia using a mixture of ketamine and xylazine (16.6 and 0.6 mg/ml, respectively). Mice were then transcardially perfused using ice-cold 0.1 M phosphate-buffered saline and 4% paraformaldehyde in 0.1-M phosphate-buffered saline solution (PBS), with a pH of 7.4. Brains were removed and post-fixed for 3 hours. Following that, brains were cryoprotected in 30% sucrose in PBS for 48 hours at 4°C. After sucrose cryoprotection, a freezing sliding microtome was used to cut 30 µm sections. Sections were collected in a six-well plate with cryoprotectant (50% sodium

phosphate buffer, 30% ethylene glycol, 20% glycerol) for storage, and were kept at −20°C.

3.2.4.2. Fluorescent immunohistochemistry, confocal imaging, analysis of perisomatic puncta densities and fluorescent intensities

The PFC-containing sections were incubated for 4 hours at room temperature, in a solution containing 2% Triton X-100 and 10% normal donkey serum (NDS) in 0.1 M PB. Then, sections were incubated at 4°C for four days in a solution containing 2% Triton X-100, 10% NDS, 0.05% sodium azide, and different combinations of the following primary antibodies and reagents: mouse anti-bassoon, rabbit anti-parvalbumin, mouse anti-parvalbumin, guinea pig anti-parvalbumin, guinea pig anti-vesicular GABA transporter (vGAT), guinea pig anti-vesicular glutamate transporter 1 (vGluT1), rabbit anti-vesicular glutamate transporter 2 (vGluT2), mouse anti-potassium voltage-gated channel, Shab-related subfamily, member 1 (Kv2.1) and biotinylated *Wisteria floribunda* agglutinin (WFA) (see **Table 1**). The following secondary antibodies were used to visualize the primary antibodies: DyL405-conjugated streptavidin, Alexa Fluor 488-conjugated donkey anti-guinea pig, Alexa Fluor 488-conjugated donkey anti-rabbit, Cy3-conjugated donkey anti-mouse IgG, Cy3-conjugated donkey anti-guinea pig IgG, Alexa647-conjugated donkey anti-rabbit IgG and Alexa647-conjugated donkey anti-mouse IgG (see **Table 2**).

Confocal images were taken at 12-bit depth with 1024 X 1024 pixel resolution using a Nikon A1R microscope fitted with an oil-immersion apochromatic lens (CFI Plan Apo VC60x Oil, NA 1.40; z step size: 0.5 μm; xy: 0.11 μm/pixel). The density of puncta surrounding the soma of PV neurons and Kv2.1 immunoreactive putative pyramidal neurons was analyzed using a similar methodology. In the mPFC, 40 to 50 putative pyramidal neurons were imaged per mouse in three different sections. 10-15 PV+ neurons were counted in each animal per subregion, since the density of PV+ interneurons was more limited. We used the NIS Elements Software (Nikon Europe; RRID:SCR_014329) for image processing. The outline of every soma (i.e. the cell membrane) was delineated manually, and this manual selection was further enlarged by 0.25 μm to form a "ring" that covers the area surrounding the soma. vGluT1+Bassoon+ and vGluT2+Bassoon+ puncta in close proximity to PV+ or Kv2.1+ somata were considered to establish an apposition (i.e. form putative perisomatic synapses). Bassoon is a presynaptic release site

marker [191], while vGluT1 and vGluT2 indicate excitatory intracortical and extracortical inputs, respectively [192–194], and Kv2.1 immunoreactivity was used to identify pyramidal cells in layer 5 of the mPFC [195].

Using custom scripts in Fiji, labeling intensities of the perisomatic region and PV somata were quantified in arbitrary units as the mean of all selected pixels. Intensities of single neurons were plotted. Previously drawn regions of interest (ROIs) were used to measure mean fluorescent intensity and integrated density in the area ±0.25 μm from the cell border with the use of custom scripts [196].

Table 1. **Overview of primary antibodies or reagents used in this study**

Reagent	**Source**	**Catalog No.**	**Host**	**Dilution**	**RRID**
Bassoon	Abcam	SAP7F407	Mouse	1:1000	AB_1860018
c-Fos	Synaptic Systems	226 004	Guinea pig	1:4000 1:3000 IF	AB_2619946
Parvalbumin	Swant	PV27	Rabbit	1:5000 1:2500	AB_2631173
Parvalbumin	Sigma-Aldrich	P3088	Mouse	1:5000	AB_477329
Parvalbumin	Synaptic Systems	195 004	Guinea pig	1:2000	AB_2156476
vGAT	Synaptic Systems	131 004	Guinea pig	1:1000	AB_88787
vGluT1	Synaptic Systems	135 304	Guinea pig	1:1000	AB_887878
vGluT2	Synaptic Systems	135 402	Rabbit	1:1000	AB_2187539
Voltage-gated potassium channel type 2.1 (Kv2.1)	Neuromab	75-014	Mouse	1:1000	AB_10673392
Wisteria floribunda agglutinin (WFA)	Sigma-Aldrich	L1516	—	1:500	AB_2620171

Table 2. Overview of secondary antibodies used in this study.

Antibody	Source	Catalog No.	Host	Dilution	RRID
Alexa Fluor 488 anti-guinea pig IgG	Jackson ImmunoResearch	706-545-148	Donkey	1:200	AB_2340472
Alexa Fluor 488 anti-mouse IgG	Jackson ImmunoResearch	715-545-151	Donkey	1:500	AB_2341099
Alexa Fluor 488 anti-rabbit IgG	Jackson ImmunoResearch	711-545-152	Donkey	1:500	AB_2313584
Alexa Fluor 488 conjugated streptavidin	Jackson ImmunoResearch	016-540-084		1:500	AB_2337249
Alexa Fluor 647 anti-mouse IgG	Jackson ImmunoResearch	715-605-150	Donkey	1:500	AB_2340862
Alexa Fluor 647 anti-guinea pig IgG	Jackson ImmunoResearch	706-605-148	Donkey	1:500	AB_2340476
Alexa Fluor 647 anti-rabbit IgG	Jackson ImmunoResearch	711-605-152	Donkey	1:200	AB_2492288
Alexa Fluor 647 anti-rabbit IgG	Jackson ImmunoResearch	111-605-003	Goat	1:500	AB_2338072
Biotin conjugated anti-guinea pig IgG	Jackson ImmunoResearch	706-065-148	Donkey	1:1000	AB_2340451
Cy3-conjugated anti-guinea pig IgG	Jackson ImmunoResearch	106-165-003	Goat	1:500	AB_2337423
Cy3-conjugated anti-guinea pig IgG	Jackson ImmunoResearch	706-165-148	Donkey	1:500	AB_2340460
Cy3-conjugated anti-mouse IgG	Jackson ImmunoResearch	715-165-151	Donkey	1:200	AB_2315777
Cy3-conjugated anti-rabbit IgG	Jackson ImmunoResearch	711-165-152	Donkey	1:500	AB_2307443
DyL405 anti-mouse	Jackson ImmunoResearch	115-475-003	Goat	1:500	AB_2338786
DyL405 conjugated streptavidin	Jackson ImmunoResearch	016-470-084		1:500	AB_2337248

3.2.5. Statistical analysis

Data are expressed as mean ± standard error of the mean (SEM). Differences between groups were analyzed in the Prism (GraphPad Prism Software Inc. San Diego, California, USA) or Statistica 13.5 (Tibco, Palo Alto, CA, USA) softwares using Student's t-test, or Mann-Whitney U test when the requirements for t-tests were not fulfilled (i.e. when data did not follow a normal distribution, as verified through the D'Agostino and Pearson normality test). In the case of the delay discounting and sucrose preference tests, repeated measures ANOVA was employed. We used two-way ANOVA for c-Fos activation and PNN-dependent analysis of puncta densities, followed by Fisher's post hoc analyses. During the statistical analysis of individual cell numbers as a function of group, we implemented both the factor "housing" and "animal identity" in an additive fashion to a two-way ANOVA model. This way, the explanatory effects of the social environment and individual variability of animals could be independently determined. When performing the latter analyses, we used the R Statistical Environment (R Core Team, 2022). The significance level was set at $p < 0.05$ throughout.

4. Results

4.1. Fluoxetine and social learning in adulthood in PWSI rats

4.1.1. PWSI induces abnormal aggression in the resident-intruder test

In order to study the effects of PWSI on aggressive behavior, a resident-intruder test was performed after the 8-week isolational period (**RI Test 1**) (see **Fig. 3.** for timeline). Similarly to earlier studies from our research group, PWSI induced abnormal aggression compared to rats reared in social groups: PWSI rats displayed a higher number of biting attacks ($F(1,121) = 25.21$, $p < 0.0001$) and a greater portion of these attacks were aimed at vulnerable body parts of the opponent (i.e. the head, throat or belly; $F(1,121) = 12.19$, $p < 0.001$; **Fig. 6A**, left side). Additionally, the number of bites delivered shifted from less damaging attack types in social rats to the more damaging hard bites in PWSI rats (rearing x bite type interaction, $F(2,242) = 4.23$, $p < 0.05$, **Fig. 6A**, right side).

4.1.2. PWSI rats are capable of social learning

Huddling during sleep was measured as an indicator of social cohesion during the 3-week treatment period. On the first day, PWSI rats displayed low levels of huddling, but the differences between the huddling behavior of social and PWSI animals gradually disappeared over 1 week (day x rearing interaction, $F(20, 580) = 6.88$; $p < 0.0001$; fluoxetine did not show any effects alone or in interaction; data not shown). Beginning with the second week of treatment, huddling no longer differentiated the 4 groups (i.e. RegVEH, RegFLX, ResVEH and ResFLX).

4.1.3. Social learning diminishes PWSI-induced abnormal aggression only when combined with fluoxetine

To investigate the impact of treatments on aggressive behavior, rats reared in PWSI underwent a second RI-test (**RI Test 2**) after the 3-week treatment period, on PN98 (see **Fig. 3.** for timeline). The treatments altered aggressive behavior when compared to RI Test 1 (bite counts: $F(4,90) = 4.26$, $p < 0.01$; vulnerable bites: $F(4,90) = 3.13$, $p < 0.02$), but each treatment showed prominent differences in their efficacy (**Fig. 6B**). While resocialization alone decreased the number of biting attacks compared to RI Test 1 (repeated-measures ANOVA, test x resocialization interaction: $F(1,48) = 9.18$, $p < 0.01$), the percentage of vulnerable bites delivered was decreased only in the group that received

the combined treatment (fluoxetine x resocialization interaction: $F(1,48) = 7.98$, $p < 0.01$). Chronic administration of fluoxetine in itself did not affect any form of aggressive behavior studied here. Importantly, the combined treatment ameliorated all three measures of excessive and abnormal aggression: bite counts (4.2 ± 0.7) and the percentage of bites aimed at vulnerable targets ($14.1 \pm 5.5\%$) decreased to reflect the levels seen in socially-reared rats (shown on **Fig. 6B** left side, $p > 0.05$ for both parameters, two-tailed unpaired t-test), while attack types shifted to less damaging ones, i.e. skin pulls became more dominant than hard bites **(Fig. 6B** right side).

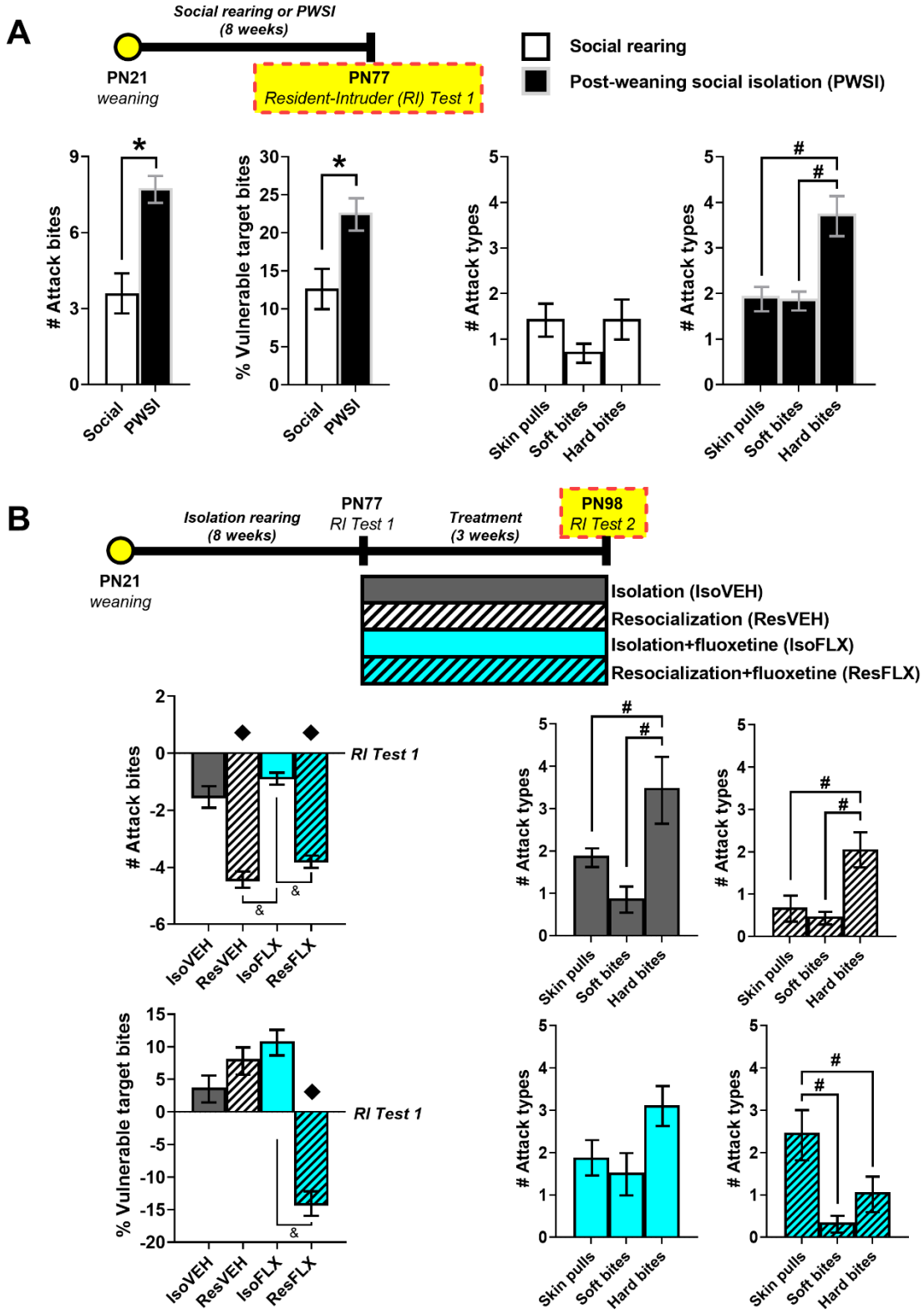

Figure 6. Behavioral effects of PWSI, resocialization and chronic fluoxetine treatment.

A, *Experimental timeline and aggressive behavior recorded during the first resident-*

intruder test. Following weaning on PN21, rats were subjected to social rearing or PWSI for 8 weeks. After reaching adulthood, rats underwent a resident-intruder test (RI Test 1) on PN77. During RI Test 1, PWSI rats delivered more biting attacks and a larger percentage of these attacks were aimed at the vulnerable body parts of the opponent (head, throat or belly) compared to socially-reared rats. When differentiating between attack types, PWSI rats showed a preference for the more damaging hard bites over soft bites or skin pulls. ***B,*** *Following 3 weeks of treatment in adulthood, PWSI rats were subjected to a second resident-intruder test, RI Test 2 on PN98. While resocialization alone was able to decrease the number of attack bites when compared to RI Test 1, only the combination of resocialization and chronic fluoxetine treatment was able to decrease both quantitative and qualitative aspects of aggression, i.e. the number of attacks, and the share of attacks aimed at vulnerable targets. The combined treatment also shifted the preference for hard bites towards the less damaging skin pulls. Data are presented as mean ± SEM. *p < 0.05, #p < 0.05, ♦p < 0.05, &p < 0.05. IsoFLX, isolation+fluoxetine; IsoVEH, isolation+vehicle; PN, postnatal day; PWSI, post-weaning social isolation; ResFLX, resocialization+fluoxetine; ResVEH, resocialization+vehicle; RI, resident-intruder test.*

The effects of chronic fluoxetine treatment in adulthood in socially-reared rats were studied separately from PWSI rats because the social learning component of resocialization was absent during the regrouping of socially-reared rats. In socially-reared rats that were regrouped for 3 weeks to mimic the resocialization of PWSI rats, chronic fluoxetine treatment decreased the number of attack bites ($F(1,23) = 4.03$, $p < 0.05$), but did not affect the percentage of vulnerable attacks ($F(1,23) = 1.26$, $p > 0.05$, **Fig. 7**). When compared to RI Test 1, neither treatment (regrouping alone or regrouping+fluoxetine) affected behavior in RI Test 2 (number of attack bites: $F(2,62) = 0.91$, $p > 0.05$); percentage of vulnerable target bites: $F(2,62) = 0.64$, $p > 0.5$, **Fig. 7**).

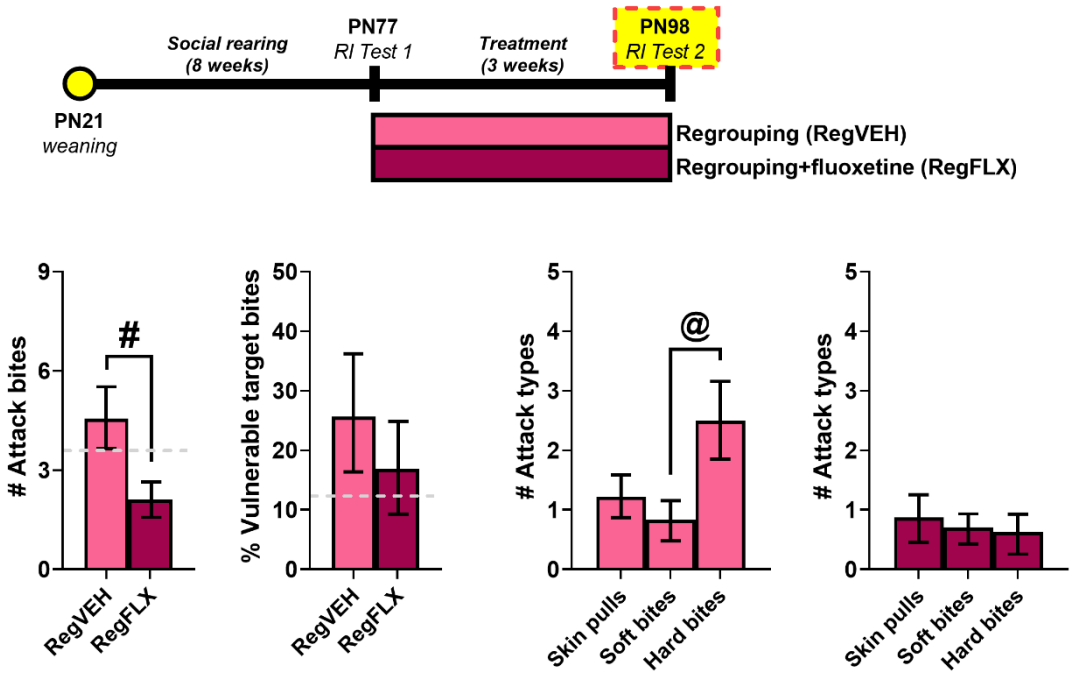

Figure 7. The effect of chronic fluoxetine treatment on aggression in rats reared in social groups. *Rats subjected to social rearing underwent 3 weeks of treatment in adulthood (PN77). Social rats were then regrouped into groups of 4 where at least 2 rats were unfamiliar with each other. Half of regrouped rats received chronic fluoxetine treatment (RegFLX). Regrouping alone or in combination with fluoxetine did not change aggressive behavior in the RI Test 2 when compared to the RI Test 1. There were no differences in the share of vulnerable target bites. Rats submitted to regrouping+fluoxetine delivered significantly less attacks compared to rats submitted to regrouping alone and showed a reduction in the dominance of hard bites over soft bites. Grey horizontal dashed lines indicate the mean observed in RI Test 1. #p < 0.05; @p < 0.05 (Fisher post hoc test). PN, postnatal day; PWSI, post-weaning social isolation; RegFLX, regrouping+fluoxetine; RegVEH, regrouping+vehicle; RI, resident-intruder test.*

4.2. Behavioral characterization of PWSI in mice and the effects of PWSI on prefrontal PV+ neurons and PNNs

4.2.1. PWSI induces abnormal aggression, disrupted behavioral organization and behavioral fragmentation

In the second set of experiments, we sought to characterize the long-term behavioral changes induced by PWSI in mice via subjecting them to post-weaning social isolation for 6 weeks followed by a behavioral test battery designed to investigate social and emotional domains (refer to **Fig. 5** for detailed timeline).

PWSI mice displayed heightened aggression compared to socially-reared mice as shown in the second RI test (see **Fig. 8A** for simplified timeline). Particularly, PWSI mice showed a decreased latency of attack ($U = 28$, $p = 0.005$; **Fig. 8B**) and delivered more biting attacks overall ($U = 25.5$, $p = 0.001$; **Fig. 8B**). Detailed analysis of aggressive interactions also revealed that PWSI mice directed more attacks toward the vulnerable body parts of the opponents, i.e. the head, throat or belly ($U = 24.5$, $p = 0.002$; **Fig. 8B**). Moreover, PWSI mice delivered more violent hard bites compared to social mice ($U = 27$, $p = 0.003$; **Fig. 8B**).

PWSI mice exhibited higher frequencies of offensive ($U = 12$, $p < 0.001$; **Fig. 8C**) and defensive ($U = 36.5$, $p = 0.010$; **Fig. 8C**) behavior and displayed less submissive behavior ($U = 20$, $p < 0.001$; **Fig. 8C**) compared to the social group. Interestingly, we also observed that PWSI mice often engaged in vigilance-like behavior (i.e. agitated observation of the intruder from a distance, with the body constantly being directed toward the intruder) [186,187] compared to social mice ($U = 6$, $p < 0.001$; **Fig. 8C**). A reduction in non-aggressive social sniffing revealed that PWSI mice spent less time with social investigation ($U = 22$, $p = 0.001$; **Fig. 8D**). In turn, there was an increase in grooming behavior ($U = 35.5$, $p = 0.011$; **Fig. 8D**) compared to social mice. Importantly, the observed changes in offensive and sniffing behaviors considerably increased the ratio of offense/sniffing events in PWSI mice ($U = 16$, $p < 0.001$; **Fig. 8E**). PWSI also induced a fragmented behavioral phenotype, shown by the increased number of behavioral transitions (i.e. PWSI mice displayed rapid shifting between behavioral elements) ($U = 16$, $p < 0.001$; **Fig. 8F**).

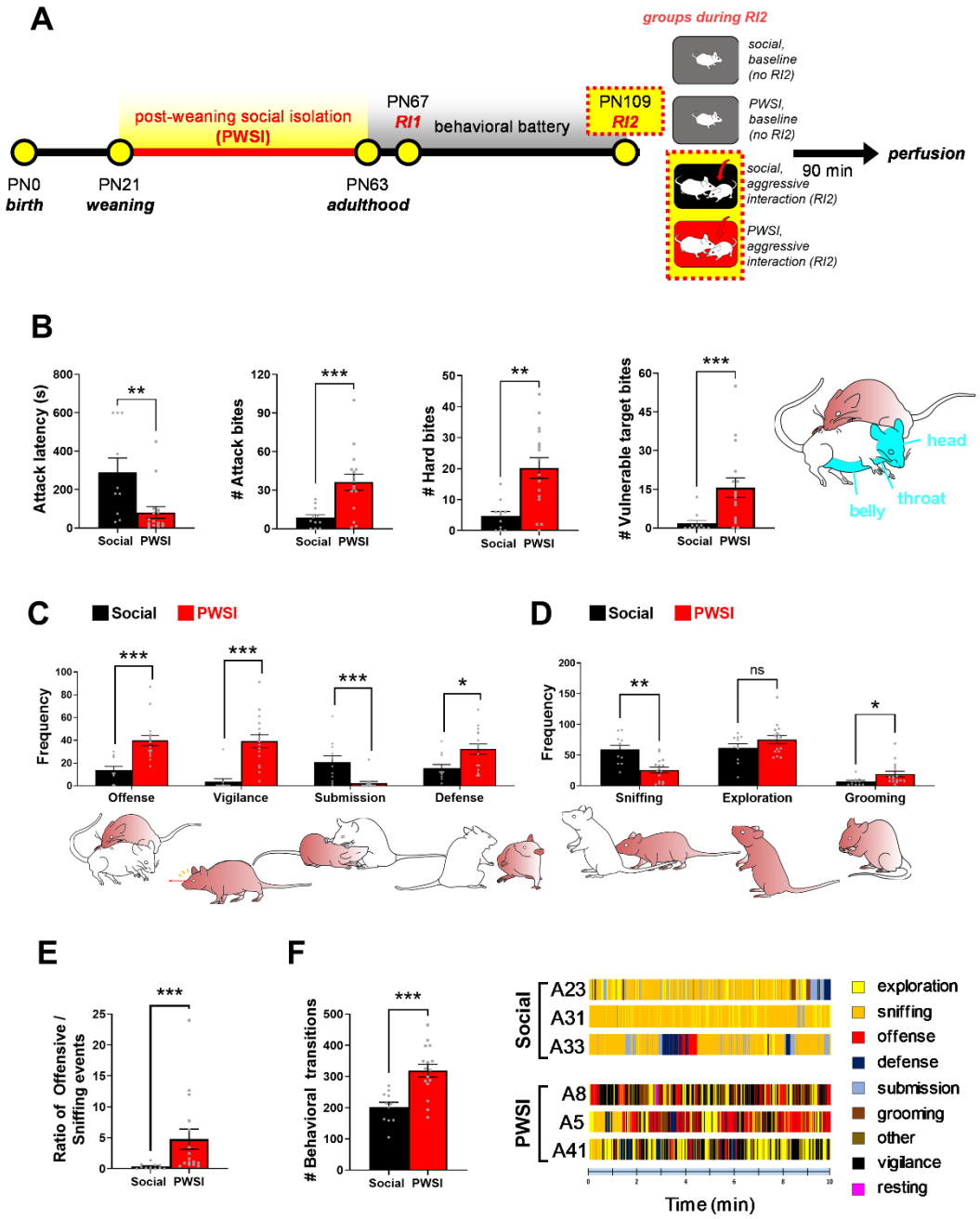

Figure 8. Post-weaning social isolation (PWSI) induced abnormal aggression in conjunction with disrupted behavioral organization and behavioral fragmentation. A, *Simplified experimental timeline. Following weaning on PN21, mice were housed in groups of 4 (social) or were housed alone (PWSI) for 6 weeks, until adulthood (PN63). Mice were then subjected to a behavioral battery that lasted until PN109. Results shown in* ***B-F*** *are from the second resident-intruder test (RI2) conducted on PN109, highlighted here with red-bordered yellow.* ***B,*** *PWSI decreased attack latency, increased number of*

attack bites and also increased the number of hard bites compared to socially-reared mice. ***B,*** *Far right: schematic drawing displaying the vulnerable body parts in blue (head, throat, belly). PWSI mice targeted these vulnerable areas more often when attacking.* ***C,*** *Frequency of agonistic behaviors recorded during the RI test. PWSI led to increased frequency of offense, vigilance, defense and reduced submission.* ***D,*** *Frequency of non-agonistic behaviors observed during the RI test. PWSI reduced sniffing and increased grooming frequency.* ***E,*** *PWSI mice showed an increased ratio of offensive/sniffing events in the RI test.* ***F,*** *PWSI induced behavioral fragmentation as shown by the number of behavioral transitions in the RI test (left). Representative temporal raster plots comparing the behavioral organization of three social (top panels) and three PWSI (bottom panels) mice during the RI test (right). All data are represented as mean ± SEM. *p < 0.05, **p < 0.01, ***p < 0.001. A, animal; PN, postnatal day; PWSI, post-weaning social isolation; RI, resident-intruder test.*

In order to verify the PWSI-induced aggressive phenotype previously reported in our studies of PWSI rats [168,169] and to see whether PWSI-induced aggression remained present after the behavioral battery, we subjected mice to an RI test after the end of the post-weaning social isolation period and to another RI test following the behavioral battery, before perfusion. Abnormal aggressive behavior was already present during the first RI, conducted on PN67 (see **Fig. 8A** for simplified timeline) (significant differences between PWSI and social mice in total attack bites during first RI, $U = 95$, $p = 0.0152$; percentage of vulnerable target bites, $U = 70$, $p = 0.0008$; **Fig. 9.**) and PWSI-induced abnormal aggression was persistent over time, with the number of attack bites ($U = 25.5$, $p = 0.001$; **Fig. 9.**) and share of vulnerable target bites ($U = 33$, $p = 0.0048$; **Fig. 9.**) remaining significantly elevated compared to social controls even following the behavioral battery.

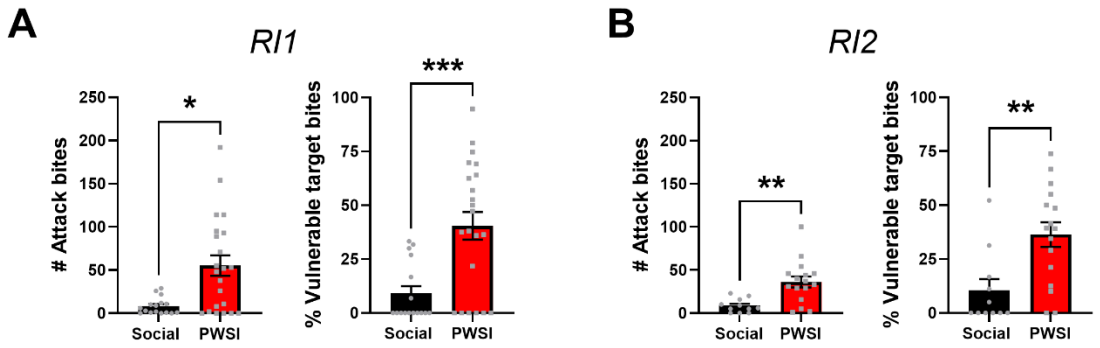

Figure 9. PWSI-induced abnormal aggression remained persistent over time. A, *PWSI-induced abnormal aggression was already present in the first RI test (RI1) at PN67, right after the isolation period, as indicated by the increased number of attack bites and larger share of bites aimed at vulnerable targets (head, throat or belly).* ***B,*** *Abnormal aggression remained persistent over time, indicated by the increased number of attack bites and larger share of bites aimed at vulnerable targets in the second RI (RI2) test at the end of the behavioral battery (PN109). All data are represented as mean ± SEM. *p < 0.05, **p < 0.01, ***p < 0.001. PWSI, post-weaning social isolation; RI, resident-intruder test.*

Additionally, since emotionally driven reactive aggression is often characterized by excessive aggressive outbursts to a perceived provocation [197], we predicted that PWSI could amplify social instigation-evoked escalated aggression [185] (**Fig. 10.**). Consistent with our hypothesis, PWSI mice subjected to social instigation showed a robust elevation in the frequency of total attack bites ($U = 67.5$, $p < 0.001$; **Fig. 10**), hard bites ($U = 93.5$, $p = 0.007$; **Fig. 10.**) and bites aimed at vulnerable body parts ($U = 54$, $p < 0.001$; **Fig. 10.**) compared to social controls.

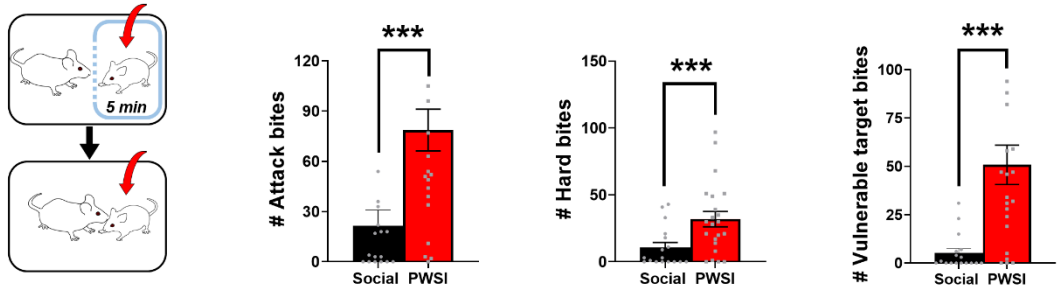

Figure 10. PWSI augmented escalation-evoked aggression. *Left: schematic presentation of the escalation procedure at PN70. Escalation increased the number of*

*attack bites, hard bites and bites aimed at vulnerable targets in PWSI mice. All data are represented as mean ± SEM. ***p < 0.001. PWSI, post-weaning social isolation.*

4.2.2. PWSI-induced disturbances are limited to social and reward-related domains and do not affect non-social anxiety

Since PWSI-induced disturbances heavily affected the social behavioral domain, we wondered if reciprocal social interactions could also be affected in a context that is less aggression-promoting. As such, to investigate how PWSI affects social behavior in neutral territory (i.e. unfamiliar for subjects) when engaging with a same-sized, unfamiliar adult conspecific, we performed a social interaction test (SI, **Fig. 11.**). PWSI mice displayed reduced sniffing frequency (U = 91, p = 0.005; **Fig. 11.**), a trend toward increased defensive behavior (U = 127, p = 0.078; **Fig. 11.**), and an increase in the ratio of aggressive/social behavior compared to socially-reared mice (U = 87, p = 0.003; **Fig. 11.**). Non-social parameters remained unaffected by PWSI, as PWSI mice showed a similar frequency of exploration (U = 171, p = 0.833; **Fig. 11.**), grooming (U = 162.5, p = 0.642; **Fig. 11.**), and digging (U = 147.5, p = 0.354; **Fig. 11.**) in comparison to the social group.

Collectively, our data provide strong evidence that PWSI in mice leads to marked social deficits, including increased and abnormal forms of aggression.

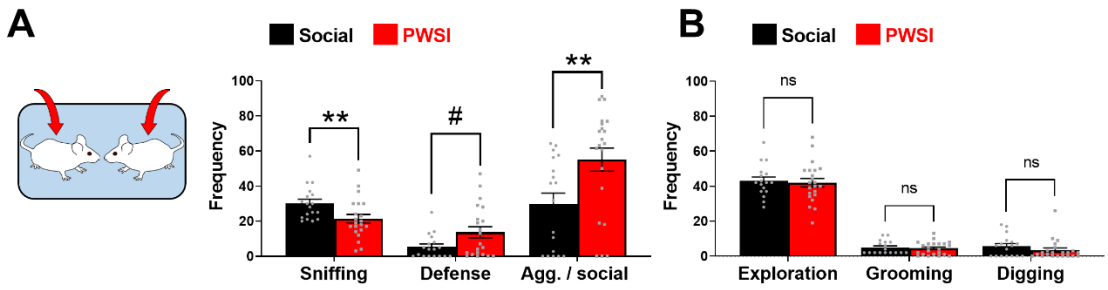

Figure 11. PWSI-induced social deficits in the social interaction test. A, *Schematic depiction of the social interaction test at PN72 (left). Frequency of social behaviors observed during the social interaction test. PWSI reduced frequency of sniffing and marginally increased frequency of defensive behaviors.* ***B,*** *Frequency of non-social behaviors was unaltered in PWSI mice during the social interaction test. J, PWSI mice showed an increase in the percentage of offensive/social events compared to social mice*

*in the social interaction test. All data are represented as mean ± SEM. #p= 0.078, **p < 0.01. Agg, aggression.*

Anxiety-like behavior was investigated via the open-field test (OF, **Fig. 12A**) and the elevated plus-maze (EPM, **Fig. 12B**). PWSI did not affect anxiety-like behavior in the OF, since both social and PWSI mice showed similar locomotor activity (U = 161.5, p = 0.477; **Fig. 12A**), time spent in the center (U = 184, p = 0.901; **Fig. 12A**), and latency to enter the center (U = 187, p = 0.967; **Fig. 12A**). Similarly, PWSI did not affect locomotion or anxiety parameters in the EPM test such as the frequency of entries into closed arms (U=185.5, p=0.927; **Fig. 12B**), the time spent in open arms (U = 173, p = 0.666; **Fig. 12B**), and the ratio of open arm entries/total entries (U = 166.5, p = 0.535; **Fig. 12B**), suggesting that the anxiety-like domain was not affected by PWSI.

Early-life adversities have consistently been linked to altered motivational state and impulsivity in adulthood [198,199]. To investigate such implications, PWSI mice were tested in the delay discounting paradigm using operant chambers (**Fig. 12C**). During training, large reward preference showed a gradual increase in both PWSI and social groups (no group differences, data not shown). With the introduction of delay in large reward delivery, the preference for the small reward increased in both groups ($F(7, 259) = 39.845$, $p < 0.001$, **Fig. 12C**), but PWSI did not induce changes in large reward preference compared to social mice ($F(1, 37) = 1.829$, $p = 0.184$; **Fig. 12C**). However, we observed a slight but significant decrease in the number of total responses given ($F(1, 37) = 5.286$, $p = 0.027$; **Fig. 12C**) suggesting a lowered motivational state in PWSI mice.

To further study motivational and reward-related changes of PWSI, mice were subjected to the SPT (**Fig. 12D**). While PWSI did not affect water consumption ($F(1, 36) = 0.520$, $p = 0.476$; data not shown) or sucrose preference ($F(1, 36) = 1.777$, $p = 0.191$; **Fig. 12D**), PWSI led to a slight but significant decrease in sucrose consumption ($F(1, 36) = 4.157$, $p = 0.049$; **Fig. 12D**). This, coupled with the decreased number of total responses in the delay discounting test might indicate a lowered reward value for sucrose in PWSI mice.

Overall, the above results demonstrate that PWSI selectively induces marked social deficits over multiple paradigms, with a slight indication of additional motivational or reward-related disturbances.

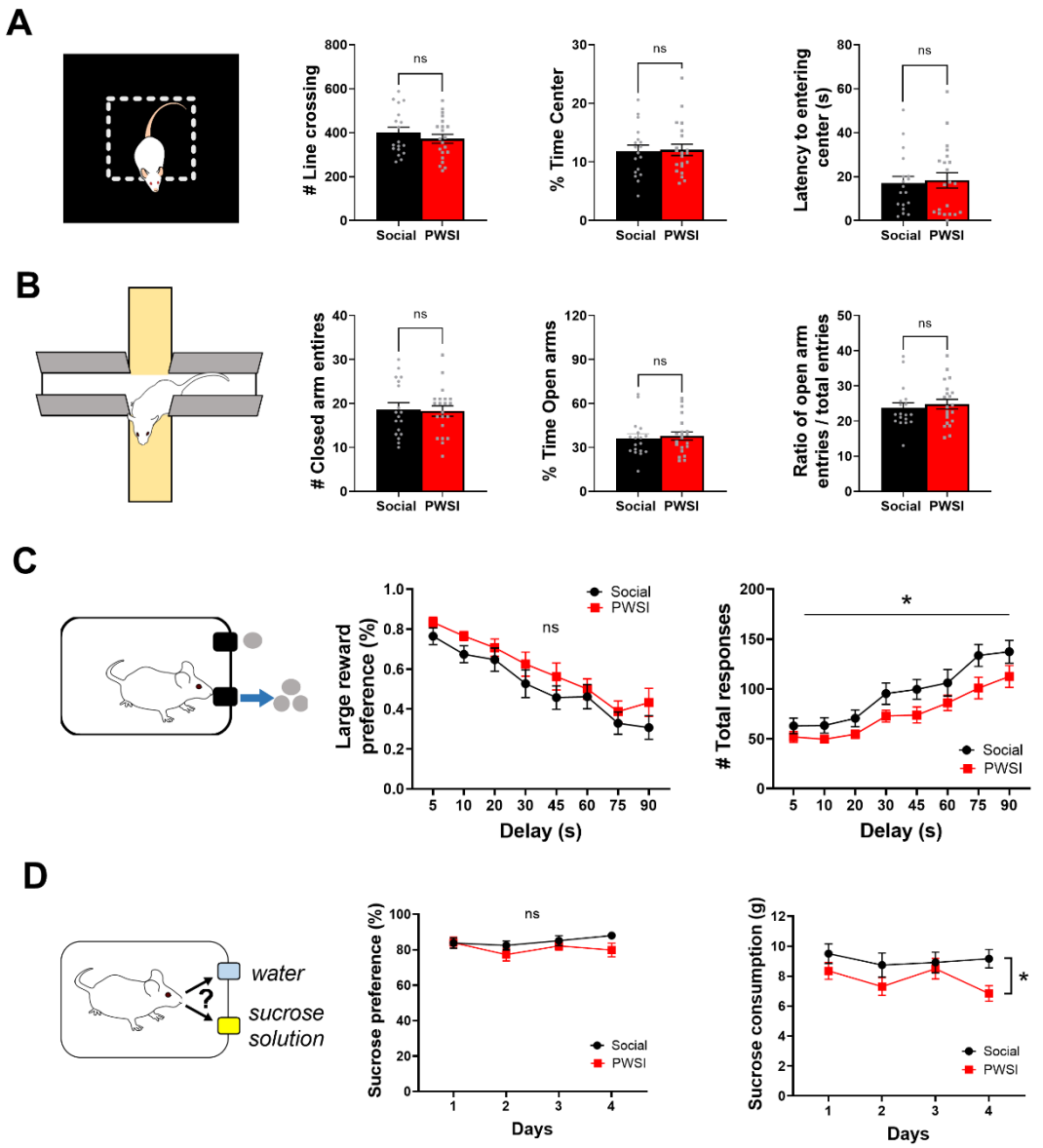

Figure 12. PWSI mice did not display non-social anxiety but showed reduced motivation and sucrose consumption. A, *Schematic drawing of the open-field (OF) test used for measuring locomotor activity and anxiety-like behavior. PWSI did not affect locomotion, time spent in the center, or latency of entering the center in the OF test.* ***B,*** *Schematic drawing of the elevated plus-maze (EPM) test used for measuring anxiety-like behavior. PWSI did not alter the frequency of entry into the closed arms, the duration of time spent in the open arms, and the ratio of open arm entries/total entries in the EPM test.* ***C,*** *Schematic drawing of the delay discounting paradigm used for measuring impulsivity and motivational states. The dynamic of large reward preference remained*

unchanged by PWSI following the initiation of the delay period. PWSI led to a reduced number of total nose poke responses following the initiation of the delay period. ***D,*** *Schematic drawing of the sucrose preference test. PWSI did not alter sucrose preference. PWSI mice showed decreased sucrose consumption. All data are represented as mean ± SEM. *p < 0.05.*

4.2.3. PWSI increased PV+ soma intensity and PNN intensity in the mPFC

Our previous studies of PWSI in rats and current study in mice (data not included in the the present thesis) highlight that PWSI induces neuronal hyperactivation in response to aggressive interaction within selective subregions of both main areas of the PFC: the mPFC and the OFC [153,170,180]. The OFC and mPFC are both heavily involved in emotion-regulation and behavioral flexibility, but subserve distinct roles within these processes [45]. In our scientific paper of which this experiment forms a part of, we have demonstrated that while both regions show marked neuronal activation (as revealed by c-Fos expression) in response to aggressive interaction (RI), in PWSI mice aggression-induced hyperactivation of the PFC was specific to the mPFC when compared to social controls [153]. This suggests that PWSI might impact the OFC and mPFC in distinct ways, warranting the investigation and comparison of both areas in PWSI-related neurobiological changes.

In the PFC, PV+ neurons play an essential role in the maintenance of synaptic excitatory/inhibitory balance during social behavior [144,200] and their function is disrupted by early-life adversity [144,201]. Additionally, exposure to adverse experiences has also been linked to aberrant PV soma and PNN intensities in the PFC [202,203].

Therefore, using high resolution confocal microscopy, we investigated how PWSI affects PV soma and PNN intensities of PV+ neurons and PV+PNN+ neurons, respectively, in the mPFC and OFC (**Fig. 13A**). Our results display that OFC and mPFC PV+ neurons in PWSI mice had significantly greater PV soma intensity (OFC, $U = 3992$, $p = 0.028$; mPFC, $U = 8612$, $p < 0.001$, **Fig. 13B**) compared to social mice. Intriguingly, PV+ neurons that are enwrapped by PNNs also showed greater PNN intensity in PWSI mice ($U = 1663$, $p < 0.001$, **Fig. 13C**). This change was specific to the mPFC, as no significant differences in the intensity of PNN was observed between groups in the OFC ($U = 1788$, $p = 0.078$, **Fig. 13C**).

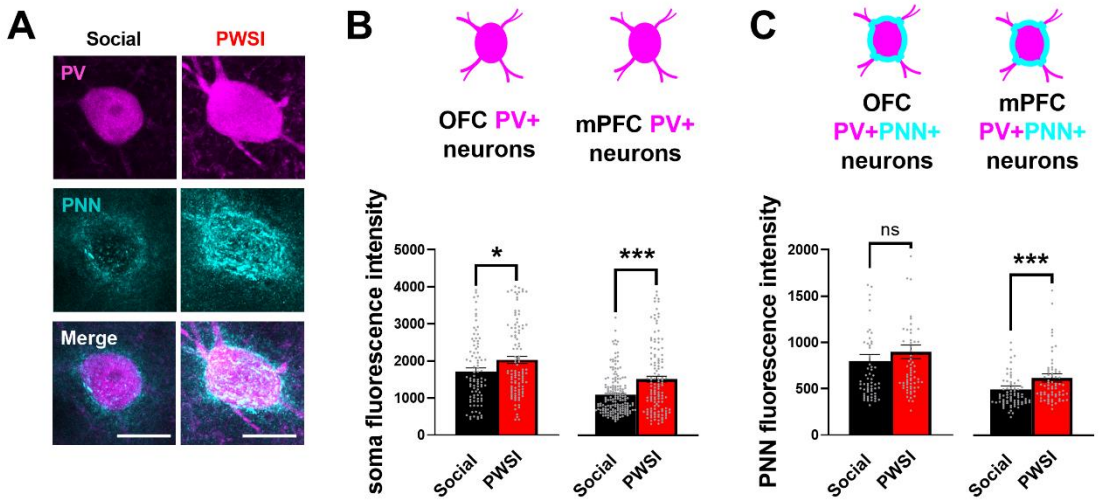

Figure 13. PWSI increased PV and PNN intensity in the mPFC. A, *Representative high resolution confocal images of PV+PNN+ neurons in the mPFC showing PWSI-induced higher PV and PNN intensity compared to social mice. Scale bar, 20 µm.* ***B,*** *Graphs showing PV intensity of PV neuron somas (OFC, n = 92 neurons from 4 social mice and n = 106 neurons from 4 PWSI mice; mPFC, n = 176 neurons from 4 social mice and n = 127 neurons from 4 PWSI mice).* ***C,*** *Graphs showing PNN intensity of PV+PNN+ neurons (OFC, n = 63 neurons from 4 social mice and n = 68 neurons from 4 PWSI mice; mPFC, n = 75 neurons from 4 social mice and n = 70 neurons from 4 PWSI mice). All data are represented as mean ± SEM. *p < 0.05, **p < 0.01, ***p < 0.001. mPFC, medial prefrontal cortex; OFC, orbitofrontal cortex; PNN, perineuronal net; PV, parvalbumin.*

4.2.4. PWSI increased the density of excitatory cortical (vGluT1+) and subcortical (vGluT2+) boutons surrounding the perisomatic region of PV+ neurons in the mPFC

Early-life adversity has been shown to affect the density of inhibitory synapses [204], therefore we tested whether PWSI affected the density of vesicular GABA transporter (vGAT+) immunoreactive inputs targeting the perisomatic region of PV+ neurons. PWSI did not affect the density of inhibitory inputs (OFC, $t(90) = 0.693$, $p = 0.490$; mPFC, $t(323) = 0.16$, $p = 0.873$ **Fig. 14A-D**).

Excitatory synaptic input can regulate the deposition of PNNs around PV+ interneurons [112,205]. Since we found that, as revealed by c-Fos staining, PWSI leads to an increase in the recruitment of PV+ neurons following aggressive interaction in the mPFC but not OFC (data not included in the thesis, refer to [153]), and that PNN

fluorescence intensity also increased around PV+ neurons in the mPFC (**Fig. 13C**), we asked whether PWSI affected the excitatory synaptic drive arriving onto the perisomatic region of PV+ neurons. Therefore, we investigated the excitatory glutamatergic inputs targeting the somata of cortical PV+ interneurons: intracortical (**Fig. 14E-H**) and subcortical inputs (**Fig. 14I-L**) which use presynaptic vesicular glutamate transporter 1 (vGluT1) and 2 (vGluT2), respectively [192–194]. By applying multiple labeling immunostaining and confocal microscopy, we assessed the density of vGluT1 immunoreactive (vGluT1+) and vGluT2 immunoreactive (vGluT2+) synaptic puncta apposing the somata of PV+ neurons in combination with the presynaptic release site marker Bassoon+ (**Fig. 14F** and **Fig. 14J**). There was a significant increase in the density of both cortical and subcortical inputs targeting the somata of PV+ neurons in the mPFC of PWSI mice compared to social mice (vGluT1+Basson+ puncta, $U = 5945$, $p < 0.002$, **Fig. 14H**; vGluT2+Basson+ puncta, $U = 6455$, $p<0.001$; **Fig. 14L**). The observed increase in the excitatory drive was specific for the mPFC since no such changes were detectable at the level of the OFC (vGluT1+Basson+ puncta, $U = 6450$, $p = 0.273$, **Fig. 14G**; vGluT2+Basson+ puncta, $U = 4445$, $p = 0.273$, **Fig. 14K**).

Based on our data, one might suggest that aggressive interaction-associated recruitment of PV+ neurons in PWSI mice could have been due to an enhanced excitatory drive arising from both cortical and subcortical sources.

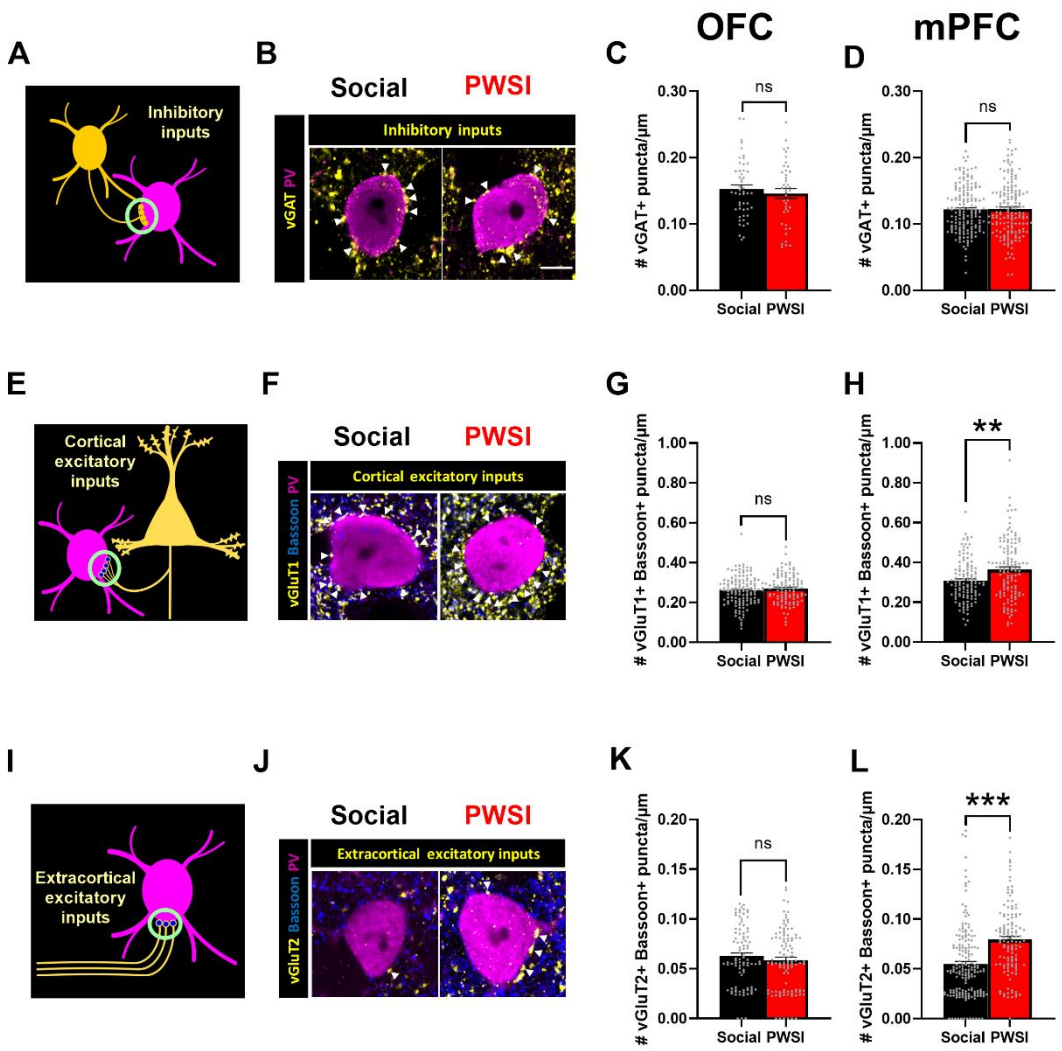

Figure 14. PWSI increased the density of excitatory cortical (vGluT1+) and subcortical (vGluT2+) inputs targeting the perisomatic region of PV+ neurons in the mPFC. A, *Schematic presentation of a local inhibitory neuron (yellow) targeting the perisomatic region of a PV+ neuron (magenta). Yellow circles depict the vesicular GABA transporter (vGAT+) immunoreactive synapses analyzed in this experiment.* ***B,*** *Representative single plane confocal images showing close appositions of vGAT+ puncta (white arrowheads) surrounding a PV+ neuron (magenta) from the mPFC of social and PWSI mice. Scale bar, 5 µm.* ***C-D****, The density of inhibitory inputs targeting the perisomatic region of PV+ neurons was unaffected by PWSI. Bar graphs showing the density of vGAT+ puncta surrounding the perisomatic region of PV+ neurons from the OFC (****C****) and mPFC (****D****), respectively (OFC, n = 50 neurons from 4 social mice and n = 42 neurons from 4 PWSI mice; mPFC, n = 163 neurons from 4 social mice and n = 162 neurons from 4 PWSI*

*mice). **E-L,** The density of excitatory inputs targeting the perisomatic region of PV+ neurons was increased by PWSI in the mPFC. **E,** Schematic drawing depicting a local putative pyramidal neuron (yellow) targeting the perisomatic region of a PV+ neuron (magenta). Yellow circles stand for vesicular glutamate transporter type 1 (vGluT1+) immunoreactive synapses, and the blue dots in the center of these circles indicate the Bassoon immunoreactive presynaptic active zones analyzed in this experiment. **F,** Representative single plane confocal images depicting close appositions of vGluT1+Bassoon+ puncta (white arrowheads) surrounding a PV+ neuron from the mPFC of social and PWSI mice. Same magnification as in **B**. Bar graphs showing the density of vGluT1+Bassoon+ puncta impinging on the perisomatic region of PV+ neurons from the OFC (**G**) and mPFC (**H**), respectively (OFC, n = 129 neurons from 4 social mice and n = 109 neurons from 4 PWSI mice; mPFC, n = 121 neurons from 4 social mice and n = 128 neurons from 4 PWSI mice). **I,** Schematic drawing displaying extracortical excitatory inputs (yellow) targeting the perisomatic region of a PV+ neuron (magenta). Yellow circles indicate vesicular glutamate transporter type 2 (vGluT2+) immunoreactive synapses with the blue dots in the center of these signaling Bassoon immunoreactive presynaptic active zones analyzed in this experiment. **J,** Representative single plane confocal images showing close appositions of vGluT2+Bassoon+ puncta (white arrowheads) surrounding a PV+ neuron from the mPFC of SOC and PWSI mice. Similar magnification as in **B**. Bar graphs showing the density of vGluT2+Bassoon+ puncta targeting the perisomatic region of PV+ neurons from the OFC (**K**) and mPFC (**L**), respectively (OFC, n = 92 neurons from 4 social mice and n = 106 neurons from 4 PWSI mice; mPFC, n = 176 neurons from 4 social mice and n = 127 neurons from 4 PWSI mice). All data are represented as mean ± SEM. ***p < 0.0001. mPFC, medial prefrontal cortex; OFC, orbitofrontal cortex; vGAT, vesicular GABA transporter; vGluT1, vesicular glutamate transporter type 1; vGluT2, vesicular glutamate transporter type 2.*

4.2.5. PWSI increased the density of excitatory inputs targeting PV+ neurons in the mPFC, irrespective of the presence of PNN

In the following, we asked whether the observed PWSI-evoked synaptic imbalances in mPFC PV+ neurons are PNN-dependent. In line with previous observations

[206], PV+PNN+ neurons received more vGAT+ inputs compared to PV+PNN- neurons ($F(1, 310) = 11.46$, $p < 0.001$, **Fig. 15A and 15D**). Accordingly, we also observed increased perisomatic vGAT fluorescence intensity around PV+PNN+ neurons ($F(1, 311) = 10.62$, $p = 0.001$), however, PWSI had no effect on the density of inhibitory inputs ($F(1, 310) = 0.054$, $p = 0.823$, **Fig. 15A and 15D**). In addition, we observed that the PNN intensities of PV+ neurons showed a positive correlation with perisomatic vGAT+ puncta intensities ($r = 0.768$, $p< 0.001$, data not shown).

In the case of cortical excitatory inputs, our results display that PV+PNN+ neurons received higher densities of vGluT1+ Bassoon+ inputs compared to PV+PNN- neurons ($F(1, 240) = 8.884$, $p = 0.003$, **Fig. 15B and 15E**). PWSI resulted in higher densities of vGluT1+ Bassoon+ inputs targeting mPFC PV+ neurons ($F(1, 240) = 12.14$, $p < 0.0001$, **Fig. 15B and 15E**), which did not depend on PNN coverage and housing interaction, ($F(1, 240) = 1.143$, $p = 0.286$). No differences were seen in the intensity of vGluT1+ staining (all p values > 0.05, data not shown). Additionally, PNN intensities of PV+ neurons positively correlated with perisomatic vGluT1+ puncta intensities ($r = 0.6182$, $p < 0.0001$, data not shown).

In the case of subcortical excitatory inputs, we detected increased vGluT2+ Bassoon+ puncta densities in the perisomatic regions of PV+PNN+ neurons compared to the PV+PNN- population ($F(1, 299) = 12.36$, $p < 0.001$, **Fig. 15C and 15F**). As with cortical excitatory inputs, the significant increase seen in the densities of vGluT2+Bassoon+ inputs of PWSI mice relative to social mice ($F(1, 299) = 29.94$, $p < 0.001$, **Fig. 15C and 15F**) did not depend on PNN coverage (PNN and housing interaction, $F(1, 299) = 0.005$, $p = 0.941$). In addition, PNN intensities of PV+ neurons positively correlated with perisomatic vGluT2+ puncta intensities ($r = 0.2425$, $p < 0.003$, data not shown).

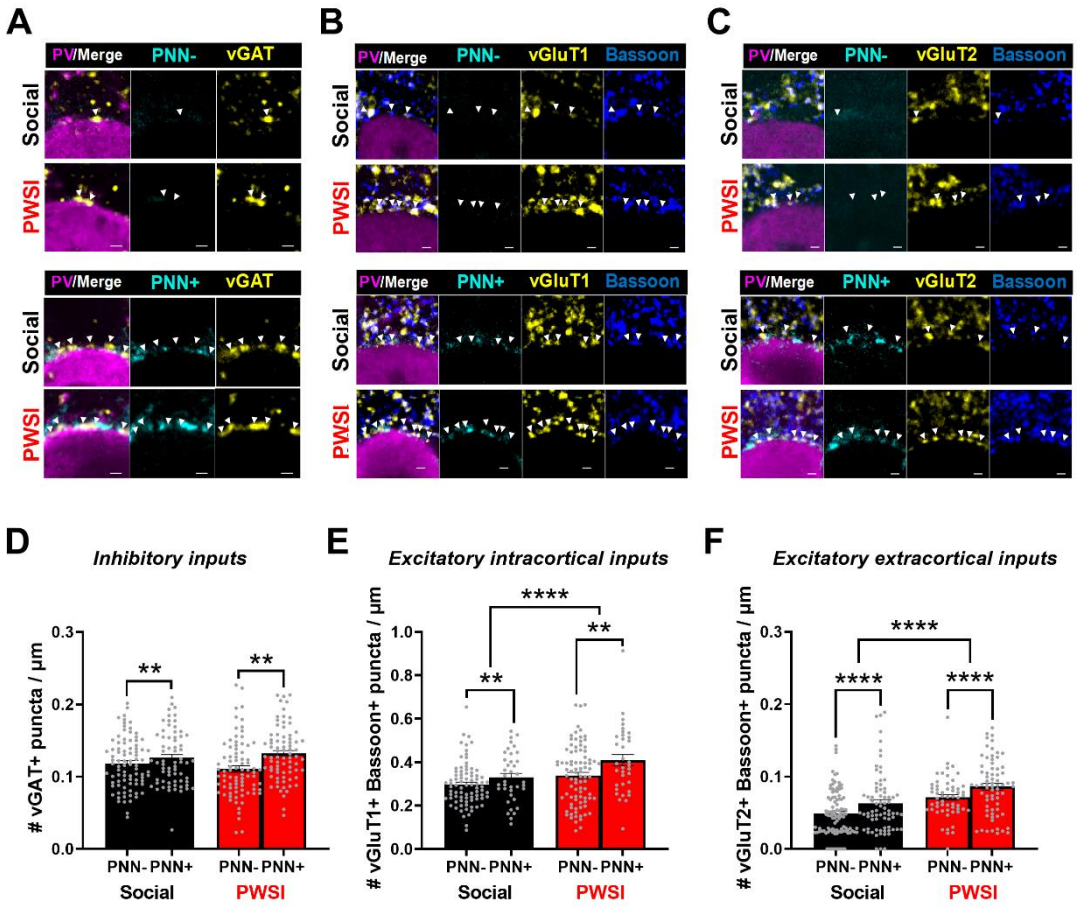

Figure 15. PWSI increased the density of perisomatic excitatory inputs targeting PV+ neurons in the mPFC, irrespective of the presence of PNN. ***A*** *and* ***D,*** *PV+PNN+ neurons receive more inhibitory inputs than PV+PNN- neurons in both social and PWSI mice.* ***A,*** *Representative single plane confocal images showing immunoreactivity for PV (magenta) and vGAT (yellow) as well as WFA staining for PNNs (cyan) for a PNN- (top panel) and a PNN+ (bottom panel) PV+ neuron from the mPFC of social and PWSI mice, respectively. White arrowheads indicate vGAT+ puncta. Scale bar, 1 µm.* ***D,*** *Bar graphs showing the density of vGAT+ puncta targeting the perisomatic region of PV+PNN- and PV+PNN+ neurons in the mPFC (n = 87 PV+PNN- and n = 67 PV+PNN+ neurons from 4 social mice and n = 83 PV+PNN- and n =77 PV+PNN+ neurons from 4 PWSI mice).* ***B, C, E,*** *and* ***F,*** *PWSI increased the density of intracortical and extracortical excitatory inputs surrounding the perisomatic region of PV+ neurons and the presence of PNN is associated with a higher densitiy of excitatory inputs.* ***B,*** *Representative single plane confocal images showing immunoreactivity for PV (magenta), vGluT1 (yellow) and Bassoon (blue) as well as WFA staining for PNNs (cyan) for a PNN- (top panel) and a*

PNN+ (bottom panel) PV+ neuron from the mPFC of social and PWSI mice, respectively. White arrowheads indicate vGluT1+Bassoon+ puncta. Scale bar, 1 μm. ***E,*** *Bar graphs showing the density of vGluT1+Bassoon+ puncta targeting the perisomatic region of PV+PNN- and PV+PNN+ neurons in the mPFC (n = 83 PV+PNN- and n = 38 PV+PNN+ neurons from 4 social mice and n = 88 PV+PNN- and n = 34 PV+PNN+ neurons from 4 PWSI mice).* ***C,*** *Representative single plane confocal images showing immunoreactivity for PV (magenta), vGluT2 (yellow) and Bassoon (blue) as well as WFA staining for PNNs (cyan) for a PNN- (top panel) and a PNN+ (bottom panel) PV+ neuron from the mPFC of social and PWSI mice, respectively. White arrowheads indicate vGluT2+Bassoon+ puncta. Scale bar, 1 μm.* ***F,*** *Bar graphs showing the density of vGluT2+Bassoon+ puncta targeting the perisomatic region of PV+PNN- and PV+PNN+ neurons in the mPFC (n = 101 PV+PNN- and n = 75 PV+PNN+ neurons from 4 social mice and n = 57 PV+PNN- and n = 70 PV+PNN+ neurons from 4 PWSI mice). All data are represented as mean ± SEM. *p < 0.05, **p < 0.01, ***p < 0.005. PNN, perineuronal net; PV, parvalbumin; vGAT, vesicular GABA transporter; vGluT1, vesicular glutamate transporter type 1; vGluT2, vesicular glutamate transporter type 2.*

4.2.6. PWSI led to a reduced density of PV+ inhibitory boutons (baskets) targeting the perisomatic region of pyramidal cells in the mPFC

PV+ basket interneurons are one of the main sources of perisomatic inhibition onto excitatory neurons (**Fig. 16A**), ensuring synchronized modulation of cortical activity via the regulation of oscillations [207,208]. To investigate whether PWSI affected the output features of PV+ interneurons, we studied the vesicular GABA transporter (vGAT+) immunoreactive inhibitory synapses of PV+ basket interneurons targeting the soma of pyramidal cells in layer 5 of mPFC, identified by Kv2.1 immunoreactivity (**Fig. 16E**) [195]. Overall, PWSI induced fewer vGAT+ puncta ($t(480) = 4.272$, $p < 0.001$, **Fig. 16C**) and PV+ puncta ($t(480) = 2.268$, $p = 0.024$, **Fig. 16B**) around pyramidal neurons. mPFC layer 5 (L5) pyramidal cells in PWSI mice received fewer inhibitory inputs from PV+ neurons, since there was a reduction in the density of PV+vGAT+ puncta surrounding Kv2.1 immunoreactive pyramidal neuron somata ($t(480) = 2.895$, $p = 0.004$, **Fig. 16D and 16E**).

Our data displays that PV+ inhibitory synaptic inputs to L5 pyramidal cells are severely reduced after PWSI, suggesting less effective perisomatic inhibition in the mPFC, which could contribute to the observed hyperactivation of the mPFC (data not included in the thesis, refer to [153]).

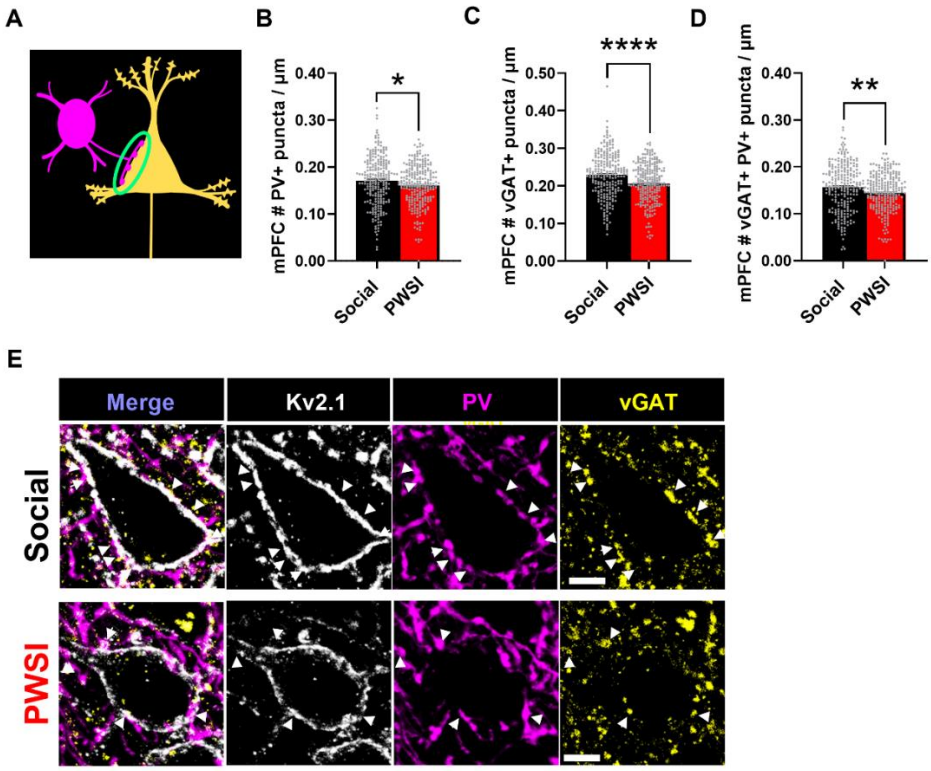

Figure 16. PWSI led to a reduced density of PV+ inhibitory boutons (baskets) targeting the perisomatic compartment of pyramidal cells in the mPFC. A, *Inhibitory axons of PV+ neurons (magenta) targeting the perisomatic region of a pyramidal neuron (yellow) forming PV immunoreactive basket-like innervation.* ***B-E,*** *PWSI decreased the inhibitory output of PV+ neurons. Bar graphs showing the density of PV+ puncta (**B**), vGAT+ puncta (**C**), and vGAT+PV+ puncta (**D**) impinging on the perisomatic region of putative pyramidal neurons (n = 239 neurons from 4 social mice and n = 243 neurons from 4 PWSI mice).* ***E,*** *Representative single plane confocal images from the mPFC showing immunoreactivity for PV (magenta) and vGAT (yellow) as well as voltage-gated potassium channel type 2.1 (Kv2.1, white, labels the perisomatic membrane of neurons) for social (top panel) and PWSI (bottom panel) mice, respectively. White arrowheads: vGAT+PV+ puncta opposing the perisomatic compartment of putative pyramidal neurons. Scale bar, 1 µm. All data are represented as mean ± SEM. *p < 0.05, **p < 0.01, ***p < 0.005.*

5. Discussion

Here, we have investigated the behavioral and plasticity-related effects of PWSI in rodents, by studying the effects of plasticity-inducing chronic fluoxetine treatment on social learning in adult PWSI animals and studying PWSI-induced changes in CP-plasticity mediators, i.e. PV+ neurons and surrounding perineuronal nets, in the prefrontal cortex, a key regulator of social behavior.

By subjecting mice to an extensive behavioral battery, we wished to achieve a detailed characterization of the behavioral effects of PWSI in mice. Our results reveal that, in line with our expectations, PWSI-induced alterations in social behavior parallel those previously described in rats [168,184]. Notably, mice also develop abnormal aggression (as shown by the decreased latency to attack, higher number of total attacks, elevated number of violent hard bites and larger percentage of bites aimed toward vulnerable body parts of the opponent), show an increase in defensive and offensive behaviors at the cost of social sniffing, and display characteristic behavioral fragmentation (i.e. rapid and inconsistent switching between behavioral elements regardless of the social context).

Our detailed analysis of social behavior in PWSI mice also revealed the presence of excessive social vigilance, a characteristic behavior that has not been investigated or described in this paradigm before, even though hypervigilance to threat and negative attention bias have often been associated with early-life maltreatment in human studies [209,210]. PWSI leads to endocrine arousal in rats [169], and clinical studies also highlight altered stress-reactivity as a consequence of neglect [211,212], providing a feasible background for hyperarousal in the presence of the social opponent.

Behavioral fragmentation suggests an inability to recognize social cues and deliver context-adequate responses, the parallels of which can also be seen in PWSI rats [168] and humans that have experienced childhood maltreatment [213,214], indicating ubiquitous social abnormalities caused by early-life adverse experiences.

In the delay discounting test, PWSI mice delivered less total responses compared to social mice. Paired with the decreased sucrose consumption in the sucrose preference test, these results potentially implicate that PWSI reduces the inherent reward value of sucrose in mice. In line with this, a study of PWSI rats has shown dulled sensitivity to sucrose in isolated rats [215]. The development of the dopaminergic system shows a peak

in adolescence, during which dopaminergic innervation of the mPFC increases progressively, and aberrant maturation induced by PWSI could underlie changes in reward value [216,217]. Studies in humans also show that early-life adversities alter reward-related accumbofrontal white matter tracts and induce behavioral alterations in reward learning [47].

Whereas social disturbances display a consistent appearance across various PWSI studies, non-social anxiety in PWSI animals varies highly over PWSI research. Some studies show that PWSI mice display increased anxiety and fear responses [218,219], however, our multi-domain test battery revealed behavioral disturbances that were mainly exclusive to the social domain. A plausible explanation is that some isolation-induced behavioral effects are strain- and test-specific or otherwise depend heavily on the population that was investigated [220]. Another possible explanation is that PWSI mice show highly variable state anxiety, and PWSI-induced trait anxiety could be hard to detect using conventional test measures. Using a novel methodological approach that reliably differentiates between state and trait anxiety, PWSI rats are indicated to have slightly increased trait anxiety, but it remains to be seen whether the same is true for mice [221].

Importantly, both of our experiments highlight that the abnormal aggressive phenotype seen in PWSI rodents is enduring and resistant to outward environmental influences: abnormal aggression was present even after three weeks of resocialization treatment in the first experiment in PWSI rats, or following the behavioral test battery in the second experiment in PWSI mice [153,184]. These findings parallel the robust, treatment-resistant phenotype of child maltreatment-associated psychiatric disorders described in human studies [222].

Though our first experiment has revealed that PWSI rats are capable of social learning, as shown by a gradual increase in huddling together during sleep under the 3-week resocialization period (as opposed to sleeping alone and far apart from each other at the start of cohabitation), resocialization in itself failed to ameliorate PWSI-induced abnormal aggression in the resident-intruder test. This decreased capacity for social learning in adulthood could reflect critical period closure in prefrontal network maturation. Indeed, in the same study we have revealed decreased levels of the activity-dependent BDNF I and IV transcripts in the infralimbic cortex (IL) of the PFC in PWSI rats compared to socially-reared rats (data not included in the thesis, refer to [184]),

suggesting decreased plasticity. Fluoxetine has been shown to induce CP-like plasticity by promoting BDNF/TrkB signalling [151], and in our study, fluoxetine restored BDNF levels in the IL to those of socially-reared rats (data not included in the thesis, see [184]). Still, chronic fluoxetine treatment alone did not affect PWSI-induced abnormal aggressive behavior, only the combination of fluoxetine and resocialization was able to successfully diminish abnormal aggression. CP-like plasticity induced by fluoxetine potentially rendered rats open to change, providing an opportunity for social experiences to guide rewiring of the social circuitry through BDNF/TrkB signalling [150,151].

In further support of this, we were able to mimic the effects of the combined treatment by pairing resocialization with IL-targeted activation of TrkB signalling using dihydroxyflavone; whereas inhibiting TrkB signalling in the IL with the TrkB antagonist ANA-12 completely abolished the effects of resocialization paired with chronic fluoxetine treatment [184]. Our retrograde tracing studies additionally revealed the potential of social network reorganization, showing an increased number of retrogradely labelled neurons of the ventral hippocampus (vHPC) projecting to the mPFC in PWSI rats that received the combined treatment. We also saw a decrease in PV+PNN+ labelling in the vHPC, indicating increased plasticity in this region. In previous studies, we have shown that aggressive interaction-induced hyperactivation in PWSI animals is not limited to the PFC and involves other hubs of the social behavioral network, e.g. the medial amygdala and mediobasal hypothalamus [170]. Together, these results suggest that disturbances in the social behavioral network as a whole could contribute to PWSI-induced social abnormalities, which are therefore not exclusively tied to the PFC. Still, the PFC is suggested to be a key player in PWSI-induced abnormal social behavior, as manipulating TrkB signalling in the IL alone was enough to abolish isolation-induced abnormal aggression [184].

BDNF is tied to a number of critical period-related processes, including the maturation of PV+ neurons, the formation of new synapses, and the pruning of unused synapses [150]. In line with decreased prefrontal BDNF levels seen in PWSI rats, our second experiment in PWSI mice revealed that PWSI also affected prefrontal PV+ neurons, as shown by increased PV+ soma fluorescent intensity and abnormalities in synaptic input and output properties. Notably, we have also seen an increase in intracortical and extracortical excitatory inputs arriving onto PV+ neurons in PWSI mice,

and a decrease in PV+ inhibitory inputs targeting pyramidal neurons **(Fig. 17**). The increase in excitatory inputs could suggest lack of synaptic pruning, since animals were deprived of social experience during the adolescent critical period of prefrontal network maturation, preventing the process of experience-dependent synaptic pruning. Supporting this notion, a study that subjected mice to isolation in adolescence found elevated dendritic spine densities in the PFC and increased levels of PSD-95, an excitatory postsynaptic marker that determines the size and strength of synapses [223,224]. The authors suggest that this could indicate precocious strengthening of synapses, making them resistant to elimination [224,225].

PNNs are involved in the stabilization of synapses [102], and deposition of PNNs around PV+ neurons commonly herald the end of cortical critical periods [52]. As such, increased PNN intensity around prefrontal PV+PNN+ neurons of PWSI mice potentially reflects decreased plasticity. Following the suggestion of Li and colleagues [224,225], higher PNN intensity could indicate precocious stabilization of synapses, rendering them resistant to change. Importantly, these alterations could potentially contribute to the robust, enduring phenotype of PWSI-induced abnormal aggression.

The elevated number of excitatory synapses arriving onto PV+ neurons could also be a compensatory mechanism for the decreased PV+ IN-mediated inhibition targeting pyramidal neurons. Paradoxically, in this study we have found that mPFC PV+PNN+ neurons of PWSI animals show heightened activation following aggressive interaction (data not included in the thesis, refer to [153]), but so does the mPFC in general [153,170,180], indicating possible functional impairment of PV+ neurons. Since PV+ INs are the most abundant interneuron-subtype in the PFC [73], abnormal function could produce widespread imbalances in excitation/inhibition and impair social information processing and action-selection. This could potentially explain behavioral fragmentation, another robust PWSI phenotype, which involves the fast, inconsistent expression of behavioral elements that disregard the social context.

Our results have further shown that PWSI-evoked synaptic imbalances did not occur in a PNN-dependent manner, i.e. PWSI did not affect PV+PNN- and PV+PNN+ interneuron synapses in a distinct way. However, correlation matrices between the c-Fos activation of the two interneuron subtypes and frequency of behaviors during the resident-intruder test indicate that PV+PNN- and PV+PNN+ neurons regulate distinct aspects of

social behavior, and PWSI-induced abnormal aggressive behavior is selectively associated with PV+PNN+ neurons [153]. Methods with a better time-scale resolution, such as calcium imaging with fiber photometry, could provide more direct proof of the involvement of PV+PNN+ neurons in PWSI-induced abnormal social behavior, however, the reliable differentiation between PV+PNN+ and PV+PNN- neurons is not feasible *in vivo* as of yet.

Taken together, our results display that PWSI-induced behavioral abnormalities are largely specific to the social domain in both rats and mice, and aberrant maturation of prefrontal PV+ interneurons potentially contribute to the PWSI behavioral phenotype. Importantly, PWSI-induced abnormal aggression is enduring and resistant to environmental influences unless plasticity is reinstated. Our work carries valuable therapeutic implications, suggesting that the combination of plasticity-inducing pharmacological treatment and psychotherapy could provide greater efficacy in the treatment of ELM-induced psychopathological disorders: by increasing plasticity, maltreatment-disrupted networks become open to change, allowing for therapeutic interventions to guide reorganization of the social circuitry.

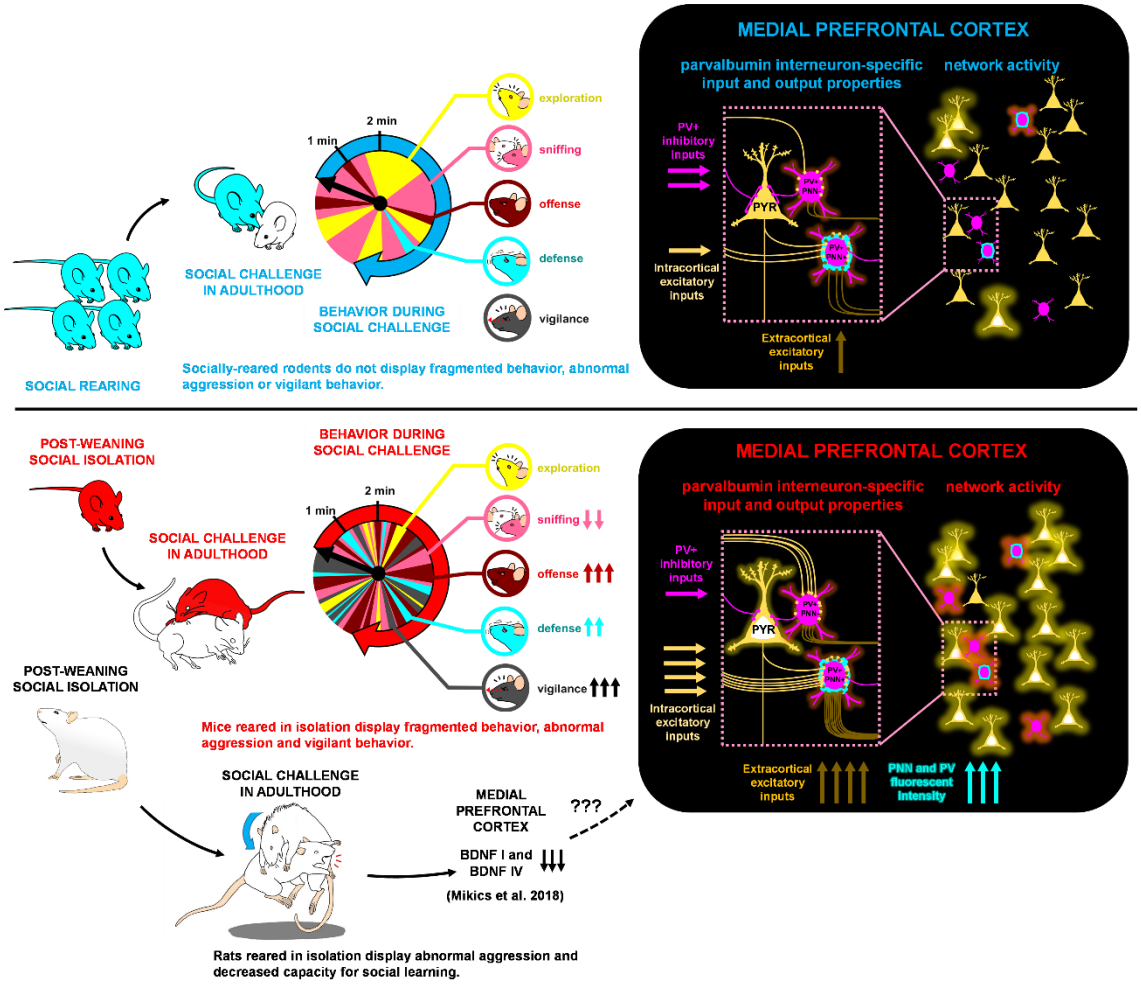

Figure 17. Summary of PWSI-induced social behavioral and neurobiological changes. *PWSI led to the appearance of abnormal aggression in adulthood in both rats and mice. Our research further revealed fragmented behavior in mice and excessive social vigilance, increased offensive and defensive behavior, and decreased sniffing. In rats, cohabitation of adult PWSI animals during resocialization revealed a capacity for social learning, but abnormal aggression remained even after resocialization. PWSI-induced behavioral changes were accompanied by changes in neuronal activity and plasticity-related markers in the medial prefrontal cortex: our first series of experiments in rats have shown decreased BDNF I and IV levels in the mPFC [184], and parallel to this, in the mPFC of PWSI mice there was an overall increase in the density of synaptic inputs targeting the perisomatic region of medial prefrontal PV+ neurons [153], including cortical excitatory (vGluT1+, light gold color) and extracortical excitatory (vGluT2+, dark gold) inputs. The increase in excitatory inputs surrounding PV+ interneurons did not depend on PNN-coverage. PWSI also led to a reduction in the density of PV+*

inhibitory boutons (magenta) targeting the perisomatic compartment of pyramidal cells in the mPFC. Additionally, mPFC PV+ IN somata and surrounding PNNs showed a higher fluorescent intensity in PWSI mice compared to social mice. BDNF, brain-derived neurotrophic factor; IN, interneuron; mPFC, medial prefrontal cortex; PNN, perineuronal net; PV, parvalbumin; PWSI, post-weaning social isolation; vGluT, vesicular glutamate transporter.

6. Conclusions

The main conclusions of our two experiments are as follows:

- ***PWSI induces abnormalities in social behavior and reward-related behavior***
    - PWSI leads to abnormal aggression, increased defensive and offensive behaviors and behavioral fragmentation as shown by the resident-intruder, social instigation and social interaction tests
    - PWSI leads to mild deficits in reward-related tasks as shown by the delay discounting and sucrose preference tests
    - Non-social anxiety was not present in PWSI mice, as revealed by the open field test and elevated plus-maze
- ***Social learning decreases in adulthood, rendering PWSI-induced abnormal aggression robust and enduring***
    - PWSI-induced abnormal aggression is resistant to resocialization in adulthood
    - PWSI-induced abnormal aggression is resistant to multiple testing (i.e. multi-domain behavioral battery of) in adulthood
- ***PWSI-induced abnormal aggression could only be successfully ameliorated by the combination of plasticity-inducing chronic fluoxetine treatment and resocialization***
    - Chronic fluoxetine treatment alone did not affect abnormal aggression in the resident-intruder test
    - Resocialization decreased quantitative (number of attack bites) but not qualitative (attacks aimed at vulnerable targets, dominance of hard bites among attack types) aspects of aggression
    - The combination of chronic fluoxetine treatment and resocialization successfully decreased both quantitative and qualitative aspects of aggression
- ***PWSI leads to altered properties of medial prefrontal parvalbumin interneurons***
    - PWSI increases PV fluorescent intensity of PV+ interneuron somata
    - PWSI increases fluorescent intensity of PNNs surrounding PV+ interneurons
    - PV+ neurons of PWSI mice receive a higher number of intracortical and subcortical excitatory inputs
    - PV+ neurons of PWSI mice send fewer inhibitory synapses onto medial prefrontal pyramidal neurons

7. Summary

Here we have shown that PWSI, a laboratory model of childhood neglect, induces abnormal aggression (shown by an increased number of total attacks, violent hard bites, and attacks aimed at vulnerable targets), increased defensive and offensive behavior, and behavioral fragmentation, i.e. rapid and inconsistent switching between behavioral elements irrespective of the social context. Although PWSI-induced behavioral deficits were mainly specific to the social domain, PWSI also affected reward-related tasks, but did not increase non-social anxiety.

The capacity for social learning was limited in PWSI animals, as resocialization alone was unable to decrease both the quantitative and qualitative aspects of aggressive behavior, rendering PWSI-induced abnormal aggression robust and enduring. Presumably, aberrant maturation of the mPFC, a key hub in the regulation of social behavior with its peak maturation coinciding with the PWSI period, contributed to the robust phenotype of abnormal aggression. Supporting this notion, we have found changes in critical regulators of cortical plasticity in the mPFC. Notably, PV+ interneurons and PNNs enwrapping them showed higher fluorescent intensity, PV+ neurons received a higher number of both intra- and subcortical excitatory synapses, and delivered less inhibitory synapses onto prefrontal pyramidal neurons. While chronic fluoxetine treatment has been shown to induce developmental plasticity, fluoxetine treatment alone was unable to affect abnormal aggression. Fluoxetine provided the opportunity for social learning by increasing plasticity, however, resocialization was also required, offering a social environment that would guide experience-dependent network reorganization of the mPFC. Accordingly, the combined treatment successfully ameliorated both quantitative and qualitative aspects of PWSI-induced abnormal aggression.

Our work carries valuable therapeutic implications, suggesting that the combination of plasticity-inducing pharmacological treatment and psychotherapy could provide greater efficacy in the treatment of child maltreatment-induced psychopathological disorders: by increasing plasticity, maltreatment-disrupted networks become open to change, allowing for therapeutic interventions to guide reorganization of the social circuitry.

8. References

1. Widom CS, Czaja SJ, Paris J. A Prospective Investigation of Borderline Personality Disorder in Abused and Neglected Children Followed Up into Adulthood. Journal of Personality Disorders. 2009 Oct;23(5):433–46.

2. Thornberry TP, Henry KL, Ireland TO, Smith CA. The Causal Impact of Childhood-Limited Maltreatment and Adolescent Maltreatment on Early Adult Adjustment. Journal of Adolescent Health. 2010 Apr;46(4):359–65.

3. Scott KM, Smith DR, Ellis PM. Prospectively Ascertained Child Maltreatment and Its Association With DSM-IV Mental Disorders in Young Adults. Arch Gen Psychiatry. 2010 Jul 1;67(7):712.

4. Varese F, Smeets F, Drukker M, Lieverse R, Lataster T, Viechtbauer W, Read J, Van Os J, Bentall RP. Childhood Adversities Increase the Risk of Psychosis: A Meta-analysis of Patient-Control, Prospective- and Cross-sectional Cohort Studies. Schizophrenia Bulletin. 2012 Jul;38(4):661–71.

5. Kisely S, Strathearn L, Najman JM. Child maltreatment and mental health problems in 30-year-old adults: A birth cohort study. Journal of Psychiatric Research. 2020 Oct;129:111–7.

6. Russotti J, Warmingham JM, Duprey EB, Handley ED, Manly JT, Rogosch FA, Cicchetti D. Child maltreatment and the development of psychopathology: The role of developmental timing and chronicity. Child Abuse & Neglect. 2021 Oct;120:105215.

7. Li M, D'Arcy C, Meng X. Maltreatment in childhood substantially increases the risk of adult depression and anxiety in prospective cohort studies: systematic review, meta-analysis, and proportional attributable fractions. Psychol Med. 2016 Mar;46(4):717–30.

8. Gilbert R, Widom CS, Browne K, Fergusson D, Webb E, Janson S. Burden and consequences of child maltreatment in high-income countries. The Lancet. 2009 Jan;373(9657):68–81.

9. Stoltenborgh M, Bakermans-Kranenburg MJ, Alink LRA, van IJzendoorn MH. The Prevalence of Child Maltreatment across the Globe: Review of a Series of Meta-Analyses: Prevalence of Child Maltreatment across the Globe. Child Abuse Rev. 2015 Jan;24(1):37–50.

10. Hildyard KL, Wolfe DA. Child neglect: developmental issues and outcomes☆. Child Abuse & Neglect. 2002 Jun;26(6–7):679–95.

11. Stoltenborgh M, Bakermans-Kranenburg MJ, van IJzendoorn MH. The neglect of child neglect: a meta-analytic review of the prevalence of neglect. Soc Psychiatry Psychiatr Epidemiol. 2013 Mar;48(3):345–55.

12. Struck N, Krug A, Yuksel D, Stein F, Schmitt S, Meller T, Brosch K, Dannlowski U, Nenadić I, Kircher T, Brakemeier EL. Childhood maltreatment and adult mental disorders – the prevalence of different types of maltreatment and associations with age of onset and severity of symptoms. Psychiatry Research. 2020 Nov;293:113398.

13. Teicher MH, Samson JA. Childhood Maltreatment and Psychopathology: A Case for Ecophenotypic Variants as Clinically and Neurobiologically Distinct Subtypes. AJP. 2013 Oct;170(10):1114–33.

14. Bernet CZ, Stein MB. Relationship of childhood maltreatment to the onset and course of major depression in adulthood. Depress Anxiety. 1999;9(4):169–74.

15. Widom CS, DuMont K, Czaja SJ. A Prospective Investigation of Major Depressive Disorder and Comorbidity in Abused and Neglected Children Grown Up. ARCH GEN PSYCHIATRY. 2007;64.

16. Agnew-Blais J, Danese A. Childhood maltreatment and unfavourable clinical outcomes in bipolar disorder: a systematic review and meta-analysis. The Lancet Psychiatry. 2016 Apr;3(4):342–9.

17. Nelson J, Klumparendt A, Doebler P, Ehring T. Childhood maltreatment and characteristics of adult depression: Meta-analysis. Br J Psychiatry. 2017 Feb;210(2):96–104.

18. Cakir S, Tasdelen Durak R, Ozyildirim I, Ince E, Sar V. Childhood trauma and treatment outcome in bipolar disorder. Journal of Trauma & Dissociation. 2016 Aug 7;17(4):397–409.

19. Nanni V, Uher R, Danese A. Childhood Maltreatment Predicts Unfavorable Course of Illness and Treatment Outcome in Depression: A Meta-Analysis. AJP. 2012 Feb;169(2):141–51.

20. Miller AB, Jenness JL, Oppenheimer CW, Gottleib ALB, Young JF, Hankin BL. Childhood Emotional Maltreatment as a Robust Predictor of Suicidal Ideation: A 3-Year Multi-Wave, Prospective Investigation. J Abnorm Child Psychol. 2017 Jan;45(1):105–16.

21. Alink LRA, Cicchetti D, Kim J, Rogosch FA. Longitudinal associations among child maltreatment, social functioning, and cortisol regulation. Developmental Psychology. 2012 Jan;48(1):224–36.

22. Johnson JG, Cohen P, Brown J, Smailes EM, Bernstein DP. Childhood Maltreatment Increases Risk for Personality Disorders During Early Adulthood. Arch Gen Psychiatry. 1999 Jul 1;56(7):600.

23. Shi Z, Bureau JF, Easterbrooks MA, Zhao X, Lyons-Ruth K. Childhood maltreatment and prospectively observed quality of early care as predictors of antisocial personality disorder features. Infant Ment Health J. 2012 Jan;33(1):55–69.

24. Gratz KL, Conrad SD, Roemer L. Risk factors for deliberate self-harm among college students. American Journal of Orthopsychiatry. 2002 Jan;72(1):128–40.

25. Gómez JM, Becker-Blease K, Freyd JJ. A Brief Report on Predicting Self-Harm: Is It Gender or Abuse that Matters? Journal of Aggression, Maltreatment & Trauma. 2015 Feb 7;24(2):203–14.

26. Angelakis I, Gillespie EL, Panagioti M. Childhood maltreatment and adult suicidality: a comprehensive systematic review with meta-analysis. Psychol Med. 2019 May;49(07):1057–78.

27. Gnanamanickam ES, Nguyen H, Armfield JM, Doidge JC, Brown DS, Preen DB, Segal L. Child maltreatment and emergency department visits: a longitudinal birth cohort study from infancy to early adulthood. Child Abuse & Neglect. 2022 Jan;123:105397.

28. Evans CBR, Burton DL. Five Types of Child Maltreatment and Subsequent Delinquency: Physical Neglect as the Most Significant Predictor. Journ Child Adol Trauma. 2013 Dec;6(4):231–45.

29. Mersky JP, Topitzes J, Reynolds AJ. Unsafe at Any Age: Linking Childhood and Adolescent Maltreatment to Delinquency and Crime. Journal of Research in Crime and Delinquency. 2012 May;49(2):295–318.

30. Vachon DD, Krueger RF, Rogosch FA, Cicchetti D. Assessment of the Harmful Psychiatric and Behavioral Effects of Different Forms of Child Maltreatment. JAMA Psychiatry. 2015 Nov 1;72(11):1135.

31. Milaniak I, Widom CS. Does child abuse and neglect increase risk for perpetration of violence inside and outside the home? Psychology of Violence. 2015 Jul;5(3):246–55.

32. Peterson C, Florence C, Klevens J. The economic burden of child maltreatment in the United States, 2015. Child Abuse & Neglect. 2018 Dec;86:178–83.

33. Klika JB, Rosenzweig J, Merrick M. Economic Burden of Known Cases of Child Maltreatment from 2018 in Each State. Child Adolesc Soc Work J. 2020 Jun;37(3):227–34.

34. Huttenlocher PR. Morphometric study of human cerebral cortex development. Neuropsychologia. 1990 Jan;28(6):517–27.

35. Giedd JN, Blumenthal J, Jeffries NO, Castellanos FX, Liu H, Zijdenbos A, Paus T, Evans AC, Rapoport JL. Brain development during childhood and adolescence: a longitudinal MRI study. Nat Neurosci. 1999 Oct;2(10):861–3.

36. Elston GN, Oga T, Fujita I. Spinogenesis and Pruning Scales across Functional Hierarchies. J Neurosci. 2009 Mar 11;29(10):3271–5.

37. Faust TE, Gunner G, Schafer DP. Mechanisms governing activity-dependent synaptic pruning in the developing mammalian CNS. Nat Rev Neurosci. 2021 Nov;22(11):657–73.

38. Lebel C, Beaulieu C. Longitudinal Development of Human Brain Wiring Continues from Childhood into Adulthood. Journal of Neuroscience. 2011 Jul 27;31(30):10937–47.

39. Wierenga L, Langen M, Ambrosino S, Van Dijk S, Oranje B, Durston S. Typical development of basal ganglia, hippocampus, amygdala and cerebellum from age 7 to 24. NeuroImage. 2014 Aug;96:67–72.

40. Lebel C, Walker L, Leemans A, Phillips L, Beaulieu C. Microstructural maturation of the human brain from childhood to adulthood. NeuroImage. 2008 Apr;40(3):1044–55.

41. Lebel C, Gee M, Camicioli R, Wieler M, Martin W, Beaulieu C. Diffusion tensor imaging of white matter tract evolution over the lifespan. NeuroImage. 2012 Mar;60(1):340–52.

42. Fletcher JL, Makowiecki K, Cullen CL, Young KM. Oligodendrogenesis and myelination regulate cortical development, plasticity and circuit function. Seminars in Cell & Developmental Biology. 2021 Oct;118:14–23.

43. Gogtay N, Giedd JN, Lusk L, Hayashi KM, Greenstein D, Vaituzis AC, Nugent TF, Herman DH, Clasen LS, Toga AW, Rapoport JL, Thompson PM. Dynamic mapping of human cortical development during childhood through early adulthood. Proc Natl Acad Sci USA. 2004 May 25;101(21):8174–9.

44. Zuo Y, Yang G, Kwon E, Gan WB. Long-term sensory deprivation prevents dendritic spine loss in primary somatosensory cortex. Nature. 2005 Jul;436(7048):261–5.

45. Lee V, Hoaken PNS. Cognition, Emotion, and Neurobiological Development: Mediating the Relation Between Maltreatment and Aggression. Child Maltreat. 2007 Aug;12(3):281–98.

46. Edmiston EE. Corticostriatal-Limbic Gray Matter Morphology in Adolescents With Self-reported Exposure to Childhood Maltreatment. Arch Pediatr Adolesc Med. 2011 Dec 1;165(12):1069.

47. Kennedy BV, Hanson JL, Buser NJ, Van Den Bos W, Rudolph KD, Davidson RJ, Pollak SD. Accumbofrontal tract integrity is related to early life adversity and feedback learning. Neuropsychopharmacol. 2021 Dec;46(13):2288–94.

48. Gee DG, Gabard-Durnam LJ, Flannery J, Goff B, Humphreys KL, Telzer EH, Hare TA, Bookheimer SY, Tottenham N. Early developmental emergence of human amygdala–prefrontal connectivity after maternal deprivation. Proc Natl Acad Sci USA. 2013 Sep 24;110(39):15638–43.

49. Jalbrzikowski M, Larsen B, Hallquist MN, Foran W, Calabro F, Luna B. Development of White Matter Microstructure and Intrinsic Functional Connectivity Between the Amygdala and Ventromedial Prefrontal Cortex: Associations With Anxiety and Depression. Biological Psychiatry. 2017 Oct;82(7):511–21.

50. Peverill M, Sheridan MA, Busso DS, McLaughlin KA. Atypical Prefrontal–Amygdala Circuitry Following Childhood Exposure to Abuse: Links With Adolescent Psychopathology. Child Maltreat. 2019 Nov;24(4):411–23.

51. Bethlehem RAI, Seidlitz J, White SR, Vogel JW, Anderson KM, Adamson C, Adler S, Alexopoulos GS, Anagnostou E, Areces-Gonzalez A, Astle DE, Auyeung B, Ayub M, Bae J, Ball G, Baron-Cohen S, Beare R, Bedford SA, Benegal V, Beyer F, Blangero J, Blesa Cábez M, Boardman JP, Borzage M, Bosch-Bayard JF, Bourke N, Calhoun VD, Chakravarty MM, Chen C, Chertavian C, Chetelat G, Chong YS, Cole JH, Corvin A, Costantino M, Courchesne E, Crivello F, Cropley VL, Crosbie J, Crossley N, Delarue M, Delorme R, Desrivieres S, Devenyi GA, Di Biase MA, Dolan R, Donald KA, Donohoe G, Dunlop K, Edwards AD, Elison JT, Ellis CT, Elman JA, Eyler L, Fair DA, Feczko E, Fletcher PC, Fonagy P, Franz CE, Galan-

Garcia L, Gholipour A, Giedd J, Gilmore JH, Glahn DC, Goodyer IM, Grant PE, Groenewold NA, Gunning FM, Gur RE, Gur RC, Hammill CF, Hansson O, Hedden T, Heinz A, Henson RN, Heuer K, Hoare J, Holla B, Holmes AJ, Holt R, Huang H, Im K, Ipser J, Jack CR, Jackowski AP, Jia T, Johnson KA, Jones PB, Jones DT, Kahn RS, Karlsson H, Karlsson L, Kawashima R, Kelley EA, Kern S, Kim KW, Kitzbichler MG, Kremen WS, Lalonde F, Landeau B, Lee S, Lerch J, Lewis JD, Li J, Liao W, Liston C, Lombardo MV, Lv J, Lynch C, Mallard TT, Marcelis M, Markello RD, Mathias SR, Mazoyer B, McGuire P, Meaney MJ, Mechelli A, Medic N, Misic B, Morgan SE, Mothersill D, Nigg J, Ong MQW, Ortinau C, Ossenkoppele R, Ouyang M, Palaniyappan L, Paly L, Pan PM, Pantelis C, Park MM, Paus T, Pausova Z, Paz-Linares D, Pichet Binette A, Pierce K, Qian X, Qiu J, Qiu A, Raznahan A, Rittman T, Rodrigue A, Rollins CK, Romero-Garcia R, Ronan L, Rosenberg MD, Rowitch DH, Salum GA, Satterthwaite TD, Schaare HL, Schachar RJ, Schultz AP, Schumann G, Schöll M, Sharp D, Shinohara RT, Skoog I, Smyser CD, Sperling RA, Stein DJ, Stolicyn A, Suckling J, Sullivan G, Taki Y, Thyreau B, Toro R, Traut N, Tsvetanov KA, Turk-Browne NB, Tuulari JJ, Tzourio C, Vachon-Presseau É, Valdes-Sosa MJ, Valdes-Sosa PA, Valk SL, Van Amelsvoort T, Vandekar SN, Vasung L, Victoria LW, Villeneuve S, Villringer A, Vértes PE, Wagstyl K, Wang YS, Warfield SK, Warrier V, Westman E, Westwater ML, Whalley HC, Witte AV, Yang N, Yeo B, Yun H, Zalesky A, Zar HJ, Zettergren A, Zhou JH, Ziauddeen H, Zugman A, Zuo XN, 3R-BRAIN, AIBL, Rowe C, Alzheimer's Disease Neuroimaging Initiative, Alzheimer's Disease Repository Without Borders Investigators, Frisoni GB, CALM Team, Cam-CAN, CCNP, COBRE, cVEDA, ENIGMA Developmental Brain Age Working Group, Developing Human Connectome Project, FinnBrain, Harvard Aging Brain Study, IMAGEN, KNE96, The Mayo Clinic Study of Aging, NSPN, POND, The PREVENT-AD Research Group, Binette AP, VETSA, Bullmore ET, Alexander-Bloch AF. Brain charts for the human lifespan. Nature. 2022 Apr 21;604(7906):525–33.

52. Hensch TK. CRITICAL PERIOD REGULATION. Annu Rev Neurosci. 2004 Jul 21;27(1):549–79.

53. Andersen SL. Trajectories of brain development: point of vulnerability or window of opportunity? Neuroscience & Biobehavioral Reviews. 2003 Jan;27(1–2):3–18.

54. Wiesel TN, Hubel DH. SINGLE-CELL RESPONSES IN STRIATE CORTEX OF KITTENS DEPRIVED OF VISION IN ONE EYE. Journal of Neurophysiology. 1963 Nov 1;26(6):1003–17.

55. Wiesel TN, Hubel DH. EFFECTS OF VISUAL DEPRIVATION ON MORPHOLOGY AND PHYSIOLOGY OF CELLS IN THE CAT'S LATERAL GENICULATE BODY. Journal of Neurophysiology. 1963 Nov 1;26(6):978–93.

56. Hubel DH, Wiesel TN. The period of susceptibility to the physiological effects of unilateral eye closure in kittens. The Journal of Physiology. 1970 Feb 1;206(2):419–36.

57. Hubel DH, Wiesel TN, LeVay S. Functional Architecture of Area 17 in Normal and Monocularly Deprived Macaque Monkeys. Cold Spring Harbor Symposia on Quantitative Biology. 1976 Jan 1;40(0):581–9.

58. Shatz CJ, Stryker MP. Ocular dominance in layer IV of the cat's visual cortex and the effects of monocular deprivation. The Journal of Physiology. 1978 Aug 1;281(1):267–83.

59. Antonini A, Stryker MP. Plasticity of geniculocortical afferents following brief or prolonged monocular occlusion in the cat. J Comp Neurol. 1996 May 20;369(1):64–82.

60. Antonini A, Gillespie DC, Crair MC, Stryker MP. Morphology of Single Geniculocortical Afferents and Functional Recovery of the Visual Cortex after Reverse Monocular Deprivation in the Kitten. J Neurosci. 1998 Dec 1;18(23):9896–909.

61. Grutzendler J, Kasthuri N, Gan WB. Long-term dendritic spine stability in the adult cortex. Nature. 2002 Dec;420(6917):812–6.

62. Sato M, Stryker MP. Distinctive Features of Adult Ocular Dominance Plasticity. J Neurosci. 2008 Oct 8;28(41):10278–86.

63. Goodman CS, Shatz CJ. Developmental mechanisms that generate precise patterns of neuronal connectivity. Cell. 1993 Jan;72:77–98.

64. Crowley JC, Katz LC. Development of ocular dominance columns in the absence of retinal input. Nat Neurosci. 1999 Dec;2(12):1125–30.

65. Tessier-Lavigne M, Goodman CS. The Molecular Biology of Axon Guidance. Science. 1996 Nov 15;274(5290):1123–33.

66. Wong ROL, Ghosh A. Activity-dependent regulation of dendritic growth and patterning. Nat Rev Neurosci. 2002 Oct 1;3(10):803–12.

67. Feller MB. Spontaneous Correlated Activity in Developing Neural Circuits. Neuron. 1999 Apr;22(4):653–6.

68. Katz LC, Shatz CJ. Synaptic Activity and the Construction of Cortical Circuits. Science. 1996 Nov 15;274(5290):1133–8.

69. Mower GD. The effect of dark rearing on the time course of the critical period in cat visual cortex. Developmental Brain Research. 1991 Feb;58(2):151–8.

70. Bartoletti A, Medini P, Berardi N, Maffei L. Environmental enrichment prevents effects of dark-rearing in the rat visual cortex. Nat Neurosci. 2004 Mar;7(3):215–6.

71. Reh RK, Dias BG, Nelson CA, Kaufer D, Werker JF, Kolb B, Levine JD, Hensch TK. Critical period regulation across multiple timescales. Proc Natl Acad Sci USA. 2020 Sep 22;117(38):23242–51.

72. Toyoizumi T, Miyamoto H, Yazaki-Sugiyama Y, Atapour N, Hensch TK, Miller KD. A Theory of the Transition to Critical Period Plasticity: Inhibition Selectively Suppresses Spontaneous Activity. Neuron. 2013 Oct;80(1):51–63.

73. Tremblay R, Lee S, Rudy B. GABAergic Interneurons in the Neocortex: From Cellular Properties to Circuits. Neuron. 2016 Jul;91(2):260–92.

74. Hu H, Gan J, Jonas P. Fast-spiking, parvalbumin $^{+}$ GABAergic interneurons: From cellular design to microcircuit function. Science. 2014 Aug;345(6196):1255263.

75. Cond F. The hierarchical development of monkey visual cortical regions as revealed by the maturation of parvalbumin-immunoreactive neurons.

76. Del Rio J, De Lecea L, Ferrer I, Soriano E. The development of parvalbumin-immunoreactivity in the neocortex of the mouse. Developmental Brain Research. 1994 Sep;81(2):247–59.

77. Shirokawa T, Ogawa T. Release of γ-aminobutyric acid by visual stimulation in the kitten visual cortex. Brain Research. 1992 Aug;589(1):157–60.

78. Chattopadhyaya B, Di Cristo G, Higashiyama H, Knott GW, Kuhlman SJ, Welker E, Huang ZJ. Experience and Activity-Dependent Maturation of Perisomatic GABAergic Innervation in Primary Visual Cortex during a Postnatal Critical Period. J Neurosci. 2004 Oct 27;24(43):9598–611.

79. Fagiolini M, Hensch TK. Inhibitory threshold for critical-period activation in primary visual cortex. Nature. 2000 Mar;404(6774):183–6.

80. Iwai Y, Fagiolini M, Obata K, Hensch TK. Rapid Critical Period Induction by Tonic Inhibition in Visual Cortex. J Neurosci. 2003 Jul 30;23(17):6695–702.

81. Katagiri H, Fagiolini M, Hensch TK. Optimization of Somatic Inhibition at Critical Period Onset in Mouse Visual Cortex. Neuron. 2007 Mar;53(6):805–12.

82. Werker JF, Hensch TK. Critical Periods in Speech Perception: New Directions. Annu Rev Psychol. 2015 Jan 3;66(1):173–96.

83. Morishita H, Cabungcal JH, Chen Y, Do KQ, Hensch TK. Prolonged Period of Cortical Plasticity upon Redox Dysregulation in Fast-Spiking Interneurons. Biological Psychiatry. 2015 Sep;78(6):396–402.

84. Cisneros-Franco JM, De Villers-Sidani É. Reactivation of critical period plasticity in adult auditory cortex through chemogenetic silencing of parvalbumin-positive interneurons. Proc Natl Acad Sci USA. 2019 Dec 26;116(52):26329–31.

85. Medina DL, Sciarretta C, Calella AM, Von Bohlen Und Halbach O, Unsicker K, Minichiello L. TrkB regulates neocortex formation through the Shc/PLCγ-mediated control of neuronal migration. EMBO J. 2004 Sep 29;23(19):3803–14.

86. Zagrebelsky M, Korte M. Form follows function: BDNF and its involvement in sculpting the function and structure of synapses. Neuropharmacology. 2014 Jan;76:628–38.

87. Mitchelmore C, Gede L. Brain derived neurotrophic factor: Epigenetic regulation in psychiatric disorders. Brain Research. 2014 Oct;1586:162–72.

88. Panja D, Bramham CR. BDNF mechanisms in late LTP formation: A synthesis and breakdown. Neuropharmacology. 2014 Jan;76:664–76.

89. Leal G, Comprido D, Duarte CB. BDNF-induced local protein synthesis and synaptic plasticity. Neuropharmacology. 2014 Jan;76:639–56.

90. Hanover TJL, Huang ZJ, Tonegawa S, Stryker MP. t Brain-Derived Neurotrophic Factor Overexpression Induces Precocious Critical Period in Mouse Visual Cortex. J Neurosci. 1999 Nov 15;19(22):RC40–RC40.

91. Huang ZJ, Kirkwood A, Pizzorusso T, Porciatti V, Morales B, Bear MF, Maffei L, Tonegawa S. BDNF Regulates the Maturation of Inhibition and the Critical Period of Plasticity in Mouse Visual Cortex. Cell. 1999 Sep;98(6):739–55.

92. Shieh PB, Hu SC, Bobb K, Timmusk T, Ghosh A. Identification of a Signaling Pathway Involved in Calcium Regulation of BDNF Expression. Neuron. 1998 Apr;20(4):727–40.

93. Pruunsild P, Kazantseva A, Aid T, Palm K, Timmusk T. Dissecting the human BDNF locus: Bidirectional transcription, complex splicing, and multiple promoters. Genomics. 2007 Sep;90(3):397–406.

94. Aid T, Kazantseva A, Piirsoo M, Palm K, Timmusk T. Mouse and ratBDNF gene structure and expression revisited. J Neurosci Res. 2007 Feb 15;85(3):525–35.

95. Hong EJ, McCord AE, Greenberg ME. A Biological Function for the Neuronal Activity-Dependent Component of Bdnf Transcription in the Development of Cortical Inhibition. Neuron. 2008 Nov;60(4):610–24.

96. Castrén E, Zafra F, Thoenen H, Lindholm D. Light regulates expression of brain-derived neurotrophic factor mRNA in rat visual cortex. Proc Natl Acad Sci USA. 1992 Oct 15;89(20):9444–8.

97. Gianfranceschi L, Siciliano R, Walls J, Morales B, Kirkwood A, Huang ZJ, Tonegawa S, Maffei L. Visual cortex is rescued from the effects of dark rearing by overexpression of BDNF. Proc Natl Acad Sci USA. 2003 Oct 14;100(21):12486–91.

98. Brückner G, Seeger G, Brauer K, Härtig W, Kacza J, Bigl V. Cortical areas are revealed by distribution patterns of proteoglycan components and parvalbumin in the Mongolian gerbil and rat. Brain Research. 1994 Sep;658(1–2):67–86.

99. Härtig W, Brauer K, Brückner G. Wisteria floribunda agglutinin-labelled nets surround parvalbumin-containing neurons: NeuroReport. 1992 Oct;3(10):869–72.

100. Celio MR, Blumcke I. Perineuronal nets — a specialized form of extracellular matrix in the adult nervous system. Brain Research Reviews. 1994 Jan;19(1):128–45.

101. Giamanco KA, Morawski M, Matthews RT. Perineuronal net formation and structure in aggrecan knockout mice. Neuroscience. 2010 Nov;170(4):1314–27.

102. Carulli D, Verhaagen J. An Extracellular Perspective on CNS Maturation: Perineuronal Nets and the Control of Plasticity. IJMS. 2021 Feb 28;22(5):2434.

103. Pizzorusso T, Medini P, Berardi N, Chierzi S, Fawcett JW, Maffei L. Reactivation of Ocular Dominance Plasticity in the Adult Visual Cortex. Science. 2002 Nov 8;298(5596):1248–51.

104. Berardi N, Pizzorusso T, Maffei L. Extracellular Matrix and Visual Cortical PlasticityFreeing the Synapse. Neuron. 2004 Dec 16;44(6):905–8.

105. Oohira A, Matsui F, Katoh-Semba R. Inhibitory effects of brain chondroitin sulfate proteoglycans on neurite outgrowth from PC12D cells. J Neurosci. 1991 Mar 1;11(3):822–7.

106. Snow DM, Brown EM, Letourneau PC. GROWTH CONE BEHAVIOR IN THE PRESENCE OF SOLUBLE CHONDROITIN SULFATE PROTEOGLYCAN (CSPG), COMPARED TO BEHAVIOR ON CSPG BOUND TO LAMININ OR FIBRONECTIN. Int j dev neurosci. 1996 Jun;14(3):331–49.

107. Asher RA, Morgenstern DA, Fidler PS, Adcock KH, Oohira A, Braistead JE, Levine JM, Margolis RU, Rogers JH, Fawcett JW. Neurocan Is Upregulated in Injured Brain and in Cytokine-Treated Astrocytes. J Neurosci. 2000 Apr 1;20(7):2427–38.

108. Vo T, Carulli D, Ehlert EME, Kwok JCF, Dick G, Mecollari V, Moloney EB, Neufeld G, De Winter F, Fawcett JW, Verhaagen J. The chemorepulsive axon guidance protein semaphorin3A is a constituent of perineuronal nets in the adult rodent brain. Molecular and Cellular Neuroscience. 2013 Sep;56:186–200.

109. Frischknecht R, Heine M, Perrais D, Seidenbecher CI, Choquet D, Gundelfinger ED. Brain extracellular matrix affects AMPA receptor lateral mobility and short-term synaptic plasticity. Nat Neurosci. 2009 Jul;12(7):897–904.

110. Härtig W, Derouiche A, Welt K, Brauer K, Grosche J, Mäder M, Reichenbach A, Brückner G. Cortical neurons immunoreactive for the potassium channel Kv3.1b subunit are predominantly surrounded by perineuronal nets presumed as a buffering system for cations. Brain Research. 1999 Sep;842(1):15–29.

111. Wang D, Fawcett J. The perineuronal net and the control of CNS plasticity. Cell Tissue Res. 2012 Jul;349(1):147–60.

112. Dityatev A, Brückner G, Dityateva G, Grosche J, Kleene R, Schachner M. Activity-dependent formation and functions of chondroitin sulfate-rich extracellular matrix of perineuronal nets. Devel Neurobio. 2007 Apr;67(5):570–88.

113. Larsen B, Luna B. Adolescence as a neurobiological critical period for the development of higher-order cognition. Neuroscience & Biobehavioral Reviews. 2018 Nov;94:179–95.

114. Whishaw IQ, Kolb B. Analysis of Behavior in Laboratory Rats. In: The Laboratory Rat [Internet]. Elsevier; 2020 [cited 2023 Aug 21]. p. 215–42. Available from: https://linkinghub.elsevier.com/retrieve/pii/B9780128143384000088

115. Gangopadhyay P, Chawla M, Dal Monte O, Chang SWC. Prefrontal–amygdala circuits in social decision-making. Nat Neurosci. 2021 Jan;24(1):5–18.

116. Dickinson SY, Kelly DA, Padilla SL, Bergan JF. From Reductionism Toward Integration: Understanding How Social Behavior Emerges From Integrated Circuits. Front Integr Neurosci. 2022 Apr 1;16:862437.

117. Raam T, Hong W. Organization of neural circuits underlying social behavior: A consideration of the medial amygdala. Current Opinion in Neurobiology. 2021 Jun;68:124–36.

118. Østby Y, Tamnes CK, Fjell AM, Westlye LT, Due-Tønnessen P, Walhovd KB. Heterogeneity in Subcortical Brain Development: A Structural Magnetic Resonance Imaging Study of Brain Maturation from 8 to 30 Years. J Neurosci. 2009 Sep 23;29(38):11772–82.

119. Uematsu A, Matsui M, Tanaka C, Takahashi T, Noguchi K, Suzuki M, Nishijo H. Developmental Trajectories of Amygdala and Hippocampus from Infancy to Early Adulthood in Healthy Individuals. Krueger F, editor. PLoS ONE. 2012 Oct 9;7(10):e46970.

120. Avino TA, Barger N, Vargas MV, Carlson EL, Amaral DG, Bauman MD, Schumann CM. Neuron numbers increase in the human amygdala from birth to adulthood, but not in autism. Proc Natl Acad Sci USA. 2018 Apr 3;115(14):3710–5.

121. Steinberg L, Morris AS. ADOLESCENT DEVELOPMENT. 2000;

122. Nelson EE, Leibenluft E, McCLURE EB, Pine DS. The social re-orientation of adolescence: a neuroscience perspective on the process and its relation to psychopathology. Psychol Med. 2005 Feb;35(2):163–74.

123. Fuster JM. The Prefrontal Cortex—An Update. Neuron. 2001 May;30(2):319–33.

124. Sowell ER, Thompson PM, Tessner KD, Toga AW. Mapping Continued Brain Growth and Gray Matter Density Reduction in Dorsal Frontal Cortex: Inverse Relationships during Postadolescent Brain Maturation. J Neurosci. 2001 Nov 15;21(22):8819–29.

125. Petanjek Z, Judaš M, Šimić G, Rašin MR, Uylings HBM, Rakic P, Kostović I. Extraordinary neoteny of synaptic spines in the human prefrontal cortex. Proc Natl Acad Sci USA. 2011 Aug 9;108(32):13281–6.

126. van Harmelen AL, van Tol MJ, van der Wee NJA, Veltman DJ, Aleman A, Spinhoven P, van Buchem MA, Zitman FG, Penninx BWJH, Elzinga BM. Reduced Medial Prefrontal Cortex Volume in Adults Reporting Childhood Emotional Maltreatment. Biological Psychiatry. 2010 Nov;68(9):832–8.

127. Dannlowski U, Stuhrmann A, Beutelmann V, Zwanzger P, Lenzen T, Grotegerd D, Domschke K, Hohoff C, Ohrmann P, Bauer J, Lindner C, Postert C, Konrad C, Arolt V, Heindel W, Suslow T, Kugel H. Limbic Scars: Long-Term Consequences of Childhood Maltreatment Revealed by Functional and Structural Magnetic Resonance Imaging. Biological Psychiatry. 2012 Feb;71(4):286–93.

128. Kelly PA, Viding E, Wallace GL, Schaer M, De Brito SA, Robustelli B, McCrory EJ. Cortical Thickness, Surface Area, and Gyrification Abnormalities in Children Exposed to Maltreatment: Neural Markers of Vulnerability? Biological Psychiatry. 2013 Dec;74(11):845–52.

129. Van Harmelen AL, Van Tol MJ, Dalgleish T, Van Der Wee NJA, Veltman DJ, Aleman A, Spinhoven P, Penninx BWJH, Elzinga BM. Hypoactive medial prefrontal cortex functioning in adults reporting childhood emotional maltreatment. Soc Cogn Affect Neurosci. 2014 Dec;9(12):2026–33.

130. Bounoua N, Miglin R, Spielberg JM, Sadeh N. Childhood assaultive trauma and physical aggression: Links with cortical thickness in prefrontal and occipital cortices. NeuroImage: Clinical. 2020;27:102321.

131. Delevich K, Klinger M, Okada NJ, Wilbrecht L. Coming of age in the frontal cortex: The role of puberty in cortical maturation. Seminars in Cell & Developmental Biology. 2021 Oct;118:64–72.

132. Caballero A, Tseng KY. GABAergic Function as a Limiting Factor for Prefrontal Maturation during Adolescence. Trends in Neurosciences. 2016 Jul;39(7):441–8.

133. Caballero A, Granberg R, Tseng KY. Mechanisms contributing to prefrontal cortex maturation during adolescence. Neuroscience & Biobehavioral Reviews. 2016 Nov;70:4–12.

134. Caballero A, Flores-Barrera E, Cass DK, Tseng KY. Differential regulation of parvalbumin and calretinin interneurons in the prefrontal cortex during adolescence. Brain Struct Funct. 2014 Jan;219(1):395–406.

135. Cass DK, Flores-Barrera E, Thomases DR, Vital WF, Caballero A, Tseng KY. CB1 cannabinoid receptor stimulation during adolescence impairs the maturation of GABA function in the adult rat prefrontal cortex. Mol Psychiatry. 2014 May;19(5):536–43.

136. Ueno H, Suemitsu S, Okamoto M, Matsumoto Y, Ishihara T. Parvalbumin neurons and perineuronal nets in the mouse prefrontal cortex. Neuroscience. 2017 Feb;343:115–27.

137. Gildawie KR, Honeycutt JA, Brenhouse HC. Region-specific Effects of Maternal Separation on Perineuronal Net and Parvalbumin-expressing Interneuron Formation in Male and Female Rats. Neuroscience. 2020 Jan;428:23–37.

138. Fung SJ, Webster MJ, Sivagnanasundaram S, Duncan C, Elashoff M, Weickert CS. Expression of Interneuron Markers in the Dorsolateral Prefrontal Cortex of the Developing Human and in Schizophrenia. AJP. 2010 Dec;167(12):1479–88.

139. Hoftman GD, Volk DW, Bazmi HH, Li S, Sampson AR, Lewis DA. Altered Cortical Expression of GABA-Related Genes in Schizophrenia: Illness Progression vs Developmental Disturbance. Schizophrenia Bulletin. 2015 Jan 1;41(1):180–91.

140. Xenos D, Kamceva M, Tomasi S, Cardin JA, Schwartz ML, Vaccarino FM. Loss of TrkB Signaling in Parvalbumin-Expressing Basket Cells Results in Network Activity Disruption and Abnormal Behavior. Cerebral Cortex. 2018 Oct 1;28(10):3399–413.

141. Guyon N, Zacharias LR, van Lunteren JA, Immenschuh J, Fuzik J, Märtin A, Xuan Y, Zilberter M, Kim H, Meletis K, Lopes-Aguiar C, Carlén M. Adult trkB Signaling in Parvalbumin Interneurons is Essential to Prefrontal Network Dynamics. J Neurosci. 2021 Apr 7;41(14):3120–41.

142. van Heukelum S, Mogavero F, van de Wal MAE, Geers FE, França ASC, Buitelaar JK, Beckmann CF, Glennon JC, Havenith MN. Gradient of Parvalbumin- and Somatostatin-Expressing Interneurons Across Cingulate Cortex Is Differentially Linked to Aggression and Sociability in BALB/cJ Mice. Front Psychiatry. 2019 Nov 15;10:809.

143. Liu L, Xu H, Wang J, Li J, Tian Y, Zheng J, He M, Xu TL, Wu ZY, Li XM, Duan SM, Xu H. Cell type–differential modulation of prefrontal cortical GABAergic interneurons on low gamma rhythm and social interaction. Sci Adv. 2020 Jul 24;6(30):eaay4073.

144. Bicks LK, Yamamuro K, Flanigan ME, Kim JM, Kato D, Lucas EK, Koike H, Peng MS, Brady DM, Chandrasekaran S, Norman KJ, Smith MR, Clem RL, Russo SJ, Akbarian S, Morishita H. Prefrontal parvalbumin interneurons require juvenile social experience to establish adult social behavior. Nat Commun. 2020 Feb 21;11(1):1003.

145. Drzewiecki CM, Willing J, Juraska JM. Influences of age and pubertal status on number and intensity of perineuronal nets in the rat medial prefrontal cortex. Brain Struct Funct. 2020 Nov;225(8):2495–507.

146. Baker KD, Gray AR, Richardson R. The development of perineuronal nets around parvalbumin gabaergic neurons in the medial prefrontal cortex and basolateral amygdala of rats. Behavioral Neuroscience. 2017 Aug;131(4):289–303.

147. Jakovljevic A, Agatonovic G, Aleksic D, Aksic M, Reiss G, Förster E, Stamatakis A, Jakovcevski I, Poleksic J. The impact of early life maternal deprivation on the perineuronal nets in the prefrontal cortex and hippocampus of young adult rats. Front Cell Dev Biol. 2022 Nov 28;10:982663.

148. Catale C, Martini A, Piscitelli RM, Senzasono B, Iacono LL, Mercuri NB, Guatteo E, Carola V. Early-life social stress induces permanent alterations in plasticity and perineuronal nets in the mouse anterior cingulate cortex. Eur J of Neuroscience. 2022 Nov;56(10):5763–83.

149. Sumner JA, Colich NL, Uddin M, Armstrong D, McLaughlin KA. Early Experiences of Threat, but Not Deprivation, Are Associated With Accelerated Biological Aging in Children and Adolescents. Biological Psychiatry. 2019 Feb;85(3):268–78.

150. Miskolczi C, Halász J, Mikics É. Changes in neuroplasticity following early-life social adversities: the possible role of brain-derived neurotrophic factor. Pediatr Res. 2019 Jan;85(2):225–33.

151. Umemori J, Winkel F, Didio G, Llach Pou M, Castrén E. iPlasticity: Induced juvenile-like plasticity in the adult brain as a mechanism of antidepressants: Antidepressant-induced plasticity. Psychiatry Clin Neurosci. 2018 Sep;72(9):633–53.

152. Reichelt AC, Hare DJ, Bussey TJ, Saksida LM. Perineuronal Nets: Plasticity, Protection, and Therapeutic Potential. Trends in Neurosciences. 2019 Jul;42(7):458–70.

153. Biro L, Miskolczi C, Szebik H, Bruzsik B, Varga ZK, Szente L, Toth M, Halasz J, Mikics E. Post-weaning social isolation in male mice leads to abnormal aggression and disrupted network organization in the prefrontal cortex: Contribution of

parvalbumin interneurons with or without perineuronal nets. Neurobiology of Stress. 2023 Jul;25:100546.

154. Wong DT, Perry KW, Bymaster FP. The Discovery of Fluoxetine Hydrochloride (Prozac). Nat Rev Drug Discov. 2005 Sep;4(9):764–74.

155. Bastos EF, Marcelino JLDS, Amaral AR, Serfaty CA. Fluoxetine-induced plasticity in the rodent visual system. Brain Research. 1999 Apr;824(1):28–35.

156. Vetencourt JFM, Sale A, Viegi A, Baroncelli L, De Pasquale R, F. O'Leary O, Castrén E, Maffei L. The Antidepressant Fluoxetine Restores Plasticity in the Adult Visual Cortex. Science. 2008 Apr 18;320(5874):385–8.

157. Saarelainen T, Hendolin P, Lucas G, Koponen E, Sairanen M, MacDonald E, Agerman K, Haapasalo A, Nawa H, Aloyz R, Ernfors P, Castrén E. Activation of the TrkB Neurotrophin Receptor Is Induced by Antidepressant Drugs and Is Required for Antidepressant-Induced Behavioral Effects. J Neurosci. 2003 Jan 1;23(1):349–57.

158. De Foubert G, Carney SL, Robinson CS, Destexhe EJ, Tomlinson R, Hicks CA, Murray TK, Gaillard JP, Deville C, Xhenseval V, Thomas CE, O'Neill MJ, Zetterström TSC. Fluoxetine-induced change in rat brain expression of brain-derived neurotrophic factor varies depending on length of treatment. Neuroscience. 2004;128(3):597–604.

159. Alme MN, Wibrand K, Dagestad G, Bramham CR. Chronic Fluoxetine Treatment Induces Brain Region-Specific Upregulation of Genes Associated with BDNF-Induced Long-Term Potentiation. Neural Plasticity. 2007;2007:1–9.

160. Guirado R, Perez-Rando M, Sanchez-Matarredona D, Castrén E, Nacher J. Chronic fluoxetine treatment alters the structure, connectivity and plasticity of cortical interneurons. Int J Neuropsychopharm. 2014 Oct;17(10):1635–46.

161. Karpova NN, Pickenhagen A, Lindholm J, Tiraboschi E, Kulesskaya N, Ágústsdóttir A, Antila H, Popova D, Akamine Y, Sullivan R, Hen R, Drew LJ,

Castrén E. Fear Erasure in Mice Requires Synergy Between Antidepressant Drugs and Extinction Training. Science. 2011 Dec 23;334(6063):1731–4.

162. Rygula R, Abumaria N, Domenici E, Hiemke C, Fuchs E. Effects of fluoxetine on behavioral deficits evoked by chronic social stress in rats. Behavioural Brain Research. 2006 Nov 1;174(1):188–92.

163. Cordner ZA, Marshall-Thomas I, Boersma GJ, Lee RS, Potash JB, Tamashiro KLK. Fluoxetine and environmental enrichment similarly reverse chronic social stress-related depression- and anxiety-like behavior, but have differential effects on amygdala gene expression. Neurobiology of Stress. 2021 Nov;15:100392.

164. Haller J, Harold G, Sandi C, Neumann ID. Effects of Adverse Early-Life Events on Aggression and Anti-Social Behaviours in Animals and Humans. J Neuroendocrinol. 2014 Oct;26(10):724–38.

165. Sandi C, Haller J. Stress and the social brain: behavioural effects and neurobiological mechanisms. Nat Rev Neurosci. 2015 May;16(5):290–304.

166. Jaffee SR. Child Maltreatment and Risk for Psychopathology in Childhood and Adulthood. Annu Rev Clin Psychol. 2017 May 8;13(1):525–51.

167. Widom CS. Long-Term Impact of Childhood Abuse and Neglect on Crime and Violence. Clin Psychol Sci Pract. 2017 Jun;24(2):186–202.

168. Tóth M, Halász J, Mikics É, Barsy B, Haller J. Early social deprivation induces disturbed social communication and violent aggression in adulthood. Behavioral Neuroscience. 2008 Aug;122(4):849–54.

169. Toth M, Mikics E, Tulogdi A, Aliczki M, Haller J. Post-weaning social isolation induces abnormal forms of aggression in conjunction with increased glucocorticoid and autonomic stress responses. Hormones and Behavior. 2011 Jun;60(1):28–36.

170. Toth M, Tulogdi A, Biro L, Soros P, Mikics E, Haller J. The neural background of hyper-emotional aggression induced by post-weaning social isolation. Behavioural Brain Research. 2012 Jul;233(1):120–9.

171. Miczek KA, De Boer SF, Haller J. Excessive aggression as model of violence: a critical evaluation of current preclinical methods. Psychopharmacology. 2013 Apr;226(3):445–58.

172. Tulogdi Á, Tóth M, Barsvári B, Biró L, Mikics É, Haller J. Effects of resocialization on post-weaning social isolation-induced abnormal aggression and social deficits in rats: Resocialization of Aggressive Isolated Rats With Social Deficits. Dev Psychobiol. 2014 Jan;56(1):49–57.

173. Carlén M. What constitutes the prefrontal cortex? Science. 2017 Oct 27;358(6362):478–82.

174. Montag C, Weber B, Trautner P, Newport B, Markett S, Walter NT, Felten A, Reuter M. Does excessive play of violent first-person-shooter-video-games dampen brain activity in response to emotional stimuli? Biological Psychology. 2012 Jan;89(1):107–11.

175. New AS, Hazlett EA, Newmark RE, Zhang J, Triebwasser J, Meyerson D, Lazarus S, Trisdorfer R, Goldstein KE, Goodman M, Koenigsberg HW, Flory JD, Siever LJ, Buchsbaum MS. Laboratory Induced Aggression: A Positron Emission Tomography Study of Aggressive Individuals with Borderline Personality Disorder. Biological Psychiatry. 2009 Dec;66(12):1107–14.

176. Veit R, Lotze M, Sewing S, Missenhardt H, Gaber T, Birbaumer N. Aberrant social and cerebral responding in a competitive reaction time paradigm in criminal psychopaths. NeuroImage. 2010 Feb;49(4):3365–72.

177. Yang Y, Raine A. Prefrontal structural and functional brain imaging findings in antisocial, violent, and psychopathic individuals: A meta-analysis. Psychiatry Research: Neuroimaging. 2009 Nov;174(2):81–8.

178. Halász J, Tóth M, Kalló I, Liposits Z, Haller J. The activation of prefrontal cortical neurons in aggression—A double labeling study. Behavioural Brain Research. 2006 Nov;175(1):166–75.

179. Biro L, Sipos E, Bruzsik B, Farkas I, Zelena D, Balazsfi D, Toth M, Haller J. Task Division within the Prefrontal Cortex: Distinct Neuron Populations Selectively Control Different Aspects of Aggressive Behavior via the Hypothalamus. J Neurosci. 2018 Apr 25;38(17):4065–75.

180. Biro L, Toth M, Sipos E, Bruzsik B, Tulogdi A, Bendahan S, Sandi C, Haller J. Structural and functional alterations in the prefrontal cortex after post-weaning social isolation: relationship with species-typical and deviant aggression. Brain Struct Funct. 2017 May;222(4):1861–75.

181. Homberg JR, Wöhr M, Alenina N. Comeback of the Rat in Biomedical Research. ACS Chem Neurosci. 2017 May 17;8(5):900–3.

182. Ellenbroek B, Youn J. Rodent models in neuroscience research: is it a rat race? Disease Models & Mechanisms. 2016 Oct 1;9(10):1079–87.

183. Tiraboschi E, Guirado R, Greco D, Auvinen P, Maya-Vetencourt JF, Maffei L, Castrén E. Gene Expression Patterns Underlying the Reinstatement of Plasticity in the Adult Visual System. Neural Plasticity. 2013;2013:1–8.

184. Mikics É, Guirado R, Umemori J, Tóth M, Biró L, Miskolczi C, Balázsfi D, Zelena D, Castrén E, Haller J, Karpova NN. Social Learning Requires Plasticity Enhanced by Fluoxetine Through Prefrontal Bdnf-TrkB Signaling to Limit Aggression Induced by Post-Weaning Social Isolation. Neuropsychopharmacol. 2018 Jan;43(2):235–45.

185. de Almeida R. Aggression Escalated by Social Instigation or by Discontinuation of Reinforcement ("Frustration") in Mice Inhibition by Anpirtoline: A 5-HT1B Receptor Agonist. Neuropsychopharmacology. 2002 Aug;27(2):171–81.

186. Duque-Wilckens N, Steinman MQ, Busnelli M, Chini B, Yokoyama S, Pham M, Laredo SA, Hao R, Perkeybile AM, Minie VA, Tan PB, Bales KL, Trainor BC. Oxytocin Receptors in the Anteromedial Bed Nucleus of the Stria Terminalis Promote Stress-Induced Social Avoidance in Female California Mice. Biological Psychiatry. 2018 Feb;83(3):203–13.

187. Newman EL, Covington HE, Suh J, Bicakci MB, Ressler KJ, DeBold JF, Miczek KA. Fighting Females: Neural and Behavioral Consequences of Social Defeat Stress in Female Mice. Biological Psychiatry. 2019 Nov;86(9):657–68.

188. Adriani W, Caprioli A, Granstrem O, Carli M, Laviola G. The spontaneously hypertensive-rat as an animal model of ADHD: evidence for impulsive and non-impulsive subpopulations. Neuroscience & Biobehavioral Reviews. 2003 Nov;27(7):639–51.

189. Aliczki M, Fodor A, Balogh Z, Haller J, Zelena D. The effects of lactation on impulsive behavior in vasopressin-deficient Brattleboro rats. Hormones and Behavior. 2014 Aug;66(3):545–51.

190. Dalley JW, Mar AC, Economidou D, Robbins TW. Neurobehavioral mechanisms of impulsivity: Fronto-striatal systems and functional neurochemistry. Pharmacology Biochemistry and Behavior. 2008 Aug;90(2):250–60.

191. Dani A, Huang B, Bergan J, Dulac C, Zhuang X. Superresolution Imaging of Chemical Synapses in the Brain. Neuron. 2010 Dec;68(5):843–56.

192. Takamori S, Rhee JS, Rosenmund C, Jahn R. Identification of a vesicular glutamate transporter that defines a glutamatergic phenotype in neurons. 2000;407.

193. Takamori S, Rhee JS, Rosenmund C, Jahn R. Identification of Differentiation-Associated Brain-Specific Phosphate Transporter as a Second Vesicular Glutamate Transporter (VGLUT2). J Neurosci. 2001 Nov 15;21(22):RC182–RC182.

194. Fremeau RT, Troyer MD, Pahner I, Nygaard GO, Tran CH, Reimer RJ, Bellocchio EE, Fortin D, Storm-Mathisen J, Edwards RH. The Expression of Vesicular Glutamate Transporters Defines Two Classes of Excitatory Synapse. Neuron. 2001 Aug;31(2):247–60.

195. Vereczki VK, Veres JM, Müller K, Nagy GA, Rácz B, Barsy B, Hájos N. Synaptic Organization of Perisomatic GABAergic Inputs onto the Principal Cells of the Mouse Basolateral Amygdala. Front Neuroanat [Internet]. 2016 Mar 7 [cited 2023

Mar 20];10. Available from: http://journal.frontiersin.org/Article/10.3389/fnana.2016.00020/abstract

196. Guirado R, Carceller H, Castillo-Gómez E, Castrén E, Nacher J. Automated analysis of images for molecular quantification in immunohistochemistry. Heliyon. 2018 Jun;4(6):e00669.

197. Kempes M, Matthys W, de Vries H, van Engeland H. Reactive and proactive aggression in children A review of theory, findings and the relevance for child and adolescent psychiatry. EuropChild & Adolescent Psych. 2005 Feb;14(1):11–9.

198. Birnie MT, Kooiker CL, Short AK, Bolton JL, Chen Y, Baram TZ. Plasticity of the Reward Circuitry After Early-Life Adversity: Mechanisms and Significance. Biological Psychiatry. 2020 May;87(10):875–84.

199. Sanchez EO, Bangasser DA. The effects of early life stress on impulsivity. Neuroscience & Biobehavioral Reviews. 2022 Jun;137:104638.

200. Yizhar O, Fenno LE, Prigge M, Schneider F, Davidson TJ, O'Shea DJ, Sohal VS, Goshen I, Finkelstein J, Paz JT, Stehfest K, Fudim R, Ramakrishnan C, Huguenard JR, Hegemann P, Deisseroth K. Neocortical excitation/inhibition balance in information processing and social dysfunction. Nature. 2011 Sep;477(7363):171–8.

201. Schiavone S, Sorce S, Dubois-Dauphin M, Jaquet V, Colaianna M, Zotti M, Cuomo V, Trabace L, Krause KH. Involvement of NOX2 in the Development of Behavioral and Pathologic Alterations in Isolated Rats. Biological Psychiatry. 2009 Aug;66(4):384–92.

202. Ueno H, Suemitsu S, Murakami S, Kitamura N, Wani K, Okamoto M, Matsumoto Y, Ishihara T. Region-specific impairments in parvalbumin interneurons in social isolation-reared mice. Neuroscience. 2017 Sep;359:196–208.

203. Spijker S, Koskinen MK, Riga D. Incubation of depression: ECM assembly and parvalbumin interneurons after stress. Neuroscience & Biobehavioral Reviews. 2020 Nov;118:65–79.

204. McKlveen JM, Moloney RD, Scheimann JR, Myers B, Herman JP. “Braking” the Prefrontal Cortex: The Role of Glucocorticoids and Interneurons in Stress Adaptation and Pathology. Biological Psychiatry. 2019 Nov;86(9):669–81.

205. Devienne G, Picaud S, Cohen I, Piquet J, Tricoire L, Testa D, Di Nardo AA, Rossier J, Cauli B, Lambolez B. Regulation of Perineuronal Nets in the Adult Cortex by the Activity of the Cortical Network. J Neurosci. 2021 Jul 7;41(27):5779–90.

206. Carceller H, Guirado R, Ripolles-Campos E, Teruel-Marti V, Nacher J. Perineuronal Nets Regulate the Inhibitory Perisomatic Input onto Parvalbumin Interneurons and γ Activity in the Prefrontal Cortex. J Neurosci. 2020 Jun 24;40(26):5008–18.

207. Freund TF, Katona I. Perisomatic Inhibition. Neuron. 2007 Oct;56(1):33–42.

208. Kubota Y. Untangling GABAergic wiring in the cortical microcircuit. Current Opinion in Neurobiology. 2014 Jun;26:7–14.

209. Gibb BE, Schofield CA, Coles ME. Reported History of Childhood Abuse and Young Adults’ Information-Processing Biases for Facial Displays of Emotion. Child Maltreat. 2009 May;14(2):148–56.

210. Troller-Renfree S, McDermott JM, Nelson CA, Zeanah CH, Fox NA. The effects of early foster care intervention on attention biases in previously institutionalized children in Romania. Dev Sci. 2015 Sep;18(5):713–22.

211. Koss KJ, Hostinar CE, Donzella B, Gunnar MR. Social deprivation and the HPA axis in early development. Psychoneuroendocrinology. 2014 Dec;50:1–13.

212. Peng H, Long Y, Li J, Guo Y, Wu H, Yang Y, Ding Y, He J, Ning Y. Hypothalamic-pituitary-adrenal axis functioning and dysfunctional attitude in depressed patients with and without childhood neglect. BMC Psychiatry. 2014 Dec;14(1):45.

213. Keil V, Price JM. Social information-processing patterns of maltreated children in two social domains. Journal of Applied Developmental Psychology. 2009 Jan;30(1):43–52.

214. Kay CL, Green JM. Social cognitive deficits and biases in maltreated adolescents in UK out-of-home care: Relation to disinhibited attachment disorder and psychopathology. Dev Psychopathol. 2016 Feb;28(1):73–83.

215. Wukitsch TJ, Brase EC, Moser TJ, Kiefer SW, Cain ME. Differential rearing alters taste reactivity to ethanol, sucrose, and quinine. Psychopharmacology. 2020 Feb;237(2):583–97.

216. Suri D, Teixeira CM, Cagliostro MKC, Mahadevia D, Ansorge MS. Monoamine-Sensitive Developmental Periods Impacting Adult Emotional and Cognitive Behaviors. Neuropsychopharmacol. 2015 Jan;40(1):88–112.

217. Reynolds LM, Flores C. Mesocorticolimbic Dopamine Pathways Across Adolescence: Diversity in Development. Front Neural Circuits. 2021 Sep 8;15:735625.

218. Koike H, Ibi D, Mizoguchi H, Nagai T, Nitta A, Takuma K, Nabeshima T, Yoneda Y, Yamada K. Behavioral abnormality and pharmacologic response in social isolation-reared mice. Behavioural Brain Research. 2009 Aug;202(1):114–21.

219. Liu JH, You QL, Wei MD, Wang Q, Luo ZY, Lin S, Huang L, Li SJ, Li XW, Gao TM. Social Isolation During Adolescence Strengthens Retention of Fear Memories and Facilitates Induction of Late-Phase Long-Term Potentiation. Mol Neurobiol. 2015 Dec;52(3):1421–9.

220. Võikar V, Polus A, Vasar E, Rauvala H. Long-term individual housing in C57BL/6J and DBA/2 mice: assessment of behavioral consequences: Effect of isolation on mouse behavior. Genes, Brain and Behavior. 2004 Nov 8;4(4):240–52.

221. Varga ZK, Pejtsik D, Toth M, Balogh Z, Aliczki M, Balla GY, Kontra L, Eckert Z, Borhegyi Z, Mikics E. Improving anxiety research: novel approach to reveal trait anxiety through summary measures of multiple states.

222. Teicher MH, Gordon JB, Nemeroff CB. Recognizing the importance of childhood maltreatment as a critical factor in psychiatric diagnoses, treatment, research, prevention, and education. Mol Psychiatry. 2022 Mar;27(3):1331–8.

223. Kim E, Sheng M. PDZ domain proteins of synapses. Nat Rev Neurosci. 2004 Oct;5(10):771–81.

224. Hinton EA, Li DC, Allen AG, Gourley SL. Social Isolation in Adolescence Disrupts Cortical Development and Goal-Dependent Decision-Making in Adulthood, Despite Social Reintegration. eNeuro. 2019 Sep;6(5):ENEURO.0318-19.2019.

225. Li DC, Hinton EA, Gourley SL. Persistent behavioral and neurobiological consequences of social isolation during adolescence. Seminars in Cell & Developmental Biology. 2021 Oct;118:73–82.

9. Bibliography of the candidate's publications

9.1. List of publications used for the thesis

Biro L*, **Miskolczi C***, Szebik H, Bruzsik B, Varga ZK, Szente L, Toth M, Halasz J, Mikics E.
Post-weaning social isolation in male mice leads to abnormal aggression and disrupted network organization in the prefrontal cortex: Contribution of parvalbumin interneurons with or without perineuronal nets. Neurobiol Stress. 2023 May 29;25:100546.

Miskolczi C, Halász J, Mikics É.
Changes in neuroplasticity following early-life social adversities: the possible role of brain-derived neurotrophic factor. Pediatr Res. 2019 Jan;85(2):225-233.

Mikics É, Guirado R, Umemori J, Tóth M, Biró L, **Miskolczi C**, Balázsfi D, Zelena D, Castrén E, Haller J, Karpova NN.
Social Learning Requires Plasticity Enhanced by Fluoxetine Through Prefrontal Bdnf-TrkB Signaling to Limit Aggression Induced by Post-Weaning Social Isolation. Neuropsychopharmacology. 2018 Jan;43(2):235-245.

9.2. List of publications not used for the thesis

Balázsfi D, Zelena D, Demeter K, **Miskolczi C,** Varga ZK, Nagyváradi Á, Nyíri G, Cserép C, Baranyi M, Sperlágh B, Haller J.
Differential Roles of the Two Raphe Nuclei in Amiable Social Behavior and Aggression - An Optogenetic Study. Front Behav Neurosci. 2018 Aug 2;12:163.

Zelena D, Mikics É, Balázsfi D, Varga J, Klausz B, Urbán E, Sipos E, Biró L, **Miskolczi C**, Kovács K, Ferenczi S, Haller J.
Enduring abolishment of remote but not recent expression of conditioned fear by the blockade of calcium-permeable AMPA receptors before extinction training. Psychopharmacology (Berl). 2016 Jun;233(11):2065-2076.

10. Acknowledgements

First of all, I would like to thank my supervisor, Dr. Éva Mikics, for her support throughout my scientific career. Her guidance in performing behavioral experiments and enthusiasm in translational research formed a large part in shaping my way of thinking and I am forever grateful for this experience. Éva has always provided valuable criticism and suggestions, significantly improving my publications and my thesis.

I would also like to thank her, as the group leader of the Laboratory of Translational Behavioral Neurosciences, for taking me in as a young student into her lab and providing me with the trust and opportunity to work on our projects. I would also like to thank Dr. József Haller for these reasons and for introducing me to the analysis of aggression and social behavior.

I am also very grateful to Dr. László Biró, for being one of the most reliable and knowledgeable mentors and friends, who not only guided me through scientific research but also through the illustrious bar scene of Üllői út and beyond.

I am thankful for the technical help of Huba Szebik, Dr. Zoltán Kristóf Varga, László Szente, Dr. Bíborka Bruzsik and Dr. Manó Aliczki, who are not only my colleagues but also friends I can count on. I also want to thank Dr. Kornél Demeter for always keeping the Behavioral Studies Unit (BSU) in top shape and helping me with any BSU-related problem I had.

I am grateful to Dr. Diána Balázsfi, for being my opponent in my work defense even with the short deadline given, providing valuable feedback and a much-needed motivation boost close to the finish line.

I'd also like to thank the Coffee Club members, especially Bíbor and Laci (Szente), who kept me sane throughout heavier times, and the extended Coffee Club, for giving me something to look forward to each day.

I'm eternally grateful for meeting Vanda, for making me feel like the luckiest person alive, who has supported me and inspired me continuously. (I love you so much.)

Finally, I'd like to thank my parents, family and friends for their love and support, for motivating me thoughout my doctoral studies.